TÉCNICO LISBOA

Using a Micro-Hydro Power Local Plant for Providing Energy to The Irrigation System of a Sugar Cane Plantation at the District of Magude-Mozambique

Luís Miguel Pereira Pontes

Thesis to obtain the Master of Science Degree in

Engenharia Electrotécnica e de Computadores

Supervisor(s): Prof. Dr. Paulo José da Costa Branco
Prof. Dr. Modesto Pérez Sánchez

Examination Committee

Chairperson: Prof. Dr. Célia Maria Santos Cardoso de Jesus
Supervisor: Prof. Dr. Paulo José da Costa Branco
Member of the Committee: Excel. Prof. Dr. Zacarias Marcos Mapoissane Chilengue
Member of the Committee: Excel. Prof. Dr. Nordino Martinho Muaievela

September 2021

I declare that this document is an original work of my own authorship and that it fulfills all the requirements of the Code of Conduct and Good Practices of the Universidade de Lisboa.

Any sufficiently advanced technology is indistinguishable from magic.

Clarke's Third Law

Acknowledgments

To Professor Paulo José da Costa Branco, supervisor of this thesis, and my former Professor, to whom I am in debt for providing me with the opportunity to be his master thesis student. I acknowledge both his support and the continued guidance in technical-scientific matters.

To Professor Modesto Pérez Sánchez, supervisor of this thesis, to whom I give my sincere thanks for the valuable assistance lent in the hydraulics domain, the materials provided and the patience demonstrated in explaining concepts new to me.

To the Professors and Educators, who excel at their mission to, not only transmit their knowledge, but also encourage their students to be inquisitive and skeptical, yet open minded in the pursuit of scientific knowledge. These being the professors that, while following their curricula, also find the time to know their students, listen to feedback, and let themselves be known in the process as well...for the often perceived rigidity of curricula in higher education can be at odds with what university should be: a place to learn at a more flexible pace with increased focus on personal choice and time to reflect on newly acquired knowledge, which is deeply gratifying under the right circumstances, as opposed to a system that, for the most part, turns students in fleeting repositories of very specific but dissociated information.

Last but not least, to my Family and Friends, for supporting me in the pursuit of a higher education.

Resumo

O aumento populacional que Moçambique tem verificado coloca desafios acrescidos à gestão e exploração de recursos naturais. Neste sentido, o acesso a água e energia eléctrica necessárias à irrigação são fundamentais ao desenvolvimento do sector agrícola e bem-estar das populações locais.

Neste trabalho o estudo incide numa plantação de cana-de-açúcar, Macuvulane I, localizada no distrito de Magude, província de Maputo, estando a exploração do regadio a cargo de uma associação de pequenos produtores. A irrigação é realizada por bombagem a partir do rio Incomati e, estando as bombas ligadas à rede eléctrica nacional, incorrem daqui custos energéticos avultados. Assim, determinadas as necessidades de água para esta cultura e local específicos e, tendo em consideração as características do sistema instalado, estima-se o consumo energético que assegura a correcta irrigação do regadio.

Com o objectivo de aumentar o grau de autonomia em relação à rede, estuda-se o impacto no consumo energético, originado pela instalação de uma central micro-hídrica no local. Deste modo, o caudal do rio é caracterizado para a época chuvosa, estimando-se o potencial hídrico não explorado. Discute-se a operação da turbina Kaplan, visto ser este o tipo de turbomáquina que confere o melhor desempenho face às condições do local. São analisados dois cenários distintos quanto ao tipo de aproveitamento hidroeléctrico, realizando-se um estudo de investimento e rendibilidade para cada caso. Conclui-se que não é possível isolar por completo o sistema de irrigação da rede, propondo-se a melhor solução do ponto de vista técnico e económico.

Palavras-chave: Necessidades Hídricas, Irrigação Eficiente, Central Micro-Hídrica, Turbina Kaplan, Autonomia Energética.

Abstract

The population increase Mozambique has been experiencing places additional challenges to the management and exploration of natural resources. In this regard, access to water and electricity required for irrigation are fundamental to the development of the agriculture sector and well-being of local populations.

In this work, the study is focused on a sugar cane plantation, Macuvulane I, located in the district of Magude, province of Maputo, with a smallholders association in charge of the exploration of the plantation. Irrigation is done by pumping water from the Incomati river, and with the pumps connected to the national electric grid significant energetic costs incur. With the water requirements for both the crop and location in question determined, the energy consumption required to ensure a correct irrigation of the plantation is estimated.

Faced with the goal of increasing the degree of energetic autonomy, the potential impact in energy consumption, caused by the installation of a micro-hydro power plant in the local area, is studied. Thus, the river flow is characterized for the wet season, and the unexplored hydro potential evaluated. The operation fundamentals of the Kaplan turbine are discussed, as this is the turbomachine that offers the best performance under local conditions. Two distinct scenarios as to the type of hydropower scheme are analyzed, with an investment and profitability study performed for each case. It follows that it is not possible to completely isolate the irrigation system from the grid, leading to the proposal of the best technical and economically viable solution.

Keywords: Water Requirements, Efficient Irrigation, Micro-Hydro Power Plant, Kaplan Turbine, Energetic Autonomy.

Contents

List of Tables

List of Figures

Nomenclature

Channel Design

γ	water specific weight
ρ	water density
AR	aspect ratio
A	cross section
b	width
F_r	Froude number
g	acceleration of gravity
h	water head
k	unit conversion factor
n	Gauckler–Manning coefficient
P_w	wetted perimeter
Q_{design}	design flow
R_h	hydraulic radius
S	slope
v	fluid mean velocity
y	height

Economical Analysis

c	annual mean cost of energy
d_{om}	operation and maintenance costs
E_a	annual energy produced
i'	annual charges as a percentage of investment

I_t total investment

j year under analysis

k_a sum of geometric series

n lifespan of the power plant

R currency exchange rate

r discount rate

Flow Data

Q instant flow

Q_f flood flow

Q_N modular flow

Q_{max} maximum river flow

Q_{mean} mean river flow

Q_{min} minimum river flow

Irrigation Needs

D usable water soil storage

I_G gross irrigation

I_N net irrigation

k_u uniformity coefficient

P_e effective precipitation

S soil water storage

Crop Water Needs (FAO method)

α canopy reflection coefficient

Δ slope of the saturation vapour pressure temperature relationship

δ solar declination

γ psychrometric constant

λ latent heat vaporization

ω_s sunset hour angle

ρ_a mean air density at constant pressure

σ	Stephan-Boltzmann constant
φ	latitude
c_p	air specific heat
d_r	inverse relative distance Earth-Sun
e_a	actual vapour pressure
G	soil heat flux
J	day of the year
N	daylight hours
P_a	atmospheric pressure
R_a	extraterrestrial radiation
r_a	aerodynamic resistance
R_n	net radiation
R_s	solar radiation
r_s	bulk resistance
R_{nl}	net longwave radiation
R_{ns}	net shortwave radiation
R_{so}	clear-sky solar radiation
T_{dew}	dewpoint temperature
T_{max}	maximum air temperature
T_{mean}	mean air temperature
T_{min}	minimum air temperature
u_2	wind speed at a height of 2 m
z	altitude

Reservoir

Q_{in}	reservoir inflow
Q_{out}	reservoir outflow
V	volume in reservoir
V_{max}	reservoir capacity

Pumps/Turbine

α_1 turbine lower exploration limit

α_2 turbine upper exploration limit

ϵ flow to power relative ratio

η machine efficiency

ε_T degree of reaction

E energy

H_b hydraulic head

P electric power

Q_d pump design duty

Weather Data

P_t precipitation

T temperature

Glossary

ARA-Sul	Administração Regional de Águas do Sul
AdX	Açucareira de Xinavane
AfDB	African Development Bank
EDM	Electricidade de Moçambique
EU	European Union
FAO	Food and Agriculture Organization
FDC	Flow Duration Curve
IRR	Internal Rate of Return
LCOE	Levelized Cost Of Energy
MAFAP	Monitoring and Analyzing Food and Agricultural Policies
NPV	Net Present Value
PAT	Pump As Turbine
SCS	Soil Conservation Service
SSIP	Small Scale Irrigation Project
USDA	United States Department of Agriculture

Chapter 1

Introduction

According to the World Bank about two-thirds of Mozambique's population live in rural areas [1]. Before 2016 the country had experienced accelerated economic growth, in part due to the increased importance of sectors like agriculture and industry, but this growth was later halted in light of the hidden debt the country had amassed [1]. In 2019, the devastation to infrastructure caused by the Idai and Kenneth cyclones further sent the country into an economic crisis, putting at risk the well-being of the population.

In regard to natural resources, Mozambique is an extremely rich country, but lacks much of infrastructure required to explore them in an environmentally sustainable way. In fact, while water is obsequiously abundant as the country has an important number of rivers, a direct consequence of the rise in population is the pressure exerted in the ecosystem. In this work, the case study is focused on a sugar cane plantation in the district of Magude in the Maputo province and the closest available body of water is the Incomati river, whose basin is shared between South Africa, Swaziland and Mozambique under the Tripartite Interim Agreement between theses nations, and is already under incredible strain [2].

Subsistence agriculture provides farmers with consumables for self-sustainability but also allows some level of economic independence as the agriculture sector employs much of the population in rural areas. Of all the crops explored at national level, sugar cane has outstanding weight in the country's exports. In fact, it is the high profitability of sugar that has motivated the construction and conversion of farmland into plantations, managed by a small number of companies that control this activity, or at times, by smallholders associations of local farmers. Either way, this activity is paramount to the general well being as a means to raise populations out of poverty.

1.1 Motivation

Now, one of the obstacles towards economic independence that local populations are faced with is energy availability. Mozambique's electric grid is still underdeveloped and the quality of supply is lacking [3].

In fact much of the country has no electric coverage even to fulfill basic needs and for many families and businesses the energy tariffs amount to unsustainable electrification and irrigation costs that act as barriers towards agriculture development. In light of this, there is an increased focus on the role of renewable energies in fostering opportunities and combat poverty. While solar and hydro resources are abundant, their exploration still presents a challenge to small farmer associations due to the high investment involved in such projects.

In order to ensure adequate crop yield, the irrigation system has to be able to deliver the required water duty, and despite the fact that the mean annual precipitation value for Magude is reasonably high, the bulk of precipitation occurs in summer months. So, while in these months the need for irrigation could be thought of as more demanding, in fact due to higher levels of precipitation, the critical months actually occur in winter, when despite the lower temperatures, the lack of rain causes an increased demand in water availability which the Incomati river fulfills. However, pumping water is an energy intensive activity that lowers the profit margin of farmer associations and, as a consequence, threatens the economic sustainability of local populations.

It is thus self-evident the advantage of using the available resources to complement energy requirements. For the particular case of Magude, there are, at first glance, two technical viable possibilities to approach hydro-pumping, solar generation through photo-voltaic panels and micro-hydro generation. Here, the latter is addressed.

1.2 Topic Overview

As discussed previously, while the resources are abundant, exploring them is an entirely different matter if one takes into consideration the lack of infrastructure and other issues typically associated with developing countries.

Given the mentioned weight of the agriculture sector to the country's development, it is natural to conclude that higher investment in agriculture and training towards better agricultural practices should be a top priority to combat poverty. Out of this necessity arose the concept associated with small scale irrigation projects (ISSPs) as a practical solution to tackle this problem. As such, in 2005, the EU and the AfDB, financed the construction, in Magude, of the Macuvulane I sugar cane plantation with a total command area of 187.9 ha. The irrigation is performed by sprinkler and the water is pumped from the Incomati river, located about 300 m north of the plantation. The pumping station is equipped with 3 groups of centrifugal pumps and induction motors connected to the electric grid. The plantation is divided in blocks and a smallholders association comprised of small farmers is responsible for distribution of tasks such as manual rotation of sprinklers to ensure an evenly distribution of applied water across different blocks or otherwise ensure each plot assigned to a certain farmer or family is adequately maintained.

Naturally, in order to approach the problem of renewable powered irrigation, one must first look at the crop in question, the agricultural practices employed by the farmers and the association, the infield characteristics and the local climate and seasonal variance so as to characterize the water duty of the crop and develop an efficient irrigation scheme at the lowest possible cost. From the estimated water duty, the next step should be the estimation of the energy needs required for hydro-pumping. It should be noted that due to a number of issues, the information from the field is limited. For example, the need to estimate the energy requirements follows from an unavailability of energy bills.

Since this work is focused on developing a micro-hydro powered system for irrigation and how it can be achieved in an efficient and economically viable way, what follows is a characterization of the river flow in this region. As before, an issue encountered here is that weather data for specific locations in Mozambique is hard to come by, either because of limited measurement activity or because measurements are not publicly available for consultation. Specifically, the flow of the Incomati river at station E-43 (Magude) is only available during the wet season and for the hydrological period of 2018 to 2021. As the precipitation fluctuates greatly on an annual basis, the sample set available should not be taken as significant beyond the period of years in which these parameters were measured. In this particular case, two approaches are possible in order to generate hydroelectricity. Installing a turbine in a dam structure (scenario A) or constructing additional infrastructure to limit but regularize the river flow, such as an open channel (scenario B). The latter is indicated as a possible solution.

The prospect of water storage in a reservoir for energy generation at a convenient time, by loading the channel considering the variability of river flow, is studied.

Finally, an economic analysis is carried out to determine the most interesting scenario, bearing in mind the limitations associated with the assumptions made, in the absence of detailed information.

1.3 Objectives

This work is focused on eliminating (if possible) the dependence on the grid of the irrigation system of a sugar cane plantation located in the district of Magude, Mozambique. Irrigation sustainability is a challenge, given the costs associated with electricity that are supported by the farmer's association. A study is then needed to replace or augment the current energy source powering the irrigation system with a micro-hydro based one.

As such, the main goal is to develop an integration strategy of a micro-hydro power system to achieve self-supply, taking into account the uncertainty of natural resources over time, such as rainfall or river flow, in the viability of the energy supply.

As the integration of the new power source in the irrigation system requires the design and installation of electrical and hydraulic systems as well as the necessary facilities, these aspects are also discussed.

1.4 Thesis Outline

The current work is organized in 8 chapters and 7 appendixes.

Chapter 1 is dedicated to the subject introduction. An overview of the subject is presented as well as the objectives to be met.

Chapter 2 provides a brief overview on the sugar cane crop, and how it is explored in Mozambique.

Chapter 3 presents the case study. Starting with available local climate data, more precisely, temperature and precipitation series, the water duty of the crop is derived, based in the FAO Penman-Monteith method, followed by the analysis of the irrigation system, based on existing installed pump units and the infield data concerning the sprinklers. The operation of the pumps as well as their energy consumption is characterized to the extent of data available.

Chapter 4 concerns the underlying motivation behind a self-supply system, the advantages of the hydro resource in face of a solar alternative and the evaluation of the hydroelectric potential of the Incomati river.

Chapter 5 deals with the design of the local power plant based on available data discussed in the previous chapter. Two different scenarios, A and B, representing different technical solutions based on distinct hydro schemes with different investment costs are considered.

Chapter 6 attempts to provide a superficial economical analysis, bearing in mind the difficulty in evaluating certain aspects associated with the implementation of these solutions, relating to construction costs for example.

Chapter 7 presents and discusses the results obtained throughout the work. Starting with a review of the problem and the identification of the challenges to overcome, passing through the methodology followed in attempting to meet the goal and the motivations at the origin of assumptions made.

Chapter 8 is dedicated to the conclusions reached in this work, some caveats on the limitation of available data and how it impacts the validity of the assumptions made. Provisional conclusions as well as some recommendations for future work are discussed.

Appendix A provides a detailed description of the methodology followed in determining the evapotranspiration of the sugar cane crop based on the FAO 56 guide.

Appendix B presents the flow data pertaining to each season, compiled from hydrologic bulletins available at the ARA-Sul online repository.

Appendix C presents the chronological flow series compiled from raw data.

Appendix D presents the flow duration curves resultant from the chronological daily flow series.

Appendix E provides the models used for adjusting the FDCs.

Appendix F provides the theoretical basis used in the optimization of an open rectangular channel cross section.

Appendix G provides a brief theoretical basis for determining the photo-voltaic potential discussed in chapter 4.

Chapter 2

Sugar Cane Crop

2.1 An Overview

Sugar cane is the name given to several species of perennial tall grass that thrive in warm to temperate tropical regions of the world and are cultivated for their sucrose content, reaching between 2 to 4 meters in height [4].

Most commercial sugar cane is grown between 35°N and 35°S, in zones where there is adequate moisture and high incidence of radiation. Germination occurs at an optimum temperature range of 32°C to 38°C and optimum growth is achieved for mean daily temperatures of 22°C to 38°C. In order for active growth to occur it requires a minimum temperature of approximately 20°C, which occurs during warm long seasons. The ripening phase requires a lower temperature interval, 20°C to 10°C and is directly tied to sucrose content [4]. The crop life cycle can be divided into 4 distinct growth stages, Figure 2.1.

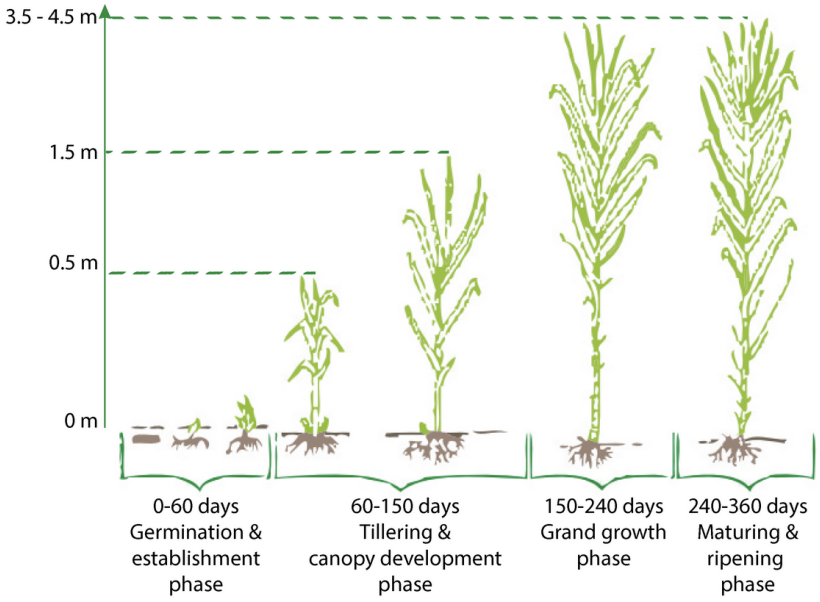

Figure 2.1: Sugar cane growth stages. Source: [5].

Higher yields depend on the length of the growing period, which is usually between 9 to 24 months, and on irrigation methods. The first crop (virgin) is usually followed by 2 to 4 ratoon crops, [4]. The ratoon practice is common for many crops as it reduces the length of the germination phase shortening the total crop length. However, to ensure high yields, after a given number of ratoon crops, up to a maximum of 8 in some cases, the crop is replanted anew. As for soil needs, the best soils are those that are more than 1 m deep and well-aerated and with a pH in the range of 5 to 8.5, with the row spacing usually between 1.1 and 1.4 m [4].

While sugar cane exploration is mostly aimed at raw sugar production, it is also cultivated for other purposes such as biofuel production. In 2018, 26 million hectares of sugar cane were cultivated worldwide with an estimated production of 1.91 billion tonnes. It is the most cultivated crop by quantity in the world [FAO].

2.2 Exploration in Mozambique

In 1908, the commercial sugar cane sector in Mozambique begun with the establishment of sugar cane estates and mills in the Zambezi and Buzi Valleys and, 6 years later, it was followed by the Xinavane plantation on the banks of the Incomati river. In the years preceding Mozambique's independence, the outflow of knowledge and skills associated with the loss of the staff, mainly Portuguese, led the production from estates and mills to sharply decrease. Moreover, the ensuing civil war (1977-1992) had detrimental effects on the sugar cane industry, leading most mills to cease their activity, Figure 2.2.

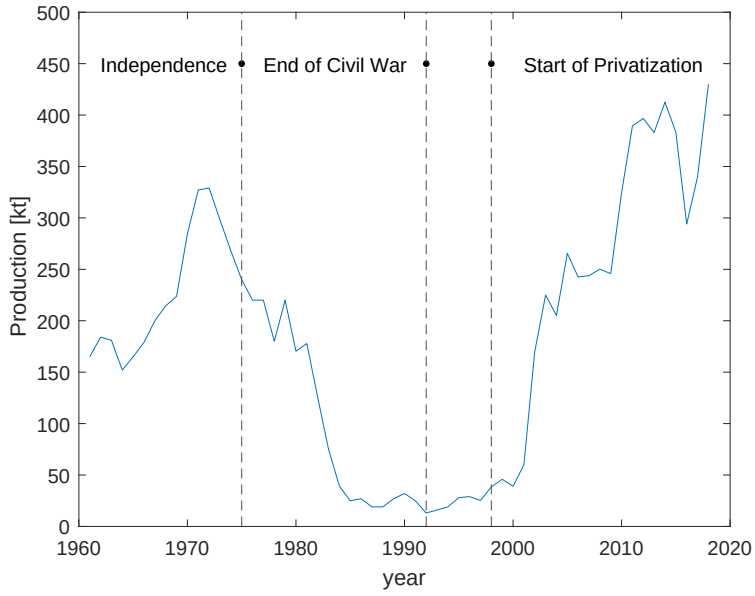

Figure 2.2: Sugar cane production in Mozambique (1961-2018) [source: FAOSTAT]

By 1992, at the end of the civil war, the Mozambican government focused on the rehabilitation of the sugar cane industry, and the results were nothing more than expected given the excellent agricultural conditions for cane production and the abundance of labour in rural areas. The sugar cane activity in Mozambique has seen major increases in output during the past few years, jumping the production from 240,000 tons in 2007 to nearly 450,000 tons in 2018 Figure 2.2.

Although the total cost of raw sugar is 260 € per ton (production costs + insurance), due to existing beneficial trade agreements, it is exported to the European market at 335 € per ton, and thus constitutes a profitable business for the Mozambican sugar industry.

In 2005, the Macuvulane I plantation was built as part of a three-phase expansion program (with over 15 sugar cane outgrower associations) implemented by the owners of AdX with the Government of Mozambique and the African Development Bank as funding agencies [6]. As far as funding modalities for this expansion program, the financing options fall between the concession of grants or loans. While the costs of the first and second phases are mainly tied to the establishment of the plantations, namely through land leveling, installation of the irrigation systems, training of the workforce and plantation of sugar cane, the third phase is financed through a loan, whereby smallholder associations are obliged to repay the costs of the first phases. In the case of Macuvulane I, the expansion project seems to be the result of a development strategy by the Mozambican government, because the first two phases did not incur costs to either the smallholders or the company, rather, they were gifted by the government [6].

The geographical location of Mozambique makes it extremely favorable for sugar cane exploration. According to a MAFAP report dated from 2013 [7], between 2005 and 2010 sugar cane accounted, on average, to 20% of the total agriculture exports of Mozambique. In 2010, production represented nearly 3.84% of the total cultivated area of the country, being dominated by four commercial industries located in the provinces of Maputo and Sofala. As mentioned, the lucrative activity benefits from preferential trade agreements with the EU. In a market structure such as this, the monopsony created by the demand and the oligopoly created by the supply act to discourage local farmers [7]. In fact, the report cites that policy decisions and the EU trade agreement have no meaningful impact for local sugar cane farmers. Moreover, the lack of strong farmer associations results in an ”unbalanced bargaining power” between farmers and sugar cane millers.

Another drawback that impacts the profitability of these associations is tied to the significant costs that pumping water for irrigation represent, raising further obstacles that thwart opportunities at development. An additional source of concern related to intensive agriculture is the pressure this activity exerts on local ecology when performed in a non environmentally sustainable way. Magude is traversed by the Incomati river, whose delta is already under great strain, with the extension of upstream irrigation for sugar cane cited as posing significant problems in the delta downstream [2].

Chapter 3

Case Study: Macuvulane I

Macuvalane I [1] is a sugar cane plantation built in 2005, as a SSIP, located in the district of Magude, province of Maputo, at coordinates (-25.028 S, 32.652 E) in Mozambique. The layout of the plantation is presented in Figure 3.1.

Figure 3.1: Macuvulane I plantation layout.

The plantation is divided in blocks with block usage and respective area given in Table 3.1. A total of fourteen blocks are used for sugar cane exploration, whereas four of the remainder, while marked as unexplored (N.E.), are actually used for subsistence agriculture, as inferred from Google Earth.

[1] PT: Macuvulana I

The last block is reserved as a nursery for when the need arises to replant a new crop [2].It should be noted that the command area for irrigation mentioned in the infield specifications, 187.9 ha is slightly decreased, in relation to the total area reported of 194.24 ha as the area correspondent to the access roads between blocks is not accounted for.

Table 3.1: Macuvulane I block usage and area.

Sugar Cane				Other	
Block	Area [ha]	Block	Area [ha]	Block	Area [ha]
1	6.85	8	19.82	N.E.	0.68
2	15.54	9	19.77	N.E.	0.68
3	20.31	10	11.86	N.E.	0.51
4	10.67	11	17.40	N.E.	0.83
5	3.67	12	19.36	Nurseries	1.83
6	10.69	13	7.74		
7	19.38	14	11.18		
Total	–	–	194.24	–	4.53

3.1 Climate Characterization

Mozambique's climate is mostly tropical humid with two distinct seasons, a humid season (summer) and a dry season (winter). The humid season is typically warm and rainy starting in October and lasting till March, whereas the dry season starts in April, ends in September and is usually colder and less rainy [8]. Annual mean precipitation is around 1000 mm, and fluctuates greatly from the coast to interior regions and from north to south [8].

Magude is located in the south interior region of the country and falls within the boundary of two distinct climate groups on the Köppen-Geiger classification, BSh to the west and Aw to the east, Figure 3.2.

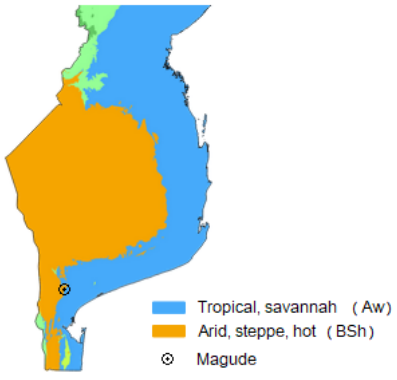

Figure 3.2: Köppen-Geiger classification map for south of Mozambique. (Adapted from Beck et al.)

[2]See ahead the discussion on the difference between virgin and ratoon sugar cane.

3.1.1 Precipitation

As far as accurate and complete precipitation records for the region in question, the data available [3] is that of two stations, Trigo de Morais (TM) and São Martinho (SM), at coordinates (25.17 S, 33.15 E) and (24.32 S, 33.00 E), respectively, for the year of 1987 [9], Table 3.2. Each of these stations is located roughly 60 km from Magude, Figure 3.3.

Table 3.2: Monthly precipitation recorded in two different stations near Magude, 1987.

Month	Jan	Feb	Mar	Apr	May	Jun	Jul	Aug	Sept	Oct	Nov	Dec
P(TM) [mm]	109.2	139.7	65.8	42.1	20.2	14.8	10.0	13.4	17.4	37.1	66.4	87.0
P(SM) [mm]	86.2	138.9	150.4	132.1	75.8	88.6	39.2	47.0	44.4	97.6	85.0	133.0

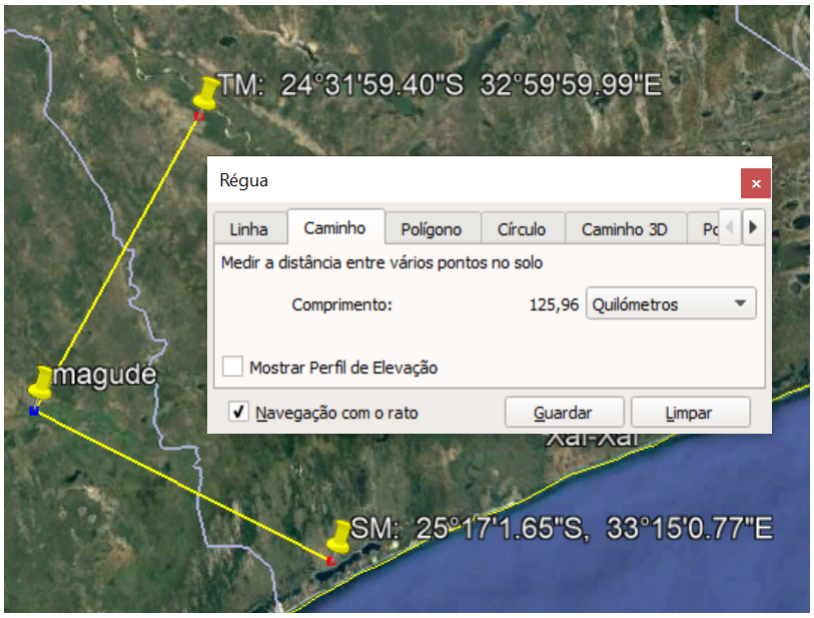

Figure 3.3: Location of TM and SM stations in relation to Magude.

Climate data for this region is hard to find and since the precipitation series of table 3.2 are not recent and only refer to one year, additional sources were consulted, Weather Atlas (WA) [10] and Climate Data (CD) [11]. However, the accuracy of the data from these online sources cannot be verified in regard to exact location and time span for which the measurements were taken.

Table 3.3: Monthly average precipitation for Maputo (unknown period).

Month	Jan	Feb	Mar	Apr	May	Jun	Jul	Aug	Sept	Oct	Nov	Dec
P(WA) [mm]	171.1	130.5	105.6	56.5	31.9	17.6	19.6	15.0	44.4	54.7	81.7	85.0
P(CD) [mm]	160.0	132.0	91.0	55.0	28.0	17.0	19.0	15.0	38.0	63.0	75.0	88.0

[3] Station E-43 in Magude is equiped to measure precipitation but records are only available for the wet season.

Reportedly, these series refer to Maputo, located 100 km to the south of Magude, and are presumably monthly averages of a larger but unknown period of years, Table 3.3.

In order to identify precipitation trends, these four series, however not akin in origin, were plotted in the same graph as depicted in Figure 3.4.

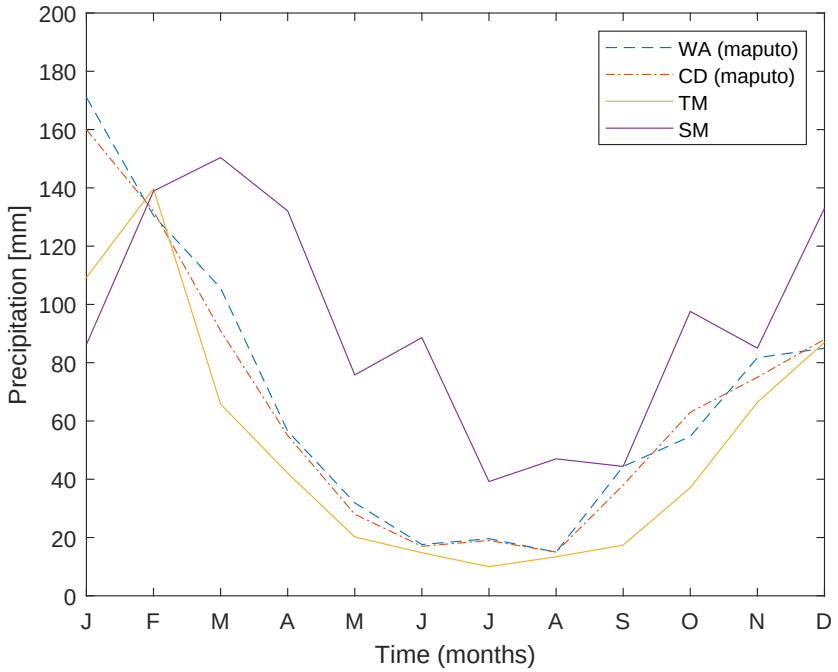

Figure 3.4: Precipitation series - 4 distinct sources.

The data from SM station was discarded because its time series does not conform with the observable trend. This is not hard to understand since this station is located at the coast, with a distinct Köppen-Geiger group (Aw), and therefore no longer in the boundary of the two previous discussed groups. Now, even considering that two of the sets are actual measurements from 1987 and the other two are averages for an unknown period, since the remaining three data sets are reasonably in accordance to each other, these were averaged to yield the results of Table 3.4.

Table 3.4: Estimated monthly average precipitation in the region.

Month	Jan	Feb	Mar	Apr	May	Jun	Jul	Aug	Sept	Oct	Nov	Dec
P [mm]	146.8	134.1	87.5	51.2	26.7	16.5	16.2	14.5	33.3	51.6	74.4	86.7

In the absence of recent actual records for a reasonable period of time, this composite series, from old data taken at a nearby station and two online sources is assumed to portrait precipitation patterns in Magude.

From Figure 3.5, it is immediate to notice that the months with higher mean precipitation values occur during the summer (south hemisphere).

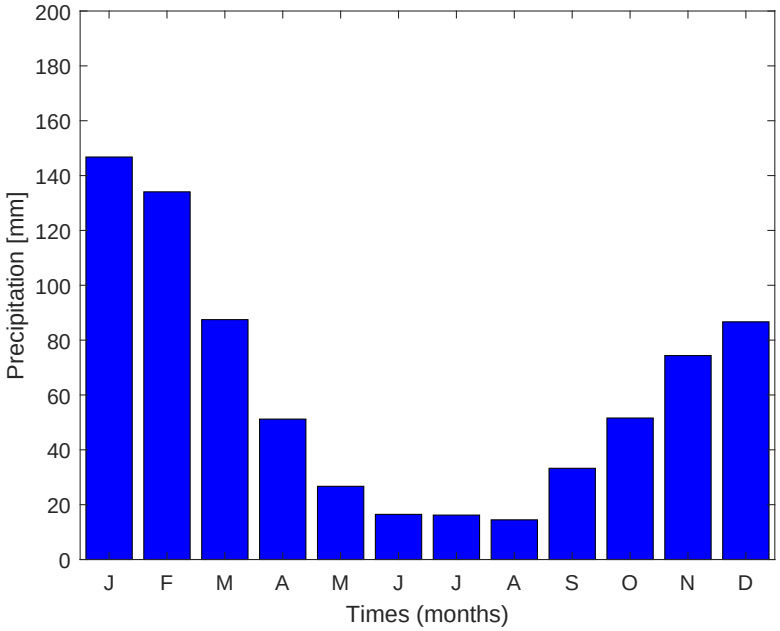

Figure 3.5: Estimated monthly average precipitation in Magude.

Adding the estimated monthly averages of Table 3.4 results in an annual mean precipitation for Magude of 739.23 mm. Comparing this value with the precipitation map of Figure 3.6, it is possible to conclude that the precipitation data used is accurate, since the mean of the three monthly average precipitation series resulted in a mean annual precipitation value that falls within the interval of expected annual precipitation in the region (650-750) mm.

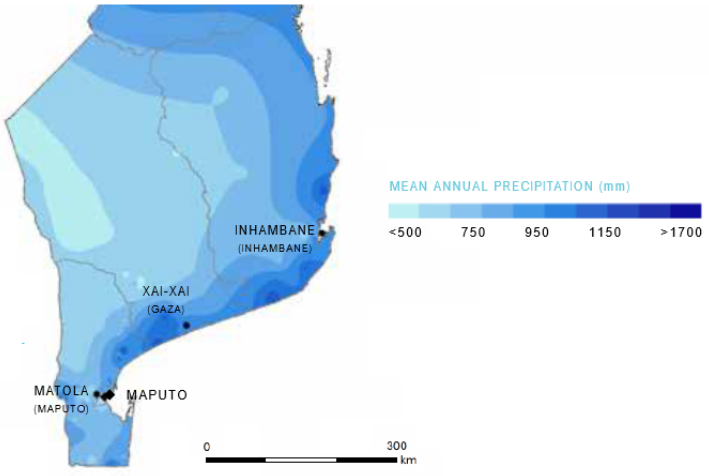

Figure 3.6: Precipitation map for south Mozambique. Adapted from [12].

3.1.2 Temperature

Due to the absence of publicly available temperature records, it was necessary to resort to the EU PVG online tool [4], which allows for the consultation of several solar databases for the African continent. For the region of Magude, the hourly daily averages of air temperature by month were obtained from the PVGIS-SARAH database, Figure 3.7.

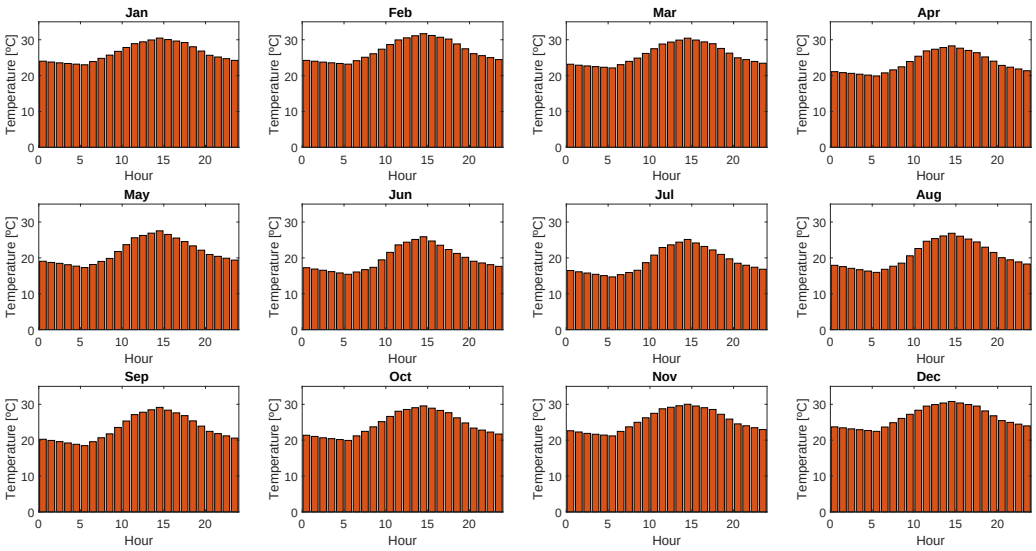

Figure 3.7: Daily average temperature by month.

3.2 Water Requirements

When planning an irrigation system, the first step lies in determining the crop water requirements. These will depend on the type of crop in question and, naturally, on some intricate relation with the local climate. Often, in more detailed studies, the type of soil is also taken into account but this will not be the case here.

The methodology adopted to determine the crop water requirements is that of guide 56 of FAO [13], where the reference evapotranspiration, ET_o [mm], which only incorporates climate parameters and is computed for a reference crop is then corrected with a crop coefficient K_c, that incorporates data about the crop, agricultural and irrigation practices, etc, to yield the desired crop evapotranspiration ET_c [mm]. With this value computed, some adjustments are performed and the final water requirements estimated.

A detailed explanation of the method used to determine both the ET_o and ET_c as well as the results obtained can be consulted in Appendix A.

[4] https://re.jrc.ec.europa.eu/pvg_tools/en/tools.html

3.2.1 Effective Precipitation

The USDA through its SCS provides a handbook, in which chapter 2 entitled 'Irrigation Water Requirements', [14] gives the basis for estimating the effective monthly precipitation.

The resulting equation for estimating effective precipitation is:

$$P_e = SF\left(0.70917 P_t^{0.82416} - 0.11556\right)\left(10^{0.02426\, ET_c}\right) \tag{3.1}$$

where

- P_e : average monthly effective precipitation [in]
- P_t : monthly mean precipitation [in]
- ET_c : average monthly crop evapotranspiration [in]
- SF : soil water storage factor

with the soil water storage factor defined as

$$SF = (0.531747 + 0.295164\, D - 0.057697\, D^2 + 0.003804\, D^3) \tag{3.2}$$

The value for D (usable water soil storage) is unknown but the document suggests a value of 50.8 mm (2 in), which is a typical value considering [15], resulting in SF = 0.9217.

Note: The quantities D, P_t, ET_c and P_e have their units expressed in inches. After computing P_e, the conversion to mm is performed.

3.2.2 Net Irrigation Requirements

Finally, the net irrigation requirements, I_N [mm] are computed from equation 3.3

$$I_N = ET_c - P_e \tag{3.3}$$

3.2.3 Gross Irrigation Requirements

In order to determine the monthly average gross irrigation requirements, I_G [mm] , it is necessary to take the net irrigation requirements I_N [mm] and apply a uniformity coefficient K_u, which accounts for the fact that water is not distributed evenly, here assumed to be $K_u = 0.9$, considering [16], after which the resulting value is increased by 10% to account for losses and other water usage, equation 3.4.

$$I_G = 1.1 \frac{I_N}{K_u} \tag{3.4}$$

3.2.4 Normalized Results

The water requirements, for both types of agriculture practice, virgin and ratoon, assuming that plantation occurs in June, with all the assumptions previously discussed and detailed in Appendix A, are presented in Tables 3.5 and 3.6, respectively.

Table 3.5: Water requirements for virgin sugar cane with plantation starting in June.

Month	ET_o[mm]	K_c	ET_c[mm]	P_t [mm]	P_e [mm]	I_N [mm]	I_G [mm]
June	77.2383	0.7250	55.9977	16.4667	10.0782	45.9195	56.1238
July	85.2581	0.7500	63.9436	16.2000	10.0772	53.8664	65.8367
August	107.8324	0.9375	101.0929	14.4667	9.6604	91.4324	111.7508
September	129.7011	1.1500	149.1562	33.2667	25.0325	124.1237	151.7068
October	145.5976	1.2500	181.9970	51.6000	40.3954	141.6016	173.0686
November	144.5500	1.2500	180.6875	74.3667	55.8526	124.8349	152.5759
December	150.2842	1.2500	187.8553	86.6667	64.9185	122.9368	150.2561
January	137.2697	1.2500	171.5871	146.7667	98.8343	72.7529	88.9202
February	126.0869	1.2500	157.6087	134.0667	88.6782	68.9305	84.2484
March	117.6411	1.2500	147.0514	87.4667	59.8262	87.2252	106.6086
April	90.8942	1.2500	113.6178	51.2000	34.5110	79.1068	96.6861
May	86.0830	1.2033	103.5837	26.7000	18.3285	85.2551	104.2007
June	77.2383	1.0917	84.3210	16.4667	10.7260	73.5950	89.9495
July	85.2581	1.0000	85.2581	16.2000	10.5608	74.6973	91.2967
August	107.8324	0.9000	97.0492	14.4667	9.5749	87.4743	106.9130
September	99.4375	0.8000	79.5500	33.2667	21.4794	58.0706	70.9752
Total	1768.2	–	1960.4	819.6	568.5	1391.8	1701.1

Table 3.6: Water requirements for ratoon sugar cane with plantation starting in June.

Month	ET_o[mm]	K_c	ET_c[mm]	P_t [mm]	P_e [mm]	I_N [mm]	I_G [mm]
June	77.2383	0.7250	55.9977	16.4667	10.0782	45.9195	56.1238
July	85.2581	0.8750	74.6008	16.2000	10.3162	64.2847	78.5702
August	107.8324	1.1758	126.7893	14.4667	10.2221	116.5672	142.4711
September	129.7011	1.2500	162.1263	33.2667	25.7568	136.3695	166.6738
October	145.5976	1.2500	181.9970	51.6000	40.3954	141.6016	173.0686
November	144.5500	1.2500	180.6875	74.3667	55.8526	124.8349	152.5759
December	150.2842	1.2500	187.8553	86.6667	64.9185	122.9368	150.2561
January	137.2697	1.2500	171.5871	146.7667	98.8343	72.7529	88.9202
February	126.0869	1.2143	153.1074	134.0667	87.8046	65.3027	79.8144
March	117.6411	0.9792	115.1942	87.4667	55.7781	59.4161	72.6196
April	48.4769	0.8125	39.3875	51.2000	29.3129	10.0746	12.3134
Total	1269.9	–	1449.3	712.5	489.3	960.1	1173.4

As the total length of the crop varies greatly according to the agriculture practice, 480 days for virgin sugar cane and 320 days for ratoon sugar cane, the determined gross water requirements are normalized to a year to establish a basis for comparison, Table 3.7.

Table 3.7: Normalization of the water requirements for both types of sugar cane practice.

Practice	Crop duration [days]	I_G [mm/(crop cycle)]	I_G [mm/year]
Virgin Cane	480	1701.1	1293.5
Ratoon Cane	320	1173.4	1338.4

Without information relative to infield practices, specifically, how many years go by before replantation of the crop occurs, i.e., how many years is ratoon practiced until a virgin crop is planted, it would be convenient for the work ahead, for example in determining energy needs associated with irrigation, to consider an annual crop with fixed length, with an annual mean water requirement given by the average normalized gross irrigation requirements, i.e, 1315.9 mm/year. However, it is best to work with monthly values to better characterize the impact of climate in the system.

As was discussed in Appendix A, several factors influence water requirements, but Figure 3.8 shows how irrigation accompanies the change in precipitation for the duration of each crop, and in line with what one may have expected, higher levels of precipitation generally imply a decrease in water requirements, and although more abundant precipitation occurs during the summer when temperature is also higher leading to increased evapotranspiration, the crop has entered its end stage requiring less water.

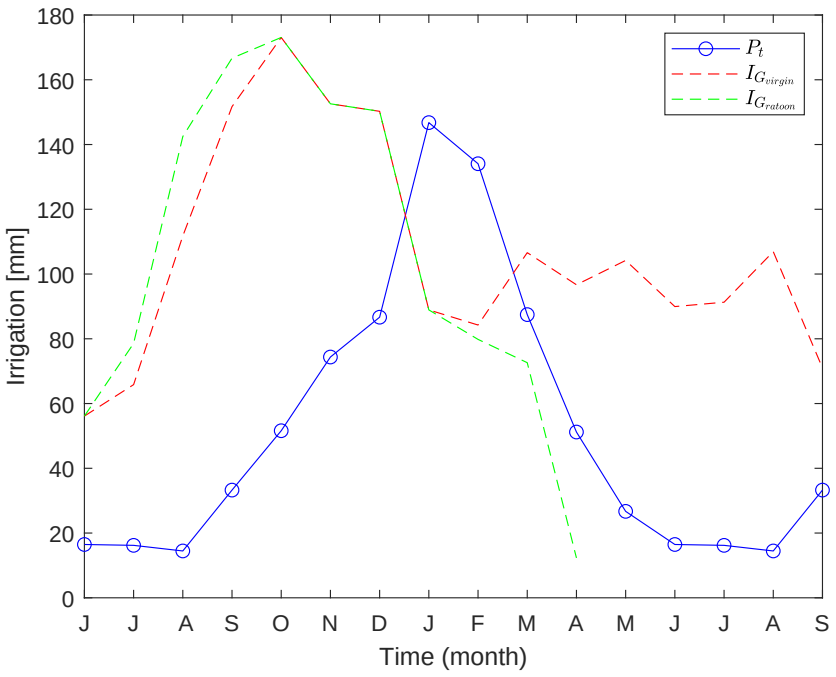

Figure 3.8: Gross irrigation requirements vs precipitation for the duration of the crop cycles.

3.3 Irrigation System

The irrigation system is composed by pumps, motors, pipes, valves, draglines and sprinklers. A schematic of the hydraulic network is presented in Figure 3.9.

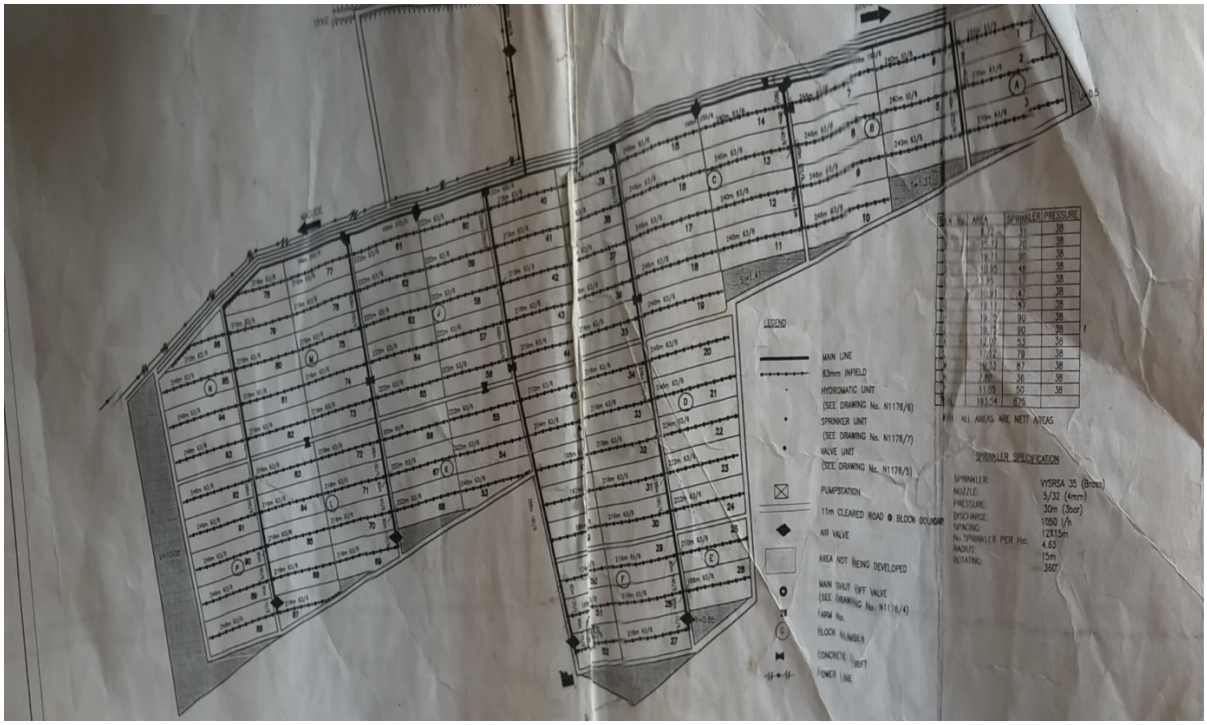

Figure 3.9: Macuvulane I hydraulic network (2005).

The pumping station is located approximately 300 m north of the plantation on the right bank of the Incomati river and is equipped with 3 groups of centrifugal pumps and respective induction motors that feed the same pipeline, Figure 3.10.

Figure 3.10: Installed pump and motor units.

The design duty of the pumps, Q_p and the nominal power of the motors, P are summarized in Table 3.8.

Table 3.8: Characteristics of installed units.

Unit	Q_p [l/s]	P [kW]
1	97.2	90
2	97.2	90
3	207.0	132
Total	401.4	312

Due to unknown issues, the larger group is disabled and it is not known what measures are being taken, if any, to correct the resultant water deficiency, because as it is discussed ahead, the two smaller pumps cannot guarantee the delivery of the required water duty in critical months.

Table 3.9 shows the distribution of sprinkler units as well as the command area for irrigation per block.

Table 3.9: Sprinkler distribution per block.

Block	Area [ha]	Sprinklers	Block	Area [ha]	Sprinklers
1	6.85	31	8	19.82	90
2	15.54	70	9	19.77	90
3	20.31	90	10	11.86	53
4	10.67	48	11	17.40	79
5	3.67	17	12	19.36	87
6	10.69	47	13	7.74	36
7	19.38	87	14	11.18	50
Total	–	–	–	194.24	875

Table 3.10: Infield specifications

Cycle Length (days)	6
Design no. Sprinklers/ha	2.57
Default Stand Time (hrs)	12
Sprinkler Gross Application (mm/hr)	4.1
Sprinkler Net Application (mm/hr)	3.3
Sprinkler Operating Pressure (kPa)	330
Pump Design Operating Pressure (kPa)	600
Gross Application (mm/cycle)	49
Net Application (mm/cycle)	39
Net Irrigation Requirement (mm/year)	1366
Target Cycles (no. Per year)	35

According to information obtained on site, and presented in Table 3.10, a given sprinkler is able to apply 49 mm/cycle (gross application), and since each cycle lasts for 6 days, with a default stand time of 12 hours (per day), the design duty of each sprinkler is 0.6806 mm/hr for a operating pressure of 330 kPa. From Figure 3.9, one knows each sprinkler covers an area with radius of 15 m, so rewriting the design duty of the sprinklers results in a value of 481 l/hr.

However, Figure 3.9 also tells us that each sprinkler has a discharge of 1050 l/hr for an operating pressure of 300 kPa (3 bar). The slight change in pressure cannot possibly explain this discrepancy, so one is led to believe that some error exists somewhere in the infield specifications.

Furthermore, from Table 3.10, one year of irrigation translates into 2520 hours (35 cyles, each with the duration of 6 days with 12 hours of irrigation per day), and considering the total command area, a net irrigation of 1366 mm/year means 1.0185×10^6 l/hr, leading to a required number of 970 sprinklers if each sprinkler discharges 1050 l/h. Now, since the total number of sprinklers in the plantation is 875, Table 3.9, they have to be rotated somehow to cover the entire field. Moreover, given that the pumps are able to output 401.4 l/s, they would be able to feed all of the sprinklers simultaneously (in terms of flow alone not considering pressure constraints). However, in the scenario where the larger pump is not working, only a fraction of sprinklers can be activated simultaneously. Even if this was not the case, given that irrigation of each plot is performed by a given smallholder or group of them, it is likely that a rotation scheme of some sort, connected to a cycle length of 6 days (presumably from Monday to Saturday), concerning sprinkler usage is in place. Since this is not known, no particular irrigation scheme will be considered.

Similarly, doubt remains on the actual duration of one cycle of irrigation, as it is defined in Table 3.10, since a sprinkler net application of 3.3 mm/hr, over a period of 12 hours results in 39 mm. In the same table, the units for this value come in mm/cycle, which implies a duration of 12 hours for each cycle (default stand time) instead of the length of the cycle (6 days). Either way, if this new value for the duration of the cycle is assumed to be correct, the sprinkler discharge becomes 2886 l/h, which seems impossible given that the sprinkler is only supposed to be able to apply 1050 l/h, as corroborated by a search for the model of the sprinkler, VYSRSA 35 (Brass), 4 mm. Adding to the mystery, Table 3.10 reports a sprinkler density of 2.57 sp/ha, but since by design from Figure 3.1 there are 875 sprinklers, and the area of the plantation is known, A = 187.9 ha, this value ought to be 4.66 sp/ha. Whatever the case, the pumps are unable to feed the entirety of sprinklers and a manual rotation for a work shift of 12 hours is assumed.

In the next chapter, the prospect of installing a micro-hydro power plant to achieve self-supply is explored, but one can anticipate for now that, as opposed to a PV powered irrigation system, highly dependent on sunshine intensity and duration, an automatic irrigation system, taking full advantage of continuous hydropower generation would be able to work, in principle, on a 24 hour cycle. For this purpose, the plantation could be divided into several areas, each corresponding to a 12 hour shift.

3.3.1 Water Duty

In previous sections the water requirements were computed based on the FAO 56 guide approach. However, a value for the net requirements is given in table 3.10 of 1366 mm/year, which is derived from:

$$\text{Net Application: } 39 \text{ mm/cycle}$$
$$\text{Target cycles per year: } 35$$
$$\text{Net Irrigation Req.: } 39 \times 35 = 1366 \text{ mm/year}$$

Comparing this value with that obtained in the normalized water requirement results (1360 mm/year), might strike one as odd, as the gross irrigation, judging by the application of some uniformity coefficient (as it was done), should not coincide with the original design net irrigation requirements. Some possible causes for this discrepancy are discussed in the results section.

Still, what is important is that, independent of the validity of the assumptions made (which can be revised provided more information exists in the future), the lengthy computations to obtain the water requirements, as described in Appendix A, now allow for the estimation of the monthly water requirements, implying that a more efficient irrigation system with adjustable cycle duration and intervals can be designed, instead of just suspending irrigation for two weeks[5] when precipitation in the region reaches 70 mm.

And perhaps, more importantly, a starting point for estimating the monthly energy consumption now exists, something that would be immediate with access to energy bills. Lastly, a new micro-hydro system can now be designed, if so wished, to cover the demand of specific months, for example months when energy demand peaks, designing in essence a self-supply system, assuming that such a thing is possible at all.

3.3.2 Water Scheduling

Doubts remain as to the irrigation scheme adopted in the plantation, specifically which groups of blocks have their lines activated at the same time and how are the sprinklers rotated between them. However, from Table 3.10, for the original designed system (3 pumps), since the cycle duration lasts 6 days (Monday to Saturday), it can be assumed that a given association of blocks comprising 1/6 of the total plantation area, A' = 31.3 ha is irrigated each day. This would depend both on the configuration of the hydraulic network, location of valves and lines in relation to the blocks and their area, and so on.

[5] Information from infield.

If this is indeed true, then the design duty of the pumps Q_{tot} [m^3/s] would be constrained by the number of cycles per year (35) required for each group of blocks with area A′ and the water duty of the crop, assumed in the original system to be $I_N = 1366$ mm/year. Then, the rationale behind the pumps design duty, Q_{tot} is understood:

$$Q_{tot} = \frac{I_N \times \frac{A}{6} \times 10^4}{35 \times 12 \times 3600} = 283\,l/s \tag{3.5}$$

Now, the water duty in terms of the net irrigation requirements does not take into account the discussion about the uniformity coefficient associated with irrigation by sprinklers, but even if this was ignored, it is highly likely that a margin was added to this value, considering that choosing a group of pumps to be associated such that the design duty would match this value would prove nearly impossible. And on top of that, a higher value of flow may be advantageous, given not only the desired operating point that must ensure stability and efficiency, considering the curve of the installation, but also, the system was probably oversized since with the pumps installed in parallel (see next section), the loss of one unit would not affect substantially the required Q_{tot}. This being said, it is not hard to imagine that the designer went from $Q_{tot} = 283\,l/s$ to $Q_{tot} = 401\,l/s$.

3.3.3 Pump Operation

Pumps are mechanical machines that move certain fluids by converting electric energy into hydraulic energy. In the present case, centrifugal pumps are installed and attached to induction motors which provide the required rotational energy to the fluid.

The hydraulic power P [W] of a turbomachine is the power available at the shaft of that machine, in the case of a pump, the power it needs to absorb, which is dependent on its imposed design flow Q [m^3/s], the head pressure it needs to overcome H [m], the fluid specific weight, γ [N/m^3], (in this case water) and the overall efficiency, η, as given by equation 3.6

$$P = \frac{\gamma\, Q\, H}{\eta} \tag{3.6}$$

3.3.3.1 H-Q Curves

The characteristic curves of the pumps could not be obtained from local inspection, but from Figure 3.10, it is possible to gather that the pumps are connected in parallel. In an arrangement such as this, the design of the system is aimed at ensuring the required total value of water duty, in this case $Q_{\text{tot}} = 2Q_{1/2} + Q_3$ where the sub indexes 1/2 and 3 denote the smaller and larger pumps, respectively, when one or two pumps are not enough to ensure Q_{tot}.

Figure 3.11 is intended to show the approximate behavior of the pumps and system, bearing in mind that the curves do not represent the installed pumps, as they could not be measured.

This type of curves, known as steadily decaying, are the most encountered type, as they lead to very stable systems. As for the system curve, generally the head increases with the flow in a quadratic form, as the pipe circuit offers increased resistance to an increased demand in Q.

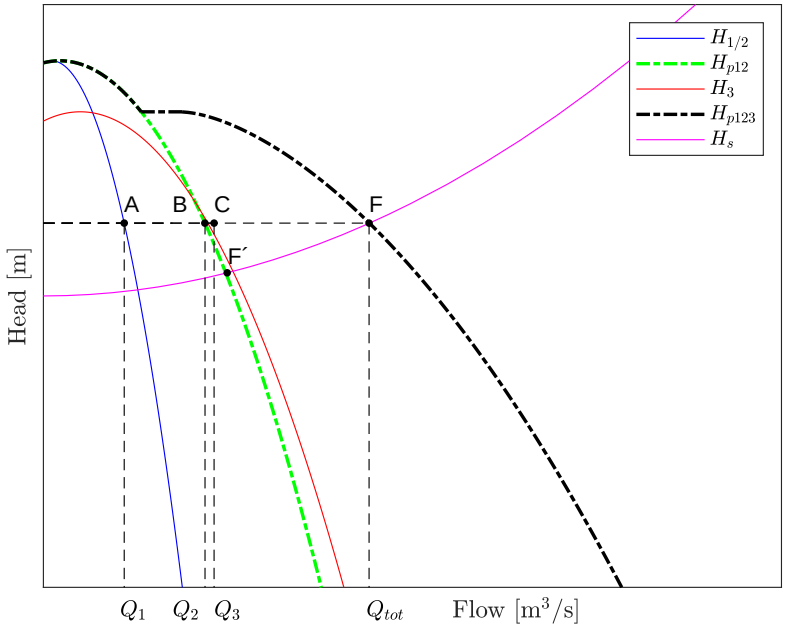

Figure 3.11: Example of parallel association of pumps.

In general, the curve that describes the change in head H [m] of the pump as a function of flow, Q [m^3/s] can be modeled by a quadratic function given by equation 3.7.

$$H = A + B\,Q - C\,Q^2 \tag{3.7}$$

Then, supposing that the smaller pumps are each represented by $H_{1/2}$ (blue), their parallel association is given by H_{p12} (green), where the parallel association of n equal pumps is obtained by rewriting equation 3.7 in equation 3.8.

$$H_p = A + \frac{B}{n}\,Q - \frac{C}{n^2}\,Q^2 \tag{3.8}$$

The larger pump, which is knocked out, could be represented by H_3 (red), as its design flow Q_3 is approximately $Q_2 = Q_1 + Q_1$, Table 3.8, i.e, its curve should be close to H_{p12} (green). By design, the 3 pumps work in parallel, H_{p123} (dashed black) and the system would be represented by something like H_s (pink) given by equation 3.9.

$$H_s = A + B\,Q^2 \tag{3.9}$$

Thus, the operating point would be defined by F, and while the real shape of the curves is unknown, Table 3.8 gives the design duty of the pumps, here expressed in cubic meters per second, and since from Table 3.10 the design operating pressure is also known, P = 600 kPa and equivalent to a water column with a pressure head H = 61.19 m, the points A (0.097, 61,19), C (0.207, 61,19) and F (0.401,61,19), are known.

The situation where the larger pump (3) is knocked out sees the operating point move to F'. One immediate advantage of the parallel association of the 3 pumps is that the total flow can be adjusted by connecting or disconnecting units from operation without compromising the overall system, as the head can be maintained by the remaining units, since $H_{\text{tot}} = H_1 = H_2 = H_3$. However, since the configuration of the system can change, as a result of actuating the several valves present throughout the plantation, the head will change according to the system characteristics [17].

One then sees how a parallel configuration allows for a greater flexibility, and redundancy in order to tackle hardware failure (case in point), allowing the system to maintain its operation with just 2 units. However, in the next section, the prospect of disconnecting one unit (or having it fail) is revisited in terms of efficiency, but without the H-Q curves of both the system and the association of pumps it is not possible to determine the new operating point. In theory, the 3 pumps were chosen so that the operating point F also coincides with the pump's best efficient point (BEP) but since the efficiency curve is also unknown, the only thing that can be said is that the new operating point F' implies a decrease in efficiency. [17].

3.3.3.2 Required Work Hours

Considering the command area, A = 187.9 ha, and the design duty of the pumps Q_p^i [l/s], where i is the number of working pumps, the water duty per hectare, W_i [l s^{-1} ha^{-1}] is given by equation 3.10:

$$\mathsf{W}_i = \frac{Q_p^i}{\mathsf{A}},\ i = \{2, 3\} \tag{3.10}$$

Alternatively, the water duty can be expressed in m^3 hr^{-1} ha^{-1}, equation 3.11,

$$\mathsf{W}_i^{'} = \mathsf{W}_i \times \frac{3600}{10^3},\ i = \{2, 3\} \tag{3.11}$$

Now, considering that the original net irrigation requirements, $\mathsf{I}_N^0 = 1366$ mm/year can also be expressed as $\mathsf{I}_N^{0'} = 13660$ m^3 ha^{-1} year^{-1}, the estimated annual required work hours of the pumps, T_i^0 [hr], are given by equation 3.12.

$$T_i^0 = \frac{\mathsf{I}_N^{0'}}{W_i^{'}},\ i = \{2, 3\} \tag{3.12}$$

By design, all 3 units work simultaneously, but accounting for the lost unit, the water duty and the estimated work hours of the pumps, as defined by equations 3.10, 3.11 and 3.12 are given in Table 3.11.

Table 3.11: Water duty and work hours for different pump arrangements.

Pumps	Q_p^i [l/s]	W_i [l s^{-1} ha^{-1}]	$\mathsf{W}_i^{'}$ [m^3 hr^{-1} ha^{-1}]	T_i^0 [hr]
2	194.4	1.0346	3.7245	3667.6
3	401.4	2.1300	7.6680	1776.8

Also, as it is costume for these sort of projects, the system is oversized in a way that only for critical months, when precipitation values decline and energy demand increases, all pumps work simultaneously. Thus, for most of the year, the 2 smaller pumps suffice to meet the water requirements, whereas in a small number of months, all of them are required. Table 3.12 presents the work hours for different pump arrangements $\mathsf{T}_i^{v/r}$ [hr], for the two types of agriculture practices and for the computed gross irrigation requirements $\mathsf{I}_G^{v/r}$ [mm], as defined by equation 3.13.

$$\mathsf{T}_i{}^{v/r} = 10 \times \frac{\mathsf{I}_G^{v/r}}{\mathsf{W}_i^{'}},\ i = \{2, 3\} \tag{3.13}$$

Table 3.12: Required pump work hours for both types of sugar cane.

	Virgin Cane				Ratoon Cane			
Month	I_G^v [mm]	T_1 [hr]	T_2 [hr]	T_3 [hr]	I_G^r [mm]	T_1 [hr]	T_2 [hr]	T_3 [hr]
June	56.1238	301	151	73	56.1238	301	151	73
July	65.8367	354	177	86	78.5702	422	211	102
August	111.7508	600	300	145	142.4711	765	383	185
September	151.7068	815	407	197	166.6738	895	448	217
October	173.0686	929	465	225	173.0686	929	465	225
November	152.5759	819	410	198	152.5759	819	410	198
December	150.2561	807	403	195	150.2561	807	403	195
January	88.9202	478	239	116	88.9202	478	239	116
February	84.2484	452	226	110	79.8144	429	214	104
March	106.6086	572	286	139	72.6196	390	195	94
April	96.6861	519	260	126	12.3134	66	33	16
May	104.2007	560	280	135	–	–	–	–
June	89.9495	483	242	116	–	–	–	–
July	91.2967	490	245	119	–	–	–	–
August	106.9130	574	287	139	–	–	–	–
September	70.9752	381	191	92	–	–	–	–
Total	1701.1	9135	4567	2212	1173.4	6301	3151	1526

Thus, if as suggested by the data from the infield specifications, the duration of a cycle or day of work is equal to 12 hours, it can be seen that, for some months, in order to ensure the required gross irrigation $\mathsf{I}_G^{v/r}$ [mm], 1 or 2 pumps are not enough (1 month of 30 days with workable 12 hour days has 360 hours).

3.3.3.3 Required Units

Since the two smaller pumps are equal, one of them working twice as long is exactly the same as two working for half as long, i.e., $T_1 \simeq 2T_2$, Table 3.12. This is not exactly true, as a change in flow will affect the efficiency of the system, but the H-Q curves are unknown. The choice then lies on how to design the irrigation system, based on whether or not irrigation can be made automated, and how are the tasks assigned to the workers. The solution that can guarantee adequate irrigation for shifts of 12 hours a day is that of Table 3.13.

Table 3.13: Required number of pumps to deliver the estimated monthly gross irrigation.

	Virgin Cane			Ratoon Cane		
Month	#P	#P	#P	#P	#P	#P
June	1	2	3	1	2	3
July	1	2	3	-	2	3
August	-	2	3	-	-	3
September	-	-	3	-	-	3
October	-	-	3	-	-	3
November	-	-	3	-	-	3
December	-	-	3	-	-	3
January	-	2	3	-	2	3
February	-	2	3	-	2	3
March	-	2	3	-	2	3
April	-	2	3	1	2	3
May	-	2	3	–	–	–
June	-	2	3	–	–	–
July	-	2	3	–	–	–
August	-	2	3	–	–	–
September	-	2	3	–	–	–

While it is known that the larger pump is disabled, and that the irrigation system can get by with only 2 pumps working for some months, this has a deleterious effect on the annual costs, because the pump in question made it so that the arrangement with the 3 working delivered a higher flow per unity of power.

3.4 Energy Consumption

In principle, the energy requirements incurring from irrigation needs could be accurately estimated from energy bills, with averages performed for each month over a large period of years.

Since no energy bills were available, energy consumption had to be indirectly estimated from the installed capacity of the motors powering the pumps and the frequency of irrigation, which implies knowing the water requirements of the crop, and preferably, how they change on a given time interval (or step), in accordance to the climate. This was the main motivation behind the previous sections.

That being said, for the original system, the results of energy consumption, E_i^o [MWh] given by equation 3.14, are presented in Table 3.14.

$$\mathsf{E}_i^o = P_i \times \mathsf{T}_i^0,\ i = \{2, 3\} \tag{3.14}$$

Table 3.14: Energy consumption for different pump arrangements with original net requirements.

Pumps	P_i [kW]	T_i^0 [hr]	E_i^0 [MWh]
2	180	3667.6	660.17
3	312	1776.8	554.36

Considering Table 3.12, energy consumption results, given by equation 3.15 for both types of sugar cane agriculture practices are presented in Table 3.15.

$$E_i^{v/r} = P_i T_i^{v/r},\ i = \{2, 3\} \tag{3.15}$$

Table 3.15: Estimated monthly energy consumption for virgin and ratoon sugar cane.

	Virgin Cane		Ratoon Cane	
Month	E_2^v [MWh]	E_3^v [MWh]	E_2^r [MWh]	E_3^r [MWh]
June	27.12	22.77	27.12	22.77
July	31.82	26.71	37.97	31.88
August	54.01	45.34	68.85	57.80
September	73.32	61.55	80.55	67.62
October	83.65	70.21	83.64	70.21
November	73.74	61.89	73.74	61.89
December	72.62	60.96	72.62	60.96
January	42.97	36.07	42.87	36.07
February	40.72	34.18	38.57	32.38
March	51.52	43.25	35.09	29.46
April	46.73	39.23	5.95	4.99
May	50.36	42.27	–	–
June	43.47	36.49	–	–
July	44.12	37.04	–	–
August	51.67	43.37	–	–
September	34.30	28.79	–	–
Total	822.12	690.14	567.08	476.05

3.5 Energy Efficiency

As the load of the system may change, according to the number of pumps or sprinklers active at one time, so do P, Q and H, which means the efficiency is not constant. For this reason, the operating point of the system, is given by the interception in the (H,Q) plane of the pump characteristic curve H = H(Q) with the curve that expresses the height in elevation of the installation as a function of Q [18].

However, as discussed before, the H-Q curves and the efficiency curve of the pumps are unknown. Assuming the system is working at the design duty point F, Figure 3.11, the combined efficiency of the unit (pump + motor) can be roughly evaluated solely from P and Q, equation 3.16.

$$\eta = \underbrace{\frac{\gamma}{H}}_{k} \frac{Q}{P} \tag{3.16}$$

Thus, if it can be assumed that both the fluid (hence γ), and the head of the installation H remain constant after the loss of the larger unit, that is, which is the same as saying that the system curve H_s in Figure 3.11 is horizontal and that point F moves to point B instead of F', the overall decrease in efficiency is given by equation 3.17.

$$\Delta\eta_{\,3\to 2} = \frac{\eta_3 - \eta_2}{\eta_3} = 1 - \frac{Q_2}{Q_3}\frac{P_3}{P_2} = 0.1597 \tag{3.17}$$

Alternatively, the impact on efficiency can be estimated by determining the relative decrease in energy consumption ΔE if the larger pump were to be repaired, equation 3.18.

$$\Delta E_{\,2\to 3} = \frac{E_2^o - E_3^o}{E_2^o} = \frac{660.17 - 554.36}{660.17} = 0.1603 \tag{3.18}$$

So, the failure of the larger pump has a deleterious effect on the annual costs, since it made it so that the arrangement with the 3 working delivered a higher value of flow per unity of power. This can be verified by comparing the efficiency of both arrangements. Referring to Table 3.10, a head (at the duty point) of P $= 600$ kPa can be converted to H $= 61.19$ meters head, and since the specific weight of water is $\gamma = \rho\, g = 9800\,\mathrm{N/m^3}$, the efficiency can be computed from equation 3.16.

$$\eta_2 = \frac{\gamma\, Q_2\, H}{P_2} = \frac{9800 \times 97.2 \times 10^{-3} \times 61.19}{90 \times 10^3} = 64.76\,\%$$
$$\eta_3 = \frac{\gamma\, Q_3\, H}{P_3} = \frac{9800 \times 401 \times 10^{-3} \times 61.19}{312 \times 10^3} = 77.07\,\%$$

With the larger pump knocked out, the remaining two need to work for a longer period to ensure the crop water requirements, and since these have a lower Q/P ratio, the energy expenditure increases if measures were put in place to compensate the loss of the larger pump. It is unknown how the association is dealing with the problem, although it is advisable to effectuate a repair.

3.6 Energy Costs

Since no consumption records are available, the estimation of energy costs can be performed assuming an agriculture tariff for monthly recorded consumption values exceeding 500 kWh, Table 3.16. In the following, a current exchange rate of R = 0.013 is assumed when converting Metical (MT) to Euro (EUR).

Table 3.16: Presumed energy tariff. [Source: EDM]

Variable Tariff V_t		Fixed Tariff F_t	
[Mt/kWh]	[€/kWh]	[Mt/month]	[€/month]
6.39	0.0831	257.97	3.3536

From the estimated energy consumption in the original scenario E_i^0 [MWh], Table 3.14, here converted to kWh, the estimated energy costs, C_i^0 [€] can be obtained by equation 3.19 and are presented in Table 3.17.

$$C_i^0 = R \times (V_t \times E_i^0 \times 10^3 + 12 \times F_t),\ i = \{2, 3\} \tag{3.19}$$

Table 3.17: Energy cost for different pump arrangements with original net requirements.

Pumps	P_i [kW]	E_i^0 [MWh]	C_i^0 [€]
2	180	660.17	54 881
3	312	554.36	46 091

If a distinction between crops is assumed and the results of Table 3.15 considered, the energy costs are computed from equation 3.20 and presented in Table 3.18.

$$C_i^{v/r} = R \times (V_t \times E_i^{v/r} \times 10^3 + n \times F_t),\ i = \{2, 3\} \tag{3.20}$$

where n is the duration of the crop cycle in months, 16 and 11 for virgin and ratoon cane practices, respectively.

Without access to the energy bills for validation this is merely an educated guess. The costs are being estimated based on the assumption that the tariff adhered to is that for ”low voltage agriculture”. However, from [3], since in 2011 there were only 55 affiliated agriculture consumers based on EDM reports, this is unlikely.

Table 3.18: Monthly energy costs for virgin and ratoon practices.

	Virgin Cane		Ratoon Cane	
Month	C_2^v [€]	C_3^v [€]	C_2^r [€]	C_3^r [€]
June	2306.8	1945.1	2290.0	1928.3
July	2696.8	2272.4	3191.2	2684.8
August	4540.0	3819.8	5756.6	4838.3
September	6144.1	5166.4	6728.2	5654.0
October	7001.7	5886.3	6984.9	5869.5
November	6179.0	5195.7	6162.2	5178.9
December	6085.9	5117.5	6069.1	5100.7
January	3623.5	3050.4	3606.7	3033.6
February	3435.9	2892.9	3241.1	2726.7
March	4333.6	3646.5	2952.3	2484.3
April	3935.2	3312.1	531.2	451.9
May	4236.9	3565.3	–	–
June	3664.8	3085.1	–	–
July	3718.9	3130.5	–	–
August	4345.8	3656.8	–	–
September	2903.0	2445.6	–	–
Total	69 152	58 188	47 514	39 951

In 2010, new legislation came into effect that introduced a medium voltage agriculture tariff, but given that the Macuvulane I plantation was built in 2005, five years prior, it is doubtful at best that an update on the equipment in order to accommodate a new voltage level (and new tariff) was performed.

Chapter 4

Self-Supply System

Considering the energy costs incurring from irrigation estimated in section 3.4, the need arises for alternatives that offer both a green and cheap source of energy. In this sense, a self-supply system refers to a system based in renewable energy, designed to replace an external power source, in this case the national electric grid, and thus able to generate and supply its own power.

While the new found autonomy in systems powered by renewable sources is an obvious advantage, providing the owner of the system direct oversight over its design and operation while benefiting from possible economic incentives often tied to renewable energy, the downside is apparent in the decrease of energy security given the variable nature of these green resources and the possible difficulty in performing self maintenance associated with the lack of technical knowledge [19]. Moreover, the abundance and/or variability of the green resource in question tied to the site physical characteristics, act as constraints in the choice of the resource, while also determining the system size [19].

4.1 Motivation for Hydro

As mentioned previously, this work is focused on developing a self-supply micro-hydro powered irrigation system for the Macuvulane I plantation. Although the exploration of the hydro resource with this goal in mind is presumably possible, given the proximity of the Incomati river, the same could be said for the solar resource, as the region of Magude has an annual photovoltaic specific yield around 1500 kWh/kWp.

However, as Figure 4.1 shows, the peak of energy demand for the original system with 3 pumps and considering the virgin and ratoon agriculture practices, E_3^v/E_3^r [MWh], which accompanies irrigation, does not coincide with the peak of photovoltaic energy production, where $E1_{pv}$ kWh is the monthly average energy produced by a single PV panel[1] (not at scale in the figure), dependent not only on the model of panel selected, but also on irradiance and temperature, the latter not depicted here.

[1] See Appendix G for details.

As an aside, if the plantation of the crop were to be delayed by 2 or 3 months, the peak demand would decrease as the water requirement curves precede the precipitation curve (in the more demanding months) by this amount of time.

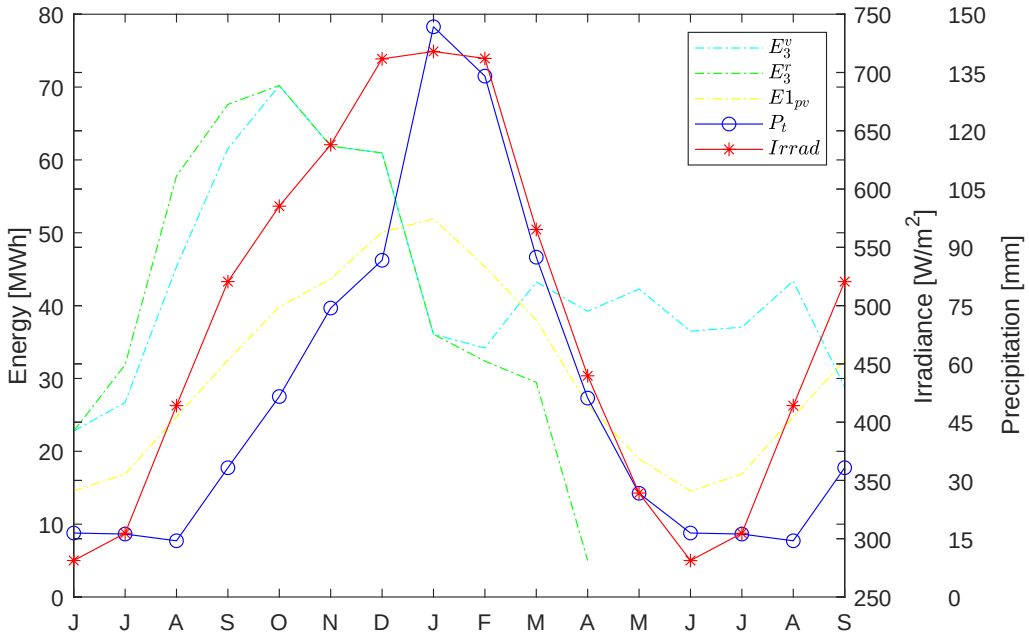

Figure 4.1: Energy demand vs precipitation and irradiance.

In this regard, the water requirements should be recomputed to assess what would be gained with this strategy, bearing in mind that typically, one cycle of 16 months of virgin cane is followed by at least 2 cycles of 11 months of ratoon, (possibly more but this is unknown). This would mean that a greater crop rotation cycle, depending exactly on the duration of each crop practice and the number of years devoted to the ratoon practice between replantation with a virgin cane would arise in which the starting month of the crop, assumed in Appendix A to be June, would begin to shift gradually, altering the water requirements for the year in question, possibly to more unfavorable situations, i.e., crop cycles with a greater lag/lead of energy demand in relation to precipitation (or irradiance), in Figure 4.1.

While the same logic is true for precipitation, and hence river flows, as the wet season coincides with the peak of precipitation (October to April), the hydro approach is not subjected to the limitations known to solar. As an example, the irrigation shifts last for 12 hours, but the number of sunlight hours, Table A.9, does not always fulfill this requirement and the irradiance varies considerably during daytime, plummeting in winter, which means a PV powered self-supply system would need to either be grossly oversized and have the ability to store energy and regulate its load to the pump demand, thus representing a high investment in hardware (PV panels) and maintenance (batteries), hampering its economical feasibility, or rely on the electric grid through a hybrid scheme to lower consumption.

As for the hydro approach, river flows do vary, but are much more constant on a daily basis[2], and the flow is available for the entirety of the irrigation shifts, and even if its mean value is reduced in the dry season, it should be possible to work with the basic river flow to power the irrigation system.

4.2 Evaluation of Hydropower Potential

What follows is a study on the possibility of powering the irrigation system solely or in part with a micro-hydro powerplant. It should be noted that the river flow is only partly characterized given that the data acquired by the ARA-Sul monitoring grid is only publicly available for the wet season. An adequate characterization of the river flow, including for the dry season and over a sufficient number of years to account for hydrological variability, as well as a study of the terrain morphology is required for an accurate project planning, namely in selecting the type of turbine that results in the best performance for the desired application.

In Mozambique, the tendency is for water consumption to increase as the number of irrigation projects for agriculture, aimed at development, increases. Although several hydro projects are planned, with some under way, to improve both water availability and electrification in rural areas, as electricity generation is to great extent performed through large-scale hydropower in Mozambique [20], the rate of access to a secure water source was still 49% in 2015 (UNICEF), and the rate of rural electrification still stands at 27%, raising doubts as to the eradication of poverty [20].

This being said, while the construction of dams, also increases the ability to regulate river flows, helping to mitigate floods or droughts, climate change is pointed as the major driver in altering the frequency of precipitation and extreme events in Mozambique, with a projected increase in temperature and decrease in precipitation, which will decreased hydroelectric generation, placing some doubt on the medium to long term reliability of this resource [20].

4.2.1 River Flow Characterization

The Incomati river has its source in South Africa at an elevation around 1800 m, and along its path of 480 km follows a general northeast direction, passing through Eswatini and Mozambique, finally reaching the Indian Ocean at Maputo Bay. Its drainage basin is shared between South Africa, Eswatini and Mozambique and has a total area of 50 000 km^2. Extensive water usage for upstream irrigation by the neighboring countries sharing the river caused tensions before a successful international agreement towards water sharing was signed in 2002 [21].

[2]This being the reason why the height of the river is typically measured daily.

In the south region of Mozambique the entity responsible for monitoring and managing water resources is ARA-Sul. Figure 4.2 was taken from a hydrological bulletin produced by ARA-Sul and shows the Incomati basin as well as a network of monitoring stations along the river path. The closest hydrometric station is E-43 located in Magude. This station is equipped to measure instant flow, height (level) and precipitation. For details on the flow data used, please refer to Appendix B.

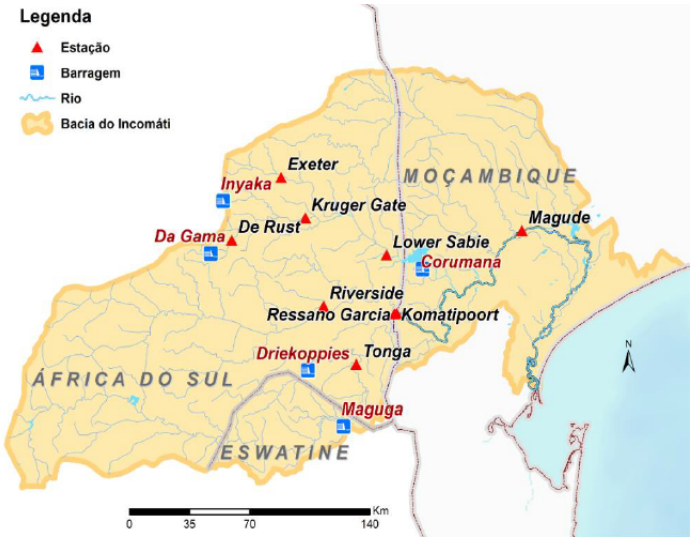

Figure 4.2: Hydrometric monitoring grid in the Incomati basin. [source: ARA-Sul]

It should be noted, that while this station is equipped to measure precipitation, the available records refer only to the wet season, this being the reason why in section 3.1.1, additional sources had to be consulted in order to work with a monthly average precipitation series.

4.2.1.1 Chronological Daily Flow Series

The chronological daily flow series for the period of 2018-2021 in which data is available, is plotted in Figure 4.3. In the same manner, the chronological flow series for each wet season, required to model the flow and estimate the producible energy, are presented in Appendix C.

For comparison, Table 4.1 presents some relevant information associated with each season.

Table 4.1: Season data indicators.

Season	Start date	End date	Data points	Q_{min} [m^3/s]	Q_{max} [m^3/s]	Q_{mean} [m^3/s]
18/19	1-nov	24-apr	173	0.94	122.25	16.03
19/20	29-nov	23-mar	112	0.64	166.73	14.97
20/21	16-nov	29-mar	132	0.17	603.12	121.56

In Mozambique the wet season typically begins in November and ends around April. One can see the river flow varies both in a single season and from season to season, and that the 2020/2021 season was marked by admittedly abnormal values of flow associated with flood alerts.

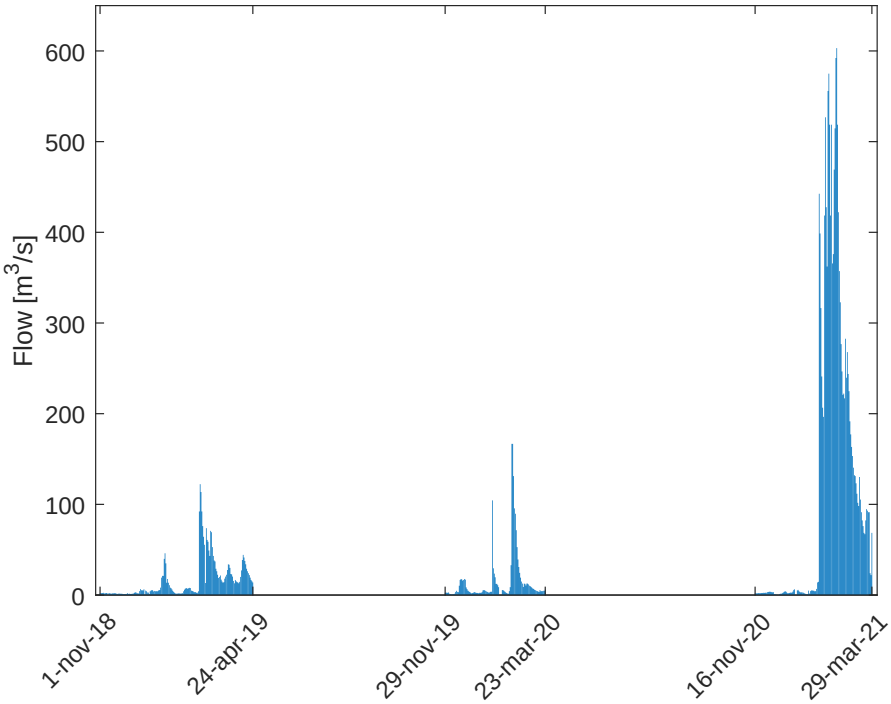

Figure 4.3: Recorded daily flows - 2018-2021, Magude - E43

Usually, in planning studies of this sort, one would work with a complete mean chronological daily flow series, but the annual series are incomplete, only records for 3 seasons are available and one of seasons was marked by floods. Therefore, it seemed unreasonable to work with a mean series in this context.

4.2.1.2 Flow Duration Curves

Sorting the chronological daily flow series, presented in Appendix C, in a decreasing manner, it is possible to obtain the so called flow duration curves (FDCs). These curves give the number of days for which a given value of flow is equaled or exceeded and can be found in Appendix D. In order to estimate the producible hydroelectric energy is it necessary to model the flow duration curves. For convenience, this is done in Appendix E.

With the flow modeled, the determination of the modular flow $Q_N\,[\mathrm{m}^3/\mathrm{s}]$, ensues. This parameter is defined as the value of flow that multiplied by an equal base of time of the flow duration curve, results in the area under the fitted flow duration curve, equation (4.1). Since the flow is measured on a daily basis, one is in fact referring to a daily modular flow, where in this case, the time is the duration in days of the wet season in question.

$$Q_N = \frac{\text{area under the curve}}{\text{time}} \tag{4.1}$$

A summary of these results is presented in Table 4.2, where the model parameters were determined in MATLAB with the *fit* function.

Table 4.2: Characterization of recorded flows.

Wet Season	Cumulative Flow [m^3/s]	Duration [days]	Model Parameters	Q_N [m^3/s]
18/19	2529	173	a = 98.83; b = 27.13	14.62
19/20	1168	112	a = 247.50	10.43
20/21	16615	132	a = 686.30; b = 25.33	125.87

4.2.2 Site Characterization

A major prerequisite in the planning of a hydro system, is a detailed knowledge of the site, as the workable value of head (that already exists or can be artificially increased), based on a topographic survey of the area is determinant in evaluating the technical feasibility of the project.

Detailed topographic maps were not available for consultation for this region, although having the limited scope of this work in mind, from Goggle Earth, it was possible to perform an elevation profile, rude as it is, as Figure 4.4 shows.

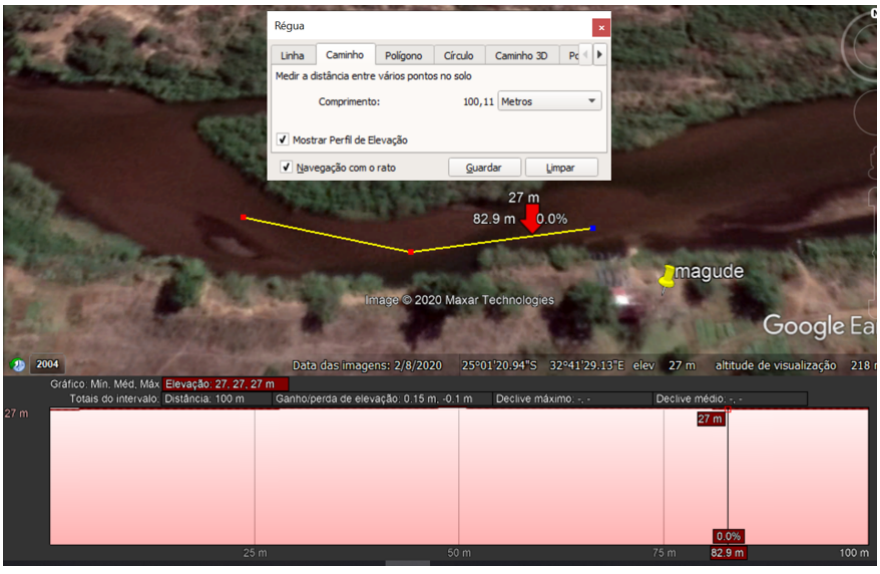

Figure 4.4: Elevation profile for the Incomati river at the pumping station site.

However incomplete and of little practical use in a more advanced phase of planning, the immediate conclusion is that, judging by the figure, the terrain is remarkably smooth. As an example, up to 100 m upstream from the pumping station, the total gain of elevation is only 0.15 m.

Chapter 5

Local Micro-Hydro Power Plant

The correct characterization of both the modular flow of the river and the topography of the site, are the two starting points to consider in the initial planning phase of the micro-hydro power plant. Without longer and continuous records, the first two seasons are considered to be typical seasons in which the values of modular flow fall in the same order of magnitude, Table 4.2. In contrast, the 2020/2021 season is considered to be atypical with a tenfold increase in magnitude of the modular flow due to a prevalence of floods, and its modular flow will therefore, not be considered in what follows.

A micro-hydro power plant typically consists of several structures as Figure 5.1 indicates.

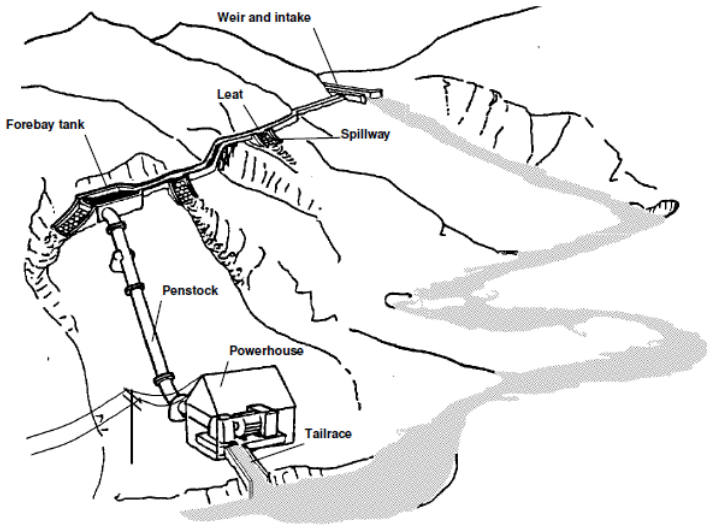

Figure 5.1: Typical small hydro scheme. Adapted from [22]

The exact configuration and additional structures may change according to site characteristics or other constraints like the the application in mind and the value of investment.

Typically, hydropower installations can be classified with respect to their size or installed capacity and according to the hydraulic head of the installation. Table 5.1 shows the recommended international definition according to installed capacity and an usual definition based on hydraulic head.

Table 5.1: Classification of small hydroplants as to installed capacity and head. Adapted from [23].

Power [MW]		Head [m]	
Micro	<0.5	Low	2-20
Mini	<2	Mini	20-150
Small	<10	Small	>150

Furthermore, hydro power plants can be classified in accordance to their storage capacity. Power plants with reservoirs are said to be storage power plants, where as, run-off-river power plants possess limited storage if any at all and lack the ability to regulate river flows. Most small hydroplants do not posses any storage capability and several configurations are possible, depending on the terrain layout, as Figure 5.2 shows, [22].

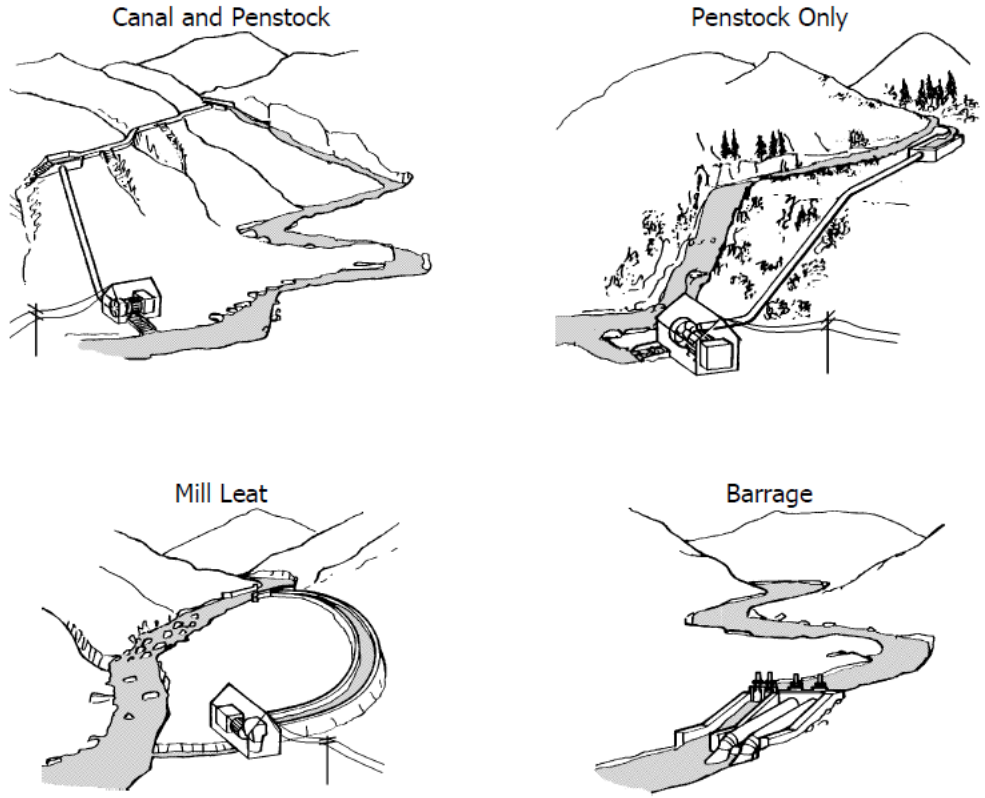

Figure 5.2: Possible small hydro configurations. Adapted from [22]

Considering the low head of the local terrain, see section 4.2.2, the choice comes down to either the mill leat or the barrage configuration. In the following, two scenarios, A and B, are considered in devising a possible solution.

In scenario A, a run-of-river hydroplant is considered in which the turbine is housed in a dam like structure, barrage type in Figure 5.2. Thus, the flow passing through the turbine is the instant flow of the river. The dam offers some ability of storage that, however limited, is more evident during the dry season.

In scenario B, a run-of-river hydroplant is still considered, but with a fraction of river flow diverted through an open channel leading to the power plant where the turbine is housed, equivalent to the mill leat configuration of Figure 5.2. Here, energy production is lower but less dependent on river flows. If the estimated mean basic flow of the river during the dry season, which is unknown, is insufficient to fully disconnect any or all pumps from the grid in a self-supply system, there is the additional option of constructing a small reservoir before the channel, akin to a forebay, and check if it is possible to maintain the required level of flow reaching the turbine for the needed duration of irrigation cycles.

While scenario B (without the optional reservoir) represents a smaller investment, it is also associated with lower energy production and, one suspects, the inability to implement a self-supply system completely autonomous, leading to a hybrid system where the irrigation system is still dependent on the grid. As for scenario A, the construction of a dam increases investment costs considerably, although allowing greater benefits in energy generation at the expense of the unexplored hydro potential. Furthermore, one sees that, with the irrigation scheme considered, based on a 12 hour cycle for the pumps, in scenario B, any surplus energy produced cannot be sold to the grid. Then, the natural solution would be to consider storage, either electric storage in batteries or water storage in a small reservoir, as in modified scenario B or scenario A. However, since the use of batteries would have to be extensive to guarantee the energy values estimated in the previous chapter, even at a partial coverage, and that this would imply high investment and maintenance costs, electric energy storage is not considered in this work.

As scenario B (without reservoir) is based in a non storage scheme, and scenario A has only a very limited storage, it is convenient to consider that, in both scenarios, the pumps continue to draw power from the grid and any energy generated in this manner is sold to the grid in a micro-generation production regime. Although, as far as it is known, Mozambique's electric grid does not support micro-generation at present, it is likely that in the coming years this will be possible at some point, and given that the introduction of renewable energy generation in special regimes is usually accompanied by economic incentives, this assumption does not seem unreasonable in moving forward with the design of the system.

If, however, for the sake of argument, no micro-generation regime is implemented in the near future, then one would have to implement a hybrid system with load regulation. In spite of this, scenario A would always result in an increased autonomy of supply at a higher investment, with the additional advantage of possibly pumping water to a higher elevation in off-periods, akin to pumped-storage hydroelectricity used in larger reservoirs. Limited as it may be, the storage capacity of this solution would allow to retain water during the dry season when the river flow is very low. As for scenario B, given the size of the optional reservoir, the irrigation system would always need to be grid connected, and so, the logical way to do this would be to connect one pump to the hydroplant (if possible) and maintain the remaining one or two pumps connected to the grid.

5.1 Mecanoelectric Equipment

Hydro generation is based in the conversion of gravitational potential energy associated with a mass of water, that experiences a decrease in hydraulic head as it passes through the prime mover. A prime mover is a machine that converts the raw resource into mechanical power. In this case the prime mover is a hydro turbine, and while, historically, this was typically some sort of wheel, designs were improved and new turbines developed as a better understanding of the physical principles behind their operation and new materials become available as a result of the industrial revolution. Mechanical power by itself is not a very useful physical quantity in modern times, and so, an additional machine is required to convert mechanical power into electric power, ready to be consumed. This machine is called a generator, and has it working principle based in Faraday's Law of Induction.

In addition to a hydro turbine and a generator, additional equipment is required, to ensure safe operation and adequate control of the system, which is dependent on site characteristics, technical constraints, investment constraints, etc, although this will not be discussed here.

5.1.1 Turbine Selection

Turbines are turbo-machines that absorb energy from a fluid and output mechanical energy [24]. Theoretically, much like an electric generator can be reversed to work as a motor, turbines can be thought of as pumps working in reverse (PAT), but in practice, the efficiency of such a machine working as both pump and turbine would drop significantly in one mode of operation, unless they were specifically designed to work in both modes as is the case of the machines installed in large hydro power plants that work as turbines in periods of high load demand and reverse their operation in off-peak hours.

A common classification of turbines is based on the value of the degree of reaction ε_T, which is defined by equation 5.1, [24].

$$\varepsilon_T = \frac{\text{pressure height absorbed by the rotor}}{\text{total height absorbed by the rotor}} \tag{5.1}$$

A turbine is said to be an action turbine if $\varepsilon_T = 0$ and conversely, a reaction turbine if $\varepsilon_T \neq 0$.

The acquisition of the turbine usually represents a considerable fraction of the cost of the micro-hydro power plant, up to 50$\%$, making it so that an adequate choice of this equipment is crucial [23]. The selection of the turbine from a technical viewpoint is essentially determined by the interaction of three parameters: flow Q [m^3/s], head H [m] and installed capacity P [kW], [23].

Usually, in a pre-selection phase, the type of turbine can be determined from graphs such as the one in Figure 5.3. For low heads and the modular flow determined, Table 4.2, the choice falls on the Kaplan type.

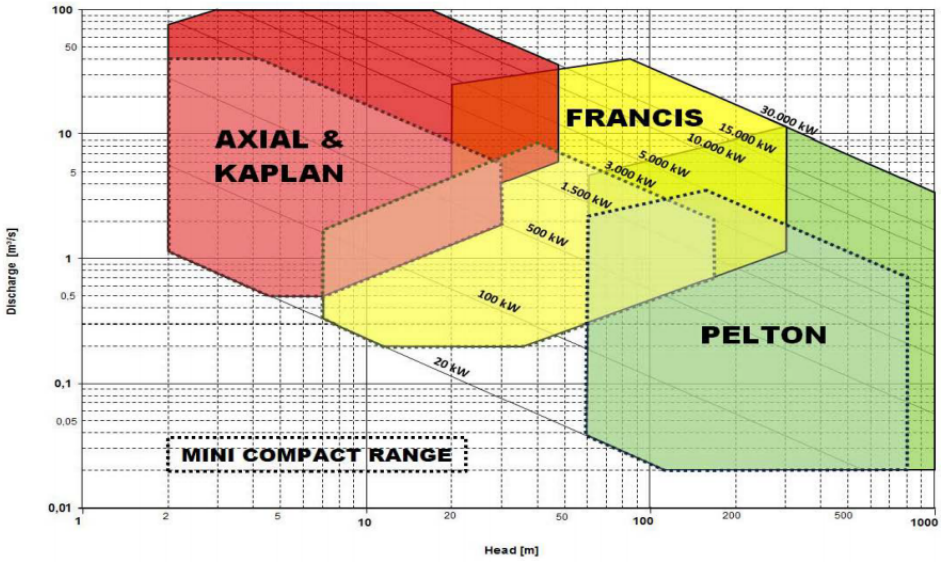

Figure 5.3: Turbine pre-selection. [Source: Andritz Hydro presentation, 2016 Energy Summit]

Since the terrain is very smooth, for the purposes of scenario A, it is considered that the useful head after the dam is built is 2 m, because this is the minimum admissible value to ensure a viable exploration of Kaplan turbines, although some manufacturers claim that some Kaplan construction types can work with as little as 1 m of head or lower.

For cases where the natural head of the river is almost non existent, the turbine is typically mounted in a water chamber [24], and the head depends both on the design of the water chamber and on the turbine dimensions and construction type, which can vary.

A more rigorous method for selecting the turbine consists in determining the specific speed of the machine defined by equation 5.2, [23].

$$n_s = \frac{N_N \sqrt{Q_N}}{(gH_u)_N^{\frac{3}{4}}} \tag{5.2}$$

where N_N is the nominal speed of the turbine (rotations per second), Q_N is the nominal flow $[\mathrm{m}^3/\mathrm{s}]$, $g\,[\mathrm{m/s}^2]$ is the acceleration of gravity and H_u [m] is the net height.

This dimensionless quantity, n_s assigns a range of values to families of turbines geometrically similar [24], is independent of the turbine dimensions, and for a Kaplan turbine is typically in the range of $n_s \in [0.19,\ 1.55]$, [23].

5.1.1.1 Kaplan Turbine

Many types or turbines exist, each suited for a specific application. In the previous section an initial selection, based on values of modular flow, $Q_N \simeq 10\,\mathrm{m}^3/\mathrm{s}$ and head, $H_b = 2\,\mathrm{m}$, pointed to a Kaplan turbine of installed capacity $P > 100\,\mathrm{kW}$, Figure 5.3. In this section, a more substantiated justification for that choice is made by exploring the design, and fundamental principles behind the design and operation of Kaplan turbines.

Fundamentally, the reasons that make Kaplan turbines so well suited for applications involving run-of-river hydro power plants which lack or otherwise have a limited ability to control or regulate river flows, are understood.

A Kaplan turbine is a reaction machine of axial flux in which the blades of the rotor are adjusted automatically in response to the change in load to achieve an optimized efficiency [24]. Reaction turbines are those where the rotor is fully submerged under water, being subjected to constant pressure, and where the turbine exit is bellow the water line.

The composition of a kaplan turbine is showed in Figure 5.4. The spiral tube is the distributor, whose function is to transform pressure into velocity, with the flux of water in the runner (rotor) being inward (centripetal turbines). The wicket-gates can be oriented to regulate the flow that passes through the turbine rotor. There is also a draft tube, used to create a depression at the exit of the runner, that by transforming dynamic pressure into static pressure helps mitigate cavitation [24].

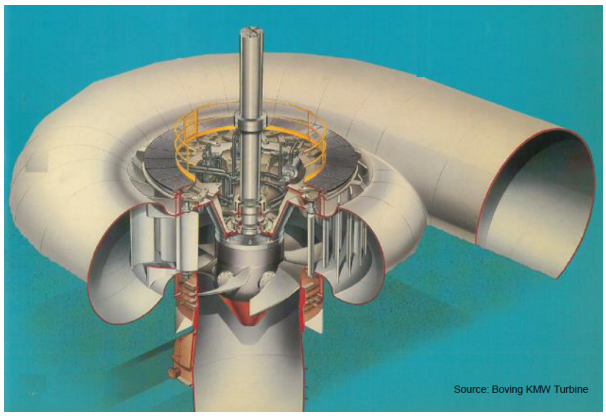

Figure 5.4: Kaplan turbine design.
[Source: Boving KMW Turbine]

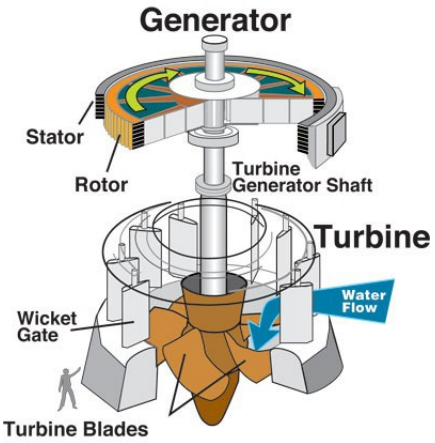

Figure 5.5: Turbine/Generator group.
[Source: https://energyeducation.ca]

Several variants of Kaplan turbines exist, either due to the adopted constructive design, or the control strategy used, resulting in a range of performances. Fundamentally, the control of Kaplan turbines is possible by acting on the wicket gates (distributor) and/or on the blades of the rotor. The efficiency curves that result from these 4 possibilities are shown in Figure 5.6.

A Kaplan turbine with the ability to control its blades is said to possess simple regulation (B), or alternatively, a regulated rotor. This is critical to widen the range of operation, resulting in a flat efficiency curve.

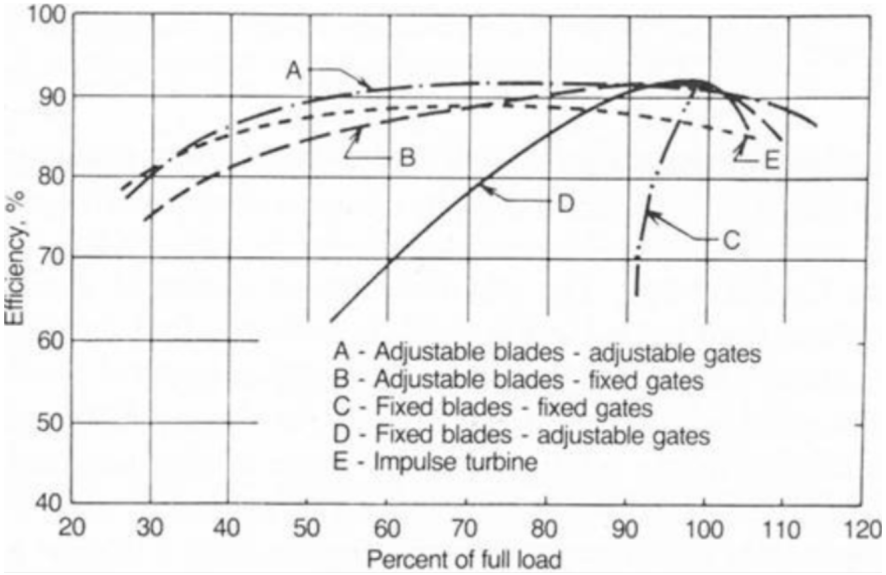

Figure 5.6: Efficiency curves of Kaplan variants. [Source: www.renewablesfirst.co.uk]

The blade adjustment for low and high values of flow is shown in Figure 5.7.

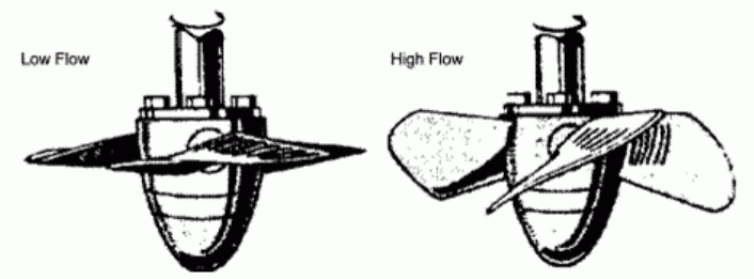

Figure 5.7: Kaplan turbine rotor with adjustable blades. [Source: www.renewablesfirst.co.uk]

If the wicket gates are also controlled, the turbine is said to have double regulation (A). This improvement, that combines both types of control, introduced by Viktor Kaplan in 1913, results from an optimization of the velocity triangles that describe a particle of fluid at the entrance and exit of the machine rotor. The application of the Euler Theorem at these points defines the torque of the machine, which can be adjusted by optimizing said triangles, and in turn maintain a nearly constant efficiency when the flow changes.

Another possibility is to simply control the wicket-gates and not the blades (D). The (B) and (D) variants are said to be semi-Kaplan, as the full Kaplan turbine possesses both types of regulation (A). A propeller turbine (C) is a particular case of a Kaplan turbine without regulation either in the rotor or the distributor.

5.1.2 Generator Selection

Generators are mecanoelectric converters that absorb mechanical energy from a prime mover, in this case a turbine, and output electric energy at a very high efficiency [25]. Fundamentally, when selecting a generator for the hydro power plant, the choice comes down to either a synchronous generator (alternator) or an asynchronous one (induction generator) [23].

Typically, small hydroelectric applications ($<$ 5 MW), are equipped with induction generators, avoiding the need for the exciter, voltage regulator and synchronizer required when using alternators, and since the excitation current in induction generators is drawn from the grid, the system where they are inserted cannot be isolated from the grid [26]. Later on it is determined that the system cannot be isolated from the grid in any technical and economically viable scenario, and as the grid connection already exists this would never be an issue.

5.2 Scenario A: Barrage

As discussed, this scenario assumes the existence of a dam with limited storage capacity. The instantaneous river flow is available to the turbine housed in the dam.

Since the minimum head requirement according to Figure 5.3 is $h = 2\,\text{m}$, and the natural head of the river and adjacent terrain is very low, it is assumed that the hydraulic head, H_b achieved after constructing the dam is $2\,\text{m}$.

5.2.1 Energy Computation

Given the scope of this work, and the lack of solid data concerning the river flow and the elevation of the site, a simplified model based in simple criteria to help determine the size of the unit in an initial planning phase [23] is adopted in the following.

5.2.1.1 Installable Power

Thus, with the nominal flow $Q_N\,[\text{m}^3/\text{s}]$ and the hydraulic head $H_b\,[\text{m}]$ evaluated in section 4.2, the nominal power P_N [W] of the turbine to be installed is estimated from equation 5.3

$$P_N = \gamma Q_N H_b \eta_c \tag{5.3}$$

where $\gamma = 9810\,\text{N}/\text{m}^3$ is the specific weight of water and η_c is the global efficiency.

A common expression to estimate the value of P_N [kW], obtained from equation 5.3 consists in assuming a global efficiency of 81.6% with the specific weight of water now expressed in kN/m^3, equation 5.4, [23].

$$P_N = 8 Q_N H_b \tag{5.4}$$

However, since the global yield is determined by the product of yields of the equipment involved, turbine, generator, etc, the global efficiency is realistically, closer to 70% [23], leading to the revised expression given by equation 5.5

$$P_N = 7 Q_N H_b \tag{5.5}$$

Since the range of power ratings available is discrete, the power is rounded up to the closest integer. Tables 5.2 summarizes these results.

Table 5.2: Power plant installable capacity.

Season	Q_N [m^3/s]	P_N [kW]
18/19	14.62	200
19/20	10.43	150
20/21	125.87	1500

5.2.1.2 Estimated Producible Energy

Since the turbine has a very low annual use of its installed capacity, as the latter is chosen for a value of flow that occurs in a very small percentage of days in the year[1], and as discussed in section 5.1.1.1, the efficiency of the turbine is directly tied to the flow, it is common to attribute exploration limits to turbines, that define the range of operation in relation to the nominal flow in which the turbine can maintain its operation without a significant variation of its efficiency [23].

Typical exploration limits α_1 and α_2, associated with different control strategies for Kaplan turbines are presented in Table 5.3.

Table 5.3: Exploration limits for two types of Kaplan turbines. Adapted from [23].

Turbine	$\alpha_1 = Q_{min}/Q_N$	$\alpha_2 = Q_{max}/Q_N$
Kaplan with double regulation	0.25	1.25
Kaplan with regulated rotor	0.40	1.00

It goes without saying that the double regulation type corresponds to curve (A) of figure 5.6 and the regulated rotor type corresponds to curve (B).

[1] In the present case the situation is even grimmer as the nominal flow determined refers solely to the wet season.

These are the two types under analysis because they are the ones in which the efficiency curves are flat resulting in wider exploration ranges, and as a consequence an increase in energy generation. As an example, the exploration area of a double regulated Kaplan turbine, for the 2018/2019 wet season is defined by the shaded area in Figure 5.8.

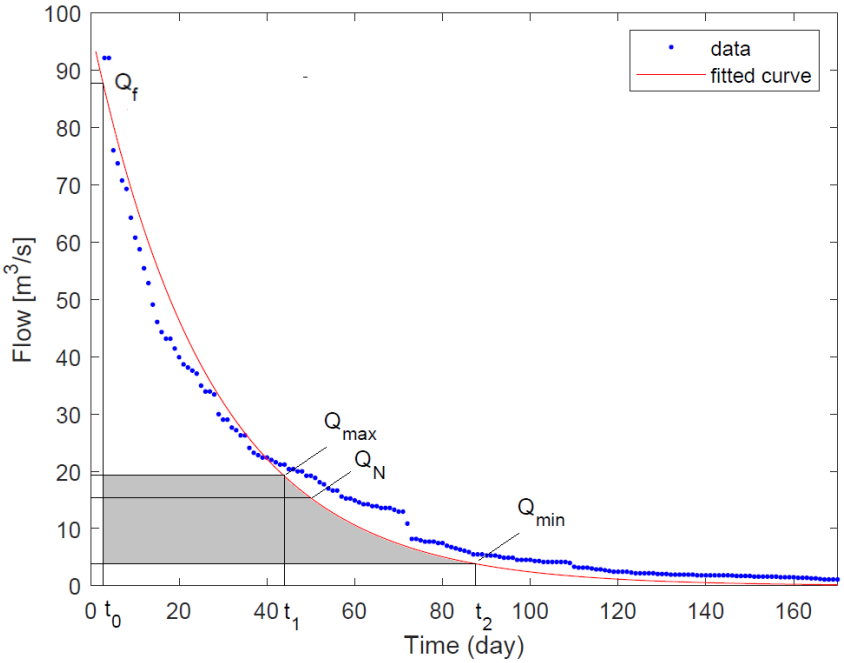

Figure 5.8: Exploration area for the 2018/2019 season using a double regulated Kaplan turbine.

Based on the determined values for the modular flow in Table 4.2, and the exploration limits for each Kaplan variant in Table 5.3, the minimum and maximum flows, Q_{min} and Q_{max} imply the determination of times t_2 and t_1 , respectively. The flood flow Q_f determines time t_0, and corresponds to the number of days where the head is insufficient to produce energy. In reality, Q_f will depend on the machine head to begin with, and the value of flow that leads to a drop in head below the minimum requirement, here assumed to be $H_b = 2$ m.

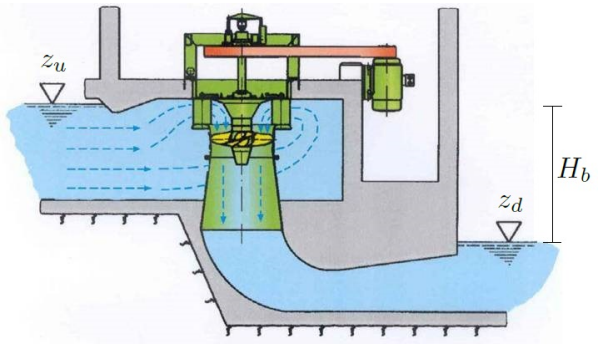

Figure 5.9: Gross height available to the turbine. [Adapted from: https://www.renewablesfirst.co.uk/]

Figure 5.9 shows a Kaplan vertical turbine construction type T that illustrates this phenomenon. Vertical axis kaplan turbines are better suited to explore lower heads than horizontal or inclined axis types. Here, z_u and z_d are the upstream and downstream height references, with the hydraulic head H_b given by equation 5.6.

$$H_b = z_u - z_d \tag{5.6}$$

As mentioned, for an initial phase of the project, a simplified energy computation model is assumed in which the hydraulic head is equal to the gross head as defined in equation 5.6.

The only missing element is knowing how the height of the river changes in response to a change in flow. This depends on the river cross section and can be inferred from the river stage discharge curve. Although not presented in this work, the river height data was compiled from the hydrologic bulletins and used to derive the river stage discharge curve seen in Figure 5.10.

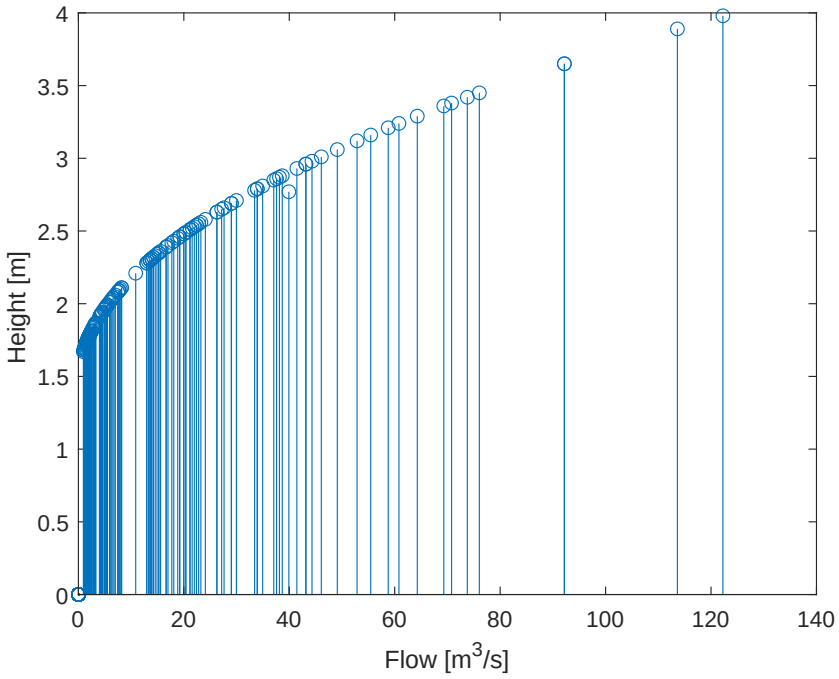

Figure 5.10: Stage-Discharge Curve, 2018/2019 Wet Season, Magude - E43

In the presence of floods, the capacity of the dam, however limited, cannot be exceeded and the height of the river increases downstream, lowering the gross head available to the machine. Assuming for a moment the basic river flow for this season is $Q_{design} = 2.5\,\mathrm{m}^3/\mathrm{s}$, then the reference height (downstream) is around $h = 1.8\,\mathrm{m}$. Now, ignoring losses in the hydraulic circuit, and without further information, if the upstream reference (in the reservoir) remains constant, as the intake gate is fixed at a certain height, and if the reference level downstream increases by a certain amount h', then H_b will drop bellow the value necessary to ensure turbine feasibility.

Based in Figure 5.10, the reference level for downstream is around $h_0 = 1.8\,\text{m}$, which means that in order for the head to be reduced by 2 m, the downstream height must increase by 2 m, $z_d = 3.8\,\text{m}$, which corresponds to a value of flow of $Q_c \simeq 110\text{m}^3/\text{s}$ that defines time t_0. Obviously, the turbine stops working properly before a null head is achieved, but without further study of the river flow or the terrain, the design of a proper turbine installment is impossible.

Integrating equation 5.5, over the exploration limits of the turbine, Table 5.3, leads to an estimate of the producible energy $E\,[\text{Wh}]$, given by the shaded area of figure 5.8 and expressed by equation 5.7 [23],

$$E = 7 \times H_b \times \left((t_1 - t_0)\alpha_2 Q_N + \int_{t_1}^{t_2} Q(t)\,dt \right) \times 24\ [\text{Wh}] \tag{5.7}$$

For the assumed exploration limits, times t_0, t_1 and t_2, in days, as well as the estimated energy (not annual) are given in Table 5.4.

Table 5.4: Estimated producible energy for two Kaplan variants (scenario A).

	Kaplan double regulated				Kaplan regulated rotor			
	t_0 [days]	t_1 [days]	t_2 [days]	E [MWh]	t_0 [days]	t_1 [days]	t_2 [days]	E [MWh]
$18/19$	2	45.27	88.95	398.44	2	51.32	76.19	322.20
$19/20$	3	18.99	94.94	203.87	3	23.74	59.34	148.86
$20/21$	44	37.31	78.07	717.32	44	42.96	66.17	598.65

Note that these results pertain only to the wet season, as the flow duration curves are incomplete due to the fact that no records for the dry season are available. In addition, it is worth repeating that the 2020/2021 season saw a spike in energy production due to a higher installed capacity connected to a higher value of modular flow, Table 5.2. In practice, the machine to be installed would have a nominal power defined by the modular flow of an average season, of which the 2018/2019 and 2019/2020 seasons are thought (and assumed) to be representative.

If the goal is to have the power plant operate all year, the modular flow of the complete FDC would decrease, lowering the installed capacity of the plant, and so, even if higher values of flow were to occur, energy production would be limited.

5.2.2 Self-Supply Condition

Judging by the results of Table 3.14, and under this original scenario, if for simplification, the energy consumption is assumed to be equally distributed for all months (since in this scenario what exists is an annual water requirement), the values of energy to be met are around $\bar{E}_2^0 = 55$ MWh/month and $\bar{E}_3^0 = 46$ MWh/month.

If, however, the scenarios in which both types of agriculture practice are considered (as these were the main motivation to characterize monthly demand), the resultant average monthly energy consumption is that of Table 3.15, with the demand peaking in October for the most unfavorable situation with $E_2^v = 83.65\,\text{MWh}$.

Now, data exists as to the producible energy in the wet season, but the seasons in which these computations were based do not have the same starting date or duration, Table 4.1, so it is not possible to establish a direct correspondence between any given month of these seasons and the energy values of Table 5.4. Were the flow duration curves complete (for a whole year), this would not be a problem.

Moreover, a close inspection of the chronological daily flow series reveals that, as expected, the value of energy produced varies according to river flows, however, ignoring this for now, if one takes the energy values of Table 5.4 and equates them to the duration in months of the respective season, an average monthly energy estimate, $\bar{E}\,[\text{MWh}/\text{month}]$ for the wet season can be obtained, Table 5.5.

Table 5.5: Estimated mean monthly energy production during the wet season.

Season	Days	Months	Kaplan double regulated		Kaplan regulated rotor	
			E [MWh]	$\bar{E}$ [MWh/month]	E [MWh]	$\bar{E}$ [MWh/month]
$18/19$	173	5.77	398.44	69.05	322.20	55.84
$19/20$	112	3.73	203.87	54.66	148.86	39.91
$20/21$	132	4.40	717.32	163.03	598.65	136.06

If one assumes the original scenario, a double regulated Kaplan turbine would at its worst produce $\bar{E} = 54.66$ MWh/month and thus be able to match, on average, the monthly demand $\bar{E}_2^0 = 55$ MWh/month for the worst case. But more data, for example, energy bills, would lower uncertainty.

As for the constructed scenarios, having in mind that all recorded seasons start either in or after November, and that the peak demand occurs in October, $E_2^v = 83.65\,\text{MWh}$, it is reasonable to state that, in that month, the power plant would not cover the required demand, although, on average, for half of wet season months (January, February and March), the energy production would satisfy demand, but a complete coverage for the wet season would not be possible.

Adding to this, as discussed, the occurrence of floods in the wet season and/or droughts in the dry season, pushes turbine operation outside its exploration limits, during which time the machine is disconnected. Simply speaking, a run-of-river plant cannot provide security of supply for the entire year as it lacks any meaningful storage capability. Anything capable of solving this problem is by definition a storage power plant, and is no longer neither a micro-hydro plant, nor it represents a realistic investment the smallholders association is capable of making, nor is physical possible for that matter.

The technical constraints make the goal of self-supply unfeasible and unrealistic under the assumptions made. A simple way do deduce this would be to considering equation 5.5, ignoring for a moment that the power to be installed is constrained by the size of the models of turbines and generators available in the market, and take P to be $P_2 = 180\,\text{kW}$ and $P_3 = 312\,\text{kW}$ and assuming a minimum required head $H_b = 2\,\text{m}$, then, the nominal flow would need to be $Q_n^2 = 12.9\,\text{m}^3/\text{s}$ and $Q_n^3 = 22.3\,\text{m}^3/\text{s}$, and although for P_2 this would seem be possible at first, considering that the average nominal flow of the first two seasons, $\bar{Q}_n = 12.5\,\text{m}^3\text{s}$, Table 4.1, this is referent only to the wet season, that is, this value will decrease if a complete flow duration curve is considered, which means that no self-supply system could be built.

The power demand is enormous, so is the energy, considering the time of irrigation tied with crop water needs, the head is too low and the flow is severely reduced in the dry season. Nonetheless, as also discussed, the system can be made to rely both on the grid and the hydro resource and/or sell surplus energy in certain periods to the grid in a microgeneration regime.

5.3 Scenario B: Channel

As mentioned, here a derivation in the river is envisioned, in this case an open channel with the additional option of an upstream reservoir loading it. The rationale here is to limit and regulate the flow reaching the turbine, resulting in a smaller machine and so too, on a smaller investment. Also, this scenario has a lower ecological impact when compared to the construction of a dam, even if small.

The power output P [W] of a turbine for a given value of flow, $Q\,[\text{m}^3/\text{s}]$ and head, H_b [m] is given by equation 5.3. One could start by asking what value of Q the channel would need to discharge so that the turbine output would match the power rating of a particular pump arrangement. Considering (or not) the outage of the larger pump, the power rating to be achieved is either $P_2 = 180\,\text{kW}$ or $P_3 = 312\,\text{kW}$.

However, simply speaking, the generator coupled to the turbine can only output its nominal power if the value of Q is constant, and considering the power requirements, this would not only result in a large and expensive channel but it also assumes that a sufficient mean river flow can be maintained for the duration of the irrigation cycle (12 hours). As it will be discussed ahead, this is not the case.

In scenario A, the conclusion reached was that the entire flow of the river (even ignoring the need to maintain an ecological flow) could not cover the demand all year. Here, if a self-supply system is not possible either way and since the flow reaching the turbine is greatly reduced in this scenario, then if the aim is to design a smaller system aimed at reducing costs, not eliminating them, it seems obvious that, as a start, the design of the channel, should be performed with the assumption that only one of the smaller pumps could in principle (to be verified) be shutoff from the grid, becoming part of a smaller self-supply hydro-powered system, while the remaining pumps (1 or 2) maintain their grid connection.

5.3.1 Channel Design

The design of the channel has to take into account not only engineering constraints but also economical ones. Several geometries of open channels are possible, circular, triangular, rectangular, trapezoidal, etc., but since, in practice rectangular channels are easier to construct, and therefore also cheaper, this will be the type of channel considered.

Although the cost of an open rectangular channel depends on its physical dimensions, both in length l [m], depth y [m] and width b [m], generally, the cost per unit length remains constant while the cost of excavation is increasingly tied to the excavation depth y. Appendix F provides an overview on how to design such a channel at the least cost. However, this approach results in a cross section with values not suited for practical application, leading to a more pragmatical solution consisting in empirically picking a set of values for the width b and depth y and check if the value of the Froude number is bellow unit to ensure a subcritical flow.

Rewriting equation 5.3, the flow that the channel needs to carry Q [m^3/s], can be expressed as a function of the required turbine output power P [W], equation 5.8.

$$Q = \frac{P}{\gamma \, \eta \, h} \tag{5.8}$$

Alternatively, from equations F.1, F.2, F.3 and F.11, Q can be expressed as a function of the channel dimensions b and h, equation 5.9

$$Q = \left(\frac{bh}{2h + b} \right)^{\frac{2}{3}} \frac{\sqrt{S}}{n} \, bh \tag{5.9}$$

Note that h is the height of water in the channel, which changes according to flow, and would in theory be included in the total hydraulic head H_b, as defined in Figure 5.9. But, whereas in scenario A, the upstream reference height would be fixed (given by the elevation of the intake gate), this being the reason why the dam could always be designed in such a way that a minimum value of $H_b = 2\,\text{m}$ could be assumed no matter the dimensions of the turbine, here however, since no dam structure exists and the terrain is smooth, the total head H_b is given by the difference between the height of water in the channel, h and the downstream reference z_d, which will depend both on the dimensions of the turbine and the power house elevation, possibly requiring a water chamber due to the very low head available.

The problem with this, however, is that in an initial planning phase such as this, in order to properly compute H_b, one would need to already have a turbine model picked, its dimensions known, and a detailed topographical survey of the site available, given that the slope of the terrain S, the channel total length l, the derivation and terminal points of the channel, would influence both H_b and the losses in the channel,

which are not considered here, given the lack of information. Then, in order to proceed, a channel with length 100 m is considered, with a slope between those points, equal to S = 0.001. This means that the head gained $\Delta h = 10\,$cm, is, on average, an order of magnitude lower than h and thus can, in a first approximation, be ignored.

Therefore, energy estimation will be performed assuming H_b is equal to h. So, even ignoring losses in the channel, the error committed in energy estimation is by default, and not by excess, (since the H_b would in reality be larger then h), which is preferable as it provides a safety margin.

It is then necessary to compute the head h as a function of the required power. Thus, substituting equation 5.8 in equation 5.9 leads to transcendental equation 5.10

$$\frac{P}{\gamma\,\eta\,h} - \left(\frac{bh}{bh+b}\right)^{\frac{2}{3}} \frac{\sqrt{S}}{n}\, bh = 0 \tag{5.10}$$

Assuming a channel made of finished concrete with a Gauckler–Manning coefficient of n = 0.012, a value of slope S = 0.001, knowing the power rating of one of the smaller pumps, P = 90 kW and fixing a value for the width of the channel, for example, b = 2 m, equation 5.10 can be solved for h, leading to a height of water in the channel of h = 1.6310 m. Plugging this value in equation 5.8 results in a value of flow in the channel of $Q_{\text{channel}} \simeq 6.25\,\text{m}^3/\text{s}$. Note that the channel height, y, can be rounded to 1.7 m.

Of course, looking at the chronological daily flow series, is it immediate to note that the recorded minimum flow Q_{min} of the river for any of the seasons is very low, see Table 4.1. For the duration of the wet season, and according to both the mean and modular flows, Q_{mean} and Q_N, the channel could be fed a constant value of $Q_{\text{channel}} \simeq 6.25\,\text{m}^3/\text{s}$ if, either the flow never decreased beyond this value or a reservoir storing a required amount of volume and discharging it according to irrigation cycles (that coincide with the periods in which the turbine would need to work) could be built.

Now, with a run-of-river powerplant such as this, the river flow cannot be controlled, and during the dry season this requirement of $Q_{\text{channel}} \simeq 6.25\,\text{m}^3/\text{s}$ cannot possibly be fulfilled, leading to the only alternative available if the desire is to isolate, at least, one pump from the grid for a few months, being the construction of a reservoir.

While this may seem conceptually similar to scenario A, in which limited storage is provided by the construction of the dam, here the reservoir would not be located directly in the river, rather it could be constructed in a location adjacent to the river where it could be charged and discharged through the channel, and for this the terrain would need to be better characterized.

5.3.2 Reservoir Loading the Channel

The reservoir function would then be to load the channel, and from the flow data, one can guess that for any reasonable reservoir size, and even limiting the system to just 1 pump, this would never work in the dry season. In order to confirm this assertion, one can consider an idealized reservoir, that experiences no losses as a result of evaporation, no change in configuration due to silt accumulation, etc. Then, the balance of water in this hypothetical reservoir is given by equation 5.11, with the adopted convention, in which the inflow Q_{in} is considered positive and the outflow Q_{out} negative.

$$\frac{dV(t)}{dt} = Q_{\text{in}}(t) - Q_{\text{out}}(t) \tag{5.11}$$

As an example, Figure 5.11 shows the charging of this reservoir through the river and its discharge through the channel for 3 irrigation cycles. Irrigation scheduling, that again, coincides with the load demand on the turbine, translates in a square wave with a duty cycle of 50% for the outflow.

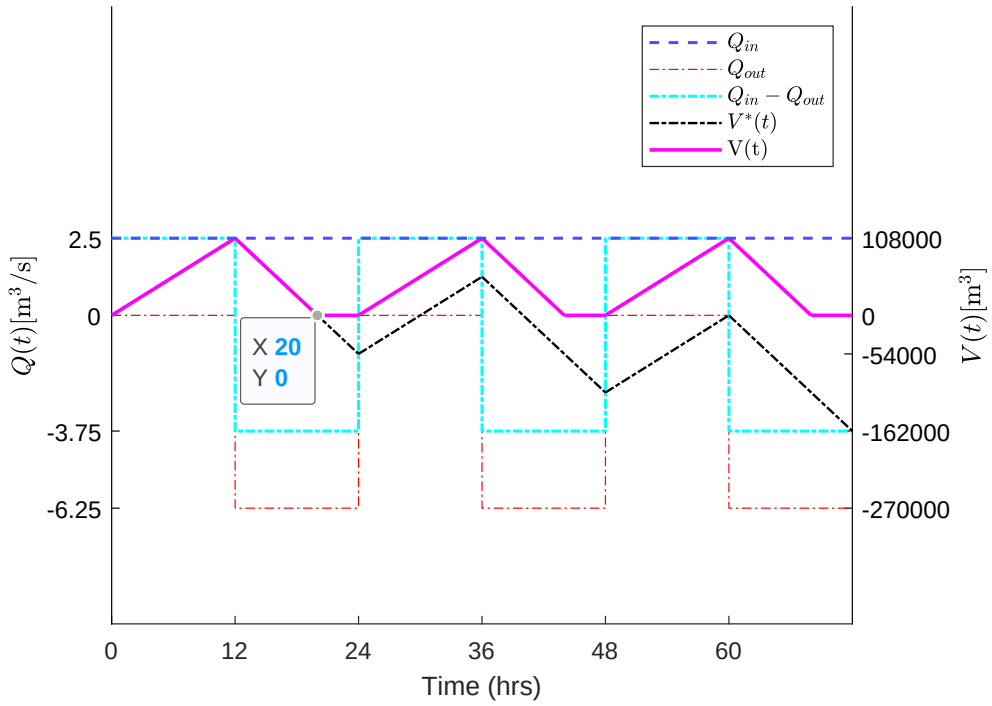

Figure 5.11: Volume of water in the reservoir as a function of time.

The reservoir is assumed to be empty at t = 0, and continually fills at a rate of $Q_{\text{in}} = 9000\,\text{m}^3/\text{hr}$ or $2.5\,\text{m}^3/\text{s}$. The rate of discharge is $Q_{\text{out}} = 13500\,\text{m}^3/\text{hr}$ or $3.75\,\text{m}^3/\text{s}$ for the second half cycle. Then, in the first cycle, the volume in the reservoir is given by equation 5.12

$$V(t) = \begin{cases} 9000\,t, & 0 \le t \le 12 \\ -13500t + 270000, & 12 \le t \le 20 \end{cases} \quad [\text{m}^3] \tag{5.12}$$

Note that, the axis of time is not meant to coincide with the hours of the day, since the exact hour at which irrigation shifts start would need to be known, but it serves to indicate that irrigation cycles last for 12 hours a day. Also, in order to ensure a fixed length of irrigation cycles, in this case 8 hours, the reservoir exit valve must only close at the end of each half-cycle. If for example, the outflow cannot be maintained for 12 hours, since the reservoir is empty at t = 20 hours, then, one could think of closing the exit valve and let the reservoir refill, but this would lead to an oscillating behavior for $V(t)$ and as a consequence for the duration of irrigation, unless the maximum capacity were to be set at 108 000 m^3.

As for the the negative volume, as it were, represented by the black dashed line, $V^*(t)$, this merely indicates a deficit of water that arises as a consequence of the reservoir's inability to maintain the required outflow in the channel for the duration in question. This means that as each irrigation cycle ends, the deficit of volume increases by 54 000 m^3 per day. If one irrigation cycle lasts for 6 days, then, the deficit will total 324 000 m^3 and this would need to be the initial condition, the volume of water in the reservoir for $t = 0$.

Imposing a positive quantity for the volume as a constraint, one obtains the real variation of volume, $V(t)$, provided the reservoir is only allowed to refill every 12 hours to avoid the metioned oscillating behavior. Therefore, the turbine can only maintain the required power for 8 hours as the reservoir is completely empty at $t = 20$ hours.

And so, for this assumed values of inflow and outflow, in order to maintain only 1 pump isolated from the grid, the capacity of the reservoir would need to be $V_{\text{max}} = 324000\,\text{m}^3$, and this is effectively a large scale dam, not a small reservoir loading a channel, which would seem to indicate, as expected, that a self-supply system based in this solution would need a storage capacity of the type found in scenario A, or as it was seen, a storage capacity far greater.

Moreover, for this reservoir to be fully emptied, the exit valve would need to be near the bottom, which means, that the reservoir could never fully charge from the river, unless a difference in head existed to begin with, which it does not seem to. Making matters worse, something that was discarded in this analysis was the necessity of maintaining an ecological flow in the river, meaning that the inflow on the reservoir would be even lower, decreasing the time in which the turbine can maintain its rated output, and so too, the duration of irrigation cycles.

In conclusion, not even one pump can be isolated from the grid in this manner, as the flow of the river is not constant and during the dry season it is substantially lower than the required value. As for the attempt at storing water to discharge it at the required rate, no reservoir short of a large dam in the river would be capable of feeding this pump, for the duration of the wet season, let alone all year. Both the basic river flow and the head are too low. Thus the pumps cannot be disconnected from the grid, but by designing a hybrid system for all 3 (or 2) the energy consumption can be reduced.

Considering the previous discussion, opting for a smaller channel seems to be the preferred solution. In this regard, a channel with cross section dimensions $b = 2\,\text{m}$ and $y = 1.5\,\text{m}$, is able to carry a maximum flow of $Q_{\text{max}} = 5.62\,\text{m}^3/\text{s}$, corresponding to a Froude number of $F_r = 0.59$. This way, the range of flows available to the turbine is limited, decreasing investment.

5.3.3 Range of Turbine Operation

As the load of the machine changes, the power available at its shaft also changes, which means that, for a constant head, the machine will not always work with the maximum flow, Q_{max}. For this reason, when considering the efficiency curve of a turbine, the flow is given as a fraction of Q_{max} which is also expressed as the percentage of gate opening. The turbine exploration limits discussed in scenario A follow from this.

In Figure 5.12, a typical efficiency curve of a Kaplan turbine is given for two types of control strategies, where the blue curve corresponds to curve (A) of figure 5.6, where as the red curve is associated with curve (D) of the same figure.

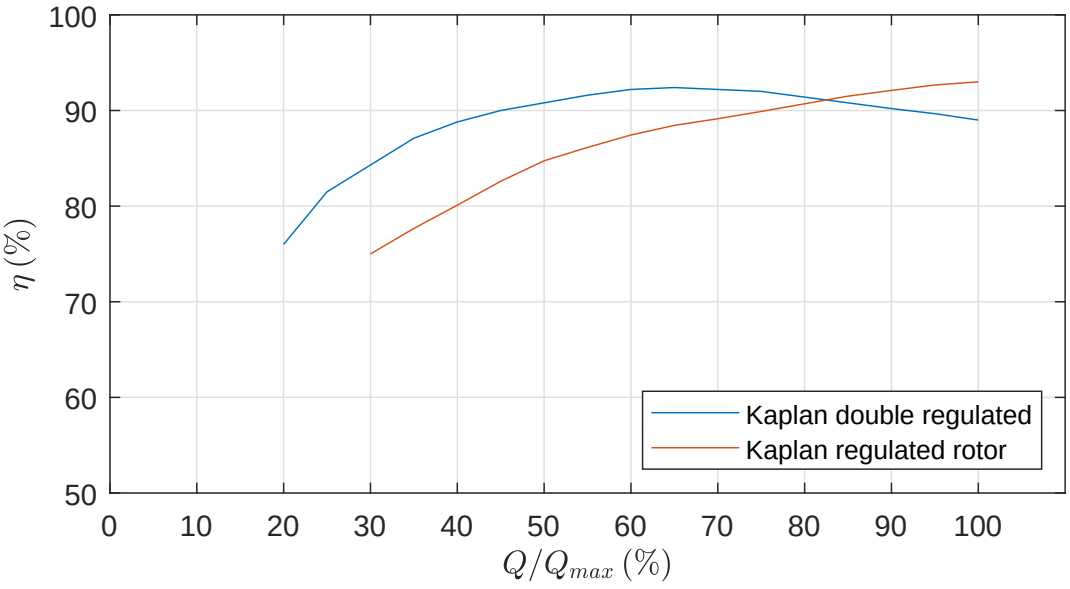

Figure 5.12: Typical efficiency curves of Kaplan turbines.

The exploration limits of a double regulated Kaplan turbine are $\alpha_1 = 0.25$ and $\alpha_2 = 1.25$, and while the efficiency curve of this turbine is flat over a large range of flows, in reality, near the edges of the interval, the efficiency drops. The same is true for a regulated rotor Kaplan turbine.

In the following analysis it is convenient to assume a constant efficiency of $\eta = 90\,\%$, which means that the opening of the intake in percentage, Q/Q_{design}, has to be bounded by $\alpha'_1 = 0.4$ and $\alpha'_2 = 1$ for a double regulated Kaplan and by $\alpha'_1 = 0.6$ and $\alpha'_2 = 1$ for a simple regulated Kaplan (regulated rotor). As such, with the design flow set, the range of flows that the turbine can work with, while maintaining a constant efficiency, can be determined.

$$\alpha'_1 \leq \frac{Q}{Q_{design}} \leq \alpha'_2 \implies \eta = 90\,\% \tag{5.13}$$

which means that the flow in the turbine should be in a range given by

$$\alpha'_1\, Q_{design} \leq Q \leq \alpha_2\,' Q_{design} \tag{5.14}$$

Then, if $Q_{design} = 2.5\,\mathrm{m}^3/\mathrm{s}$, the flow is inside the interval $Q \in [1,\, 2.5]\,\mathrm{m}^3/\mathrm{s}$ for a double regulated Kaplan and in the range $Q \in [1.5,\, 2.5]\,\mathrm{m}^3/\mathrm{s}$ for a Kaplan with regulated rotor.

If the river flow exceeds Q_{design}, the channel will still carry Q_{design}. In fact, since $Q_{\text{design}} = 2.5\,\mathrm{m}^3/\mathrm{s}$, and the maximum channel flow is $Q_{\text{max}} = 6.25\,\mathrm{m}^3/\mathrm{s}$, then, in truth, the channel can carry Q_{max} if the river flow allows it, but it can be assumed that a spillway exists in the channel and/or a forebay with a spillway loading the channel, limiting the flow to Q_{design}.

This suggests the channel can be made smaller and cheaper, as it would always be limited to Q_{design}.

$$Q_{design} \leq Q \leq Q_{\text{max}} \implies Q = Q_{\text{design}} \tag{5.15}$$

A flow in the channel $Q = Q_{design}$ results in a head of water available to the turbine of $h = 0.8105\,\mathrm{m}$, which means that the turbine size would need to be, from equation 5.3, rounded to $P = 20$ kW. This is the lower limit, as to installed power, for the exploration of Kaplan Turbines, see Figure 5.3.

As an example, the 2018/2019 season has 173 recorded flow values. The number of days for which the flow obeys the constraints given by equation 5.14 is 53. Then, for the remaining 173 - 53 = 120 days, the flow is assumed to be constant and equal to $Q_{\text{design}} = 2.5\,\mathrm{m}^3/\mathrm{s}$.

5.3.4 Estimated Producible Energy

In the following, it is worth reminding that in scenario A, the estimation of energy consisted in computing it from records of river flows, where the turbine had constant head available of 2 m. Here, given the configuration adopted, the hydropower generation is less dependent on river discharge, but will still dependent on the the assumptions made, the head H_b is the head of water in the channel h, that changes as Q changes, and the river discharge for the dry season is unknown but assumed to be $Q_{\text{mean}} = 2.5\,\mathrm{m}^3/\mathrm{s}$.

Here, with the assumption of $\eta = 0.9$, the power P [W] associated with a given value of flow $Q(i)$ in the channel is given by equation 5.16.

$$P(i) = \gamma\, Q(i)\, h(i)\, \eta \tag{5.16}$$

and since the flow $Q(i)$ is measured daily, the daily energy $E(i)$ [Wh] is computed from equation 5.17

$$E(i) = 24 \sum_{i} P(i) \tag{5.17}$$

This being said the estimated energy that could be produced, taking the 4 following assumptions is presented in Table 5.6.

- I) energy produced solely in the wet season as a result of recorded flows;

- II) energy produced in the dry season, assuming a constant basic mean flow, $Q_{\text{mean}} = 2.5\,\text{m}^3/\text{s}$, where the duration of the dry season is assumed to be 365 minus the duration of the wet season;

- III) annual energy as the sum of energy produced in the wet season (I) plus the energy produced in the dry season (II);

- IV) annual energy produced assuming the flow in the channel is constant and equal to $Q_{\text{mean}} = 2.5\,\text{m}^3/\text{s}$ all year.

Table 5.6: Estimated producible energy for different assumptions (scenario B).

Season	Kaplan double regulated			Kaplan regulated rotor		
	$E(I)$ [MWh]	$E(II)$ [MWh]	$E(III)$ [MWh]	$E(I)$ [MWh]	$E(II)$ [MWh]	$E(III)$ [MWh]
$18/19$	63.67	82.87	146.54	62.18	88.02	150.20
$19/20$	44.78	109.49	154.27	44.49	110.78	155.27
$20/21$	50.03	103.05	153.08	49.71	104.34	154.05

Note that the energy produced in scenario IV is independent of season and type of turbine, $E(IV) = 156.72\,\text{MWh}$. This should be possible due to the fact that a constant flow in the channel equal to the river basic mean flow is assumed for the the whole year. In practice, an ecological river flow would have to be maintained, so more extensive and complete records would allow to determine a more realistic value for Q_{mean} leading for a better planning of both the channel and the turbine, or even a reservoir serving as an upstream forebay. In either case, scenario B seems to offer the best solution at the lowest investment.

5.4 Proposed Solution

Although scenario B would seem to be more realistic and result on a smaller investment, it also implies smaller energy production. Adding to that, the possibility of a microgeneration production regime shifts technical constraints associated with storage and therefore, the determination of the best solution, has to be based on an economic analysis that encompasses several scenarios. This is done in the next chapter, although in the future, a proper study of the river along with a topographical survey to better estimate energy production and lead to a more accurate choice of the hydro scheme adopted, would seem the place to start, before going into further detail.

Ultimately, in projects such as this, the initial planning phase encompasses the creation of a database with information on similar projects that are physically possible, for which the investment and operation and maintenance costs are known, and that already present favorable economic indicators, such as the NPV or the IRR [23]. Then, a large number of technological solutions are evaluated using a simplified model, like the one that was used for both scenarios to estimate the producible energy, and subjected to an economic evaluation in which typical costs of operation and maintenance as well as an average price of selling energy to the grid are considered, leading to a list of options that can be ordered according to their economic interest and from which the worst solutions are eliminated [23]. The following phase consists in using detailed models that require more data, specifically on the efficiency of the equipment, such as the turbine and generator, and losses in the hydraulic circuit to reevaluate the producible energy, and redo an economic analysis from which only a couple of solutions are considered for project execution [23]. Finally opting, according to some economic criteria, for the final solution [23].

Chapter 6

Economic Analysis

Any hydro power plant project has to start with a technical study based on long records of river flows and a detailed topographical survey of the site. Once a set of possible technical solutions is devised, an economical study of the project is required to select which of those, if any, ensures feasibility or even profitability. And while a micro-hydro project is not subjected to the same detail of scrutiny as its large hydro power counterparts, given the difference in investments involved, the specific cost of hydro-power [€/kW] increases as the installed capacity decreases, which makes a correct assessment of the site, with respect to both the topography and the river, a determinant factor in lowering costs and ensuring that a well projected power plant can perform as intended.

Given the goals of this work, a more pragmatic approach would be to establish a direct line of communication with the smallholders association, determine a measure of investment capable to be made, for example proportional to annual profits, propose a certain amount of cost reduction based on that investment and provide projections on the return of investment. This would also provide the opportunity to discuss the details of operation of the irrigation system, rotation of blocks/sprinklers used, as well as agricultural practices, etc, decreasing uncertainty in all the steps that culminated in energy demand evaluation, and as a consequence impact the current analysis. While this was not possible, and a lot of assumptions had to be made, the results obtained are nonetheless considered.

6.1 Annual Mean Cost of Energy

The cost of each unit of energy produced can be obtained by computing the unitary mean annual cost, c [€/MWh], expressed as the ratio between the annual expenses D_a [€] and the annual energy produced E_a [MWh], equation 6.1, [23].

$$c = \frac{D_a}{E_a} \tag{6.1}$$

where the expenses can be further broken into a sum of terms, equation 6.2, [23]

$$D_a = i' I_t + c_d E_a \tag{6.2}$$

in which:

- i' : annual charges as a percentage of the total investment [%]
- I_t : total investment [€]
- c_d : diverse unitary costs [€/MWh]

Since the diverse unitary costs are not known a priori, they will be assumed to be included in operation and maintenance costs, whose typical values are known.

The annual mean cost is not a good metric to evaluate the economical interest of an energy source, as it can change from year to year, but it can be significant for a given year of production [23].

6.2 Discount Rate

As the entry and exit of money do not usually happen in regular and periodic time sequences the evaluation of the economical interest of a project is not trivial [23]. It is also common knowledge that is not equivalent paying the same quantity of money in different time instants, and so the discount rate allows for the conversion of financial quantities between different time instants [23].

In this way, a given payment P_j made in a period of j years can be equated with a smaller payment made today P_0 (actualized), equation 6.3 [23].

$$P_0 = \frac{P_j}{(1+r)^j} \tag{6.3}$$

6.3 Levelized Cost of Energy (LCOE)

If the evaluation period encompasses the lifespan of the power plant, a discount rate has to be considered, which means that distinct solutions can result in similar values for the annual mean cost, and yet possess very different economical interests [23].

Therefore, an often used metric is the $LCOE$, expressed as the ratio between the total costs incurred during the lifetime of the power plant and the actualized energy E_{act} produced over the same period, equation 6.4, in which the index n_c refers to the number of cost terms [23].

$$LCOE = \frac{\sum_{j=1}^{n_c} c_{ai}}{E_{act}} \tag{6.4}$$

LCOE formulas often vary as the underlying assumptions can be different, but one possibility is to consider simplified models. If, for example, the investment is made in its entirety in the initial moment, $t = 0$, the cost of investment c_{a1} [€] is just the total investment I_t, equation 6.5, [23]

$$c_{a1} = I_t \tag{6.5}$$

As for the maintenance and operation costs c_{a2}, the exploration of the power plant is assumed to start at $t = 1$, equation 6.6, where d_{om} [pu] is refered to the total investment I_t [€] in year j, [23].

$$c_{a2} = I_t \sum_{j=1}^{n} \frac{d_{omj}}{(1+r)^j} \tag{6.6}$$

The actualized total production of energy over the lifespan of the installation E_{act} [MWh] is given by equation 6.7, [23].

$$E_{act} = \sum_{j=1}^{n} \frac{E_{aj}}{(1+r)^j} \tag{6.7}$$

Since in hydro projects there are no fuel expenses associated with the production of energy, the LCOE is given by equation 6.8, where the only cost terms are c_{a1} and c_{a2}.

$$LCOE = \frac{c_{a1} + c_{a2}}{E_{act}} \tag{6.8}$$

Thus, taking a simplified model, in which the investment is assumed to be made in its entirety in the initial moment, t = 0, and the maintenance and operation costs are equally assumed constant over the lifespan of the power plant, the LCOE [€/MWh] is given by equation 6.9 [23].

$$LCOE = \frac{I_t + d_{om} I_t k_a}{E_a k_a} \tag{6.9}$$

where factor k_a expresses the sum of the geometric series given by equation 6.10 [23]

$$k_a = \sum_{j=1}^{n} \frac{1}{(1+r)^j} = \frac{(1+r)^n - 1}{r(1+r)^n} \tag{6.10}$$

6.4 Investment Indicators

The most often used evaluation indicators in energy production projects are the NPV (Net Present Value) and the IRR (Internal Rate of Return).

6.4.1 Net Present Value

The net present value (NPV), accounts for the cash-flows (difference between entries and exists of money), properly actualized for the lifespan of the power plant and is given by equation 6.11, [23].

$$NPV = \sum_{j=1}^{n} \frac{R_{Nj}}{(1+r)^j} - \sum_{j=0}^{n-1} \frac{I_j}{(1+r)^j} \tag{6.11}$$

in which n is already defined and R_{Nj} is the net cash-flow for year j given by equation 6.12, in which R_{Gj} [€] is the gross annual profit.

$$R_{Nj} = R_{Gj} - d_{omj} I_t \tag{6.12}$$

A positive NPV means the project is economically viable, i.e., that the results obtained cover the initial investment, and generate a surplus, whereas a negative NPV implies the project is not economically viable [23].

Taking the simplifying assumptions discussed before, the NPV is given by equation 6.13

$$NPV = R_N k_a - I_t \tag{6.13}$$

6.4.2 Internal Rate of Return

By definition, the internal rate of return (IRR), is the discount rate that nullifies the NPV, so from equation 6.11, it follows that the IRR can be obtained by solving equation 6.14, [23].

$$\sum_{j=1}^{n} \frac{R_{Nj}}{(1+IRR)^j} - \sum_{j=0}^{n-1} \frac{I_j}{(1+IRR)^j} = 0 \tag{6.14}$$

Since the expression given by equation 6.14 does not have a closed-form solution, the use of iterative methods is required. However, noticing how the NPV changes with the discount rate, the former can be linearized around its zero, and by use of linear interpolation, the value of the IRR can be obtained by computing two distinct values for the NPV, a positive value (NPV_1) associated with a discount rate r_1 and a negative value (NPV_2) associated with a discount rate r_2, equation 6.15, [23].

$$IRR \simeq r_1 - (r_2 - r_2) \frac{NPV_1}{NPV_2 - NPV_1} \tag{6.15}$$

6.4.3 Time of Gross Return

The time of gross return T_{gr} [years] (or payback) is a gross evaluation criteria in which the profits and expenses are assumed to be equal every year and not subjected to actualization. It is given by the

ratio between the total investment and the annual gross profit R_G discounted of the annual exploration expenses D_e, both assumed to be constant, equation 6.16 [23].

$$T_{gr} = \frac{I_t}{R_G - D_e} \tag{6.16}$$

6.4.4 Recuperation Period

A more accurate way to measure the return of investment is to consider an investment made in $t = 0$, and check how many years are required to have that investment returned (recuperation period) T_r equation 6.17, [23].

$$\sum_{j=1}^{T_r} \frac{R_{Nj}}{(1+r)^j} = I_t \tag{6.17}$$

An approximate approach to compute T_r is to consider a mean actualized net profit for the lifespan of the power plant and assume the simplified model discussed thus far, leading to equation 6.18, [23].

$$T_r = \frac{nI_t}{R_N k_a} \tag{6.18}$$

6.4.5 Return On Investment

The return on investment (ROI), is a dimensionless quantity that measures the profitability of the project for each unit of capital invested, equation 6.19, [23].

$$ROI = \frac{\sum_{j=1}^{n} \frac{R_{Nj}}{(1+r)^j}}{\sum_{j=0}^{n-1} \frac{I_j}{(1+r)^j}} \tag{6.19}$$

With the assumptions of the simplified model, equation 6.19 can be written as equation 6.20, [23].

$$ROI = \frac{R_N k_a}{I_t} \tag{6.20}$$

6.5 Estimation of Required Parameters

Typically, for small hydro projects, the lifespan of the plant is assumed to be n = 25 years, the discount rate is $r = 0.07$ and the maintenance and operation costs d_{om}, represent 1% of the investment [23].

6.5.1 Hydroplant Investment

The project of a micro-hydro powerplant is an iterative process, that encompasses the balance of expenses and income for a given installed capacity considered [23].

Since the cost of a given turbine model is hard to determine from market information because the manufacturer usually discloses this information in the acquisition process, the evaluation of the investment done here in regard to the installed capacity is superficial and based in regression models that account the cost of investment for similar projects.

Something that also undoubtedly impacts the following analysis is the fact that, for the size of the installation considered, a micro-hyro power plant, no information exists concerning the cost of similar projects in Mozambique, forcing one to use models from other regions of the world, which may not be realistic. These models depend on the installed capacity to provide a global cost of projects, even though they may differ as to the scheme adopted or additional structures and equipment needed, and since the FDCs are neither complete nor based in an average daily chronological flow series, uncertainty exists as to how realistic and accurate the estimated values for the installed capacity actually are.

For the hydro scheme contemplated in scenario A, costs regarding the planning and construction of the dam, and all adjacent structures, as well as the installation and delivery of equipment, such as the turbine, cannot be evaluated in the scope of this work, as these were discussed superficially. The same can be said for scenario B, in regard to the costs of construction of both the channel and reservoir. However, it is possible to provide a global cost estimate for the whole installation based in regression models, as discussed previously.

The unitary cost of investment for a micro hydroplant was in 2002 situated between 1500 €/kW and 6000 €/kW, with a mean value of 3750 €/kW, according to [23]. Another source [27], indicates costs for hydroplants bellow 1 MW ranging from 2000 €/kW to 8200 €/kW, with an average value of 4100 €/kW, in 2010. These values were actualized to 2020 using an online tool[1], and averaged between the two sources, Table 6.1 to yield the costs of the micro-hydro power plant according to installed capacity, Table 6.2.

Table 6.1: Typical unitary investment cost of micro-hydro (2020).

min [€/kW]	mean [€/kW]	max [€/kW]
2280	4710	9250

6.5.1.1 Scenario A

Referring to the installed capacity of the power plant, Table 5.2, where now only the first two seasons are considered, the estimated investment based in the costs of Table 6.1 is given in Table 6.2.

[1] INE, IPC - Atualização de Valores.

Table 6.2: Cost investment of micro-hydro, scenario A (2020).

Season	Power [kW]	min [€]	mean [€]	max [€]
18/19	200	456 000	942 000	1 850 000
19/20	150	342 000	707 000	1 388 000

The cost of a Kaplan turbine, with flows between $5\,\mathrm{m}^3/\mathrm{s}$ and $30\,\mathrm{m}^3/\mathrm{s}$, C [$\pounds$, 2008], can be expressed as a function of the installed capacity, P [kW] by equation 6.21, according to [28].

$$C(P) = 14000\,P^{0.35} \tag{6.21}$$

Using a present exchange rate, from pounds to euros, of $R = 1.17$, and actualizing to 2020 values, the costs of acquiring a Kaplan turbine with power ratings suited for each season are those of Table 6.3.

Table 6.3: Estimated turbine cost, scenario A (2020).

Season	Power [kW]	Cost [€]
18/19	200	116 371
19/20	150	105 227

As the turbine is not chosen to work for a particular season, rather it is projected to work based on mean flow duration curves, and given the limited number of seasons to begin with, and the discussion on the 2020/2021 season being marked by floods, it is reasonable to say that the capacity of the turbine would be either 150 kW or 200 kW. The real choice would be for a value lower than 150 kW as the dry season flows would decrease the value of modular flow, and so to, of the installed capacity. Still, with all available information, for the purposes of this analysis, the values of Table 6.3 are the ones considered.

6.5.1.2 Scenario B

In scenario B, it was determined that the installed power of a turbine projected to work with a dry season flow of $Q_{\text{mean}} = 2.5\,\mathrm{m}^3/\mathrm{s}$ is $P =$ 20 kW, with the estimated costs for this power plant given in Table 6.4 .

Table 6.4: Cost investment of micro-hydro for scenario B (2020).

Season	Power [kW]	min [€]	mean [€]	max [€]
-	20	45 600	94 200	185 000

For a Kaplan turbine, with flows between $0.5\,\mathrm{m}^3/\mathrm{s}$ and $5\,\mathrm{m}^3/\mathrm{s}$, the cost C [$\pounds$, 2008], can be expressed as a function of the installed capacity, P [kW] by equation 6.22, according to [28].

$$C(P) = 3500\,P^{0.68} \tag{6.22}$$

As before, using the same exchange rate, the cost of acquiring a Kaplan turbine with the power rating determined in scenario B is that of Table 6.5.

Table 6.5: Estimated turbine cost, scenario B (2020).

Season	Power [kW]	Cost [€]
-	20	34 926

As it can be seen, the smaller the installed capacity the more significant is the portion of the cost associated with the acquisition of the turbine.

6.5.2 Annual Produced Energy

In scenario A, the estimated energy was computed for the wet season only, and given the exploration limits of both types of Kaplan turbines and the modular flow computed for the same period, the minimum flow Q_{min} capable of being turbined would always be greater than the assumed mean flow of the river during the dry season. So, here it is assumed that the turbine is disconnected during the dry season and that the energy generated in the wet season, Table 5.4 is also the annual energy.

As for scenario B, the hypothesis in which the flow reaching the turbine through the channel is constant throughout the year is considered, $E(IV) = 156,72$ MWh.

6.5.3 Gross Profit

In the likelihood that microgeneration will be implemented in the foreseeable future, there are two options. In the first option O_1, the pumps maintain their grid connection and all generated energy is sold to the grid. In the second option O_2, energy generated by the power plant during demand periods (coinciding with irrigation) is used by the installed units in a hybrid scheme. Still, irrigation cycles last for 12 hours and in the remaining time the power plant is still producing energy and, since it is assumed that large scale energy storage is out of the question and that even limited water storage is unlikely given the size and cost of the dam and reservoir involved, energy produced in off periods would be wasted, this being the reason why assuming microgeneration is convenient.

However, given that typically, in countries where mature microgeneration technologies exist, the price of selling energy to the grid is far lower than the cost of buying energy from it, then, even if this regime were to be implemented, any possible special remuneration regime or economical incentive would not extend to the period under analysis, which means that for most of the lifespan of the power plant, typically assumed to be 25 years for hydro projects, the second option is preferable, i.e., to use energy generated for immediate consumption, lowering energy bills directly, instead of generating revenue.

Thus microgeneration would serve to generate limited revenue while also avoiding waste and taking advantage of energy produced from a green energy source. In evaluating the monthly cash-flows generated by selling energy to the grid, an average tariff of 0.041 €/kWh is assumed.

6.5.3.1 Option 1

Based on Table 5.4, the generated energy in scenario A would lead to the gross profits R_G [€] of Table 6.6:

Table 6.6: Estimated revenue for recorded flows with two Kaplan turbine variants.

	kaplan double regulated	Kaplan regulated rotor
	R_G^A [€]	R_G^A [€]
$2018/2019$	16 336	13 210
$2019/2020$	8 359	6 103

For scenario B, the gross profit associated with selling an annual energy of $E(IV) = 156,72$ MWh at the considered tariff is $R_G^B = 2952$ €.

6.5.3.2 Option 2

At first glance option 2 would seem not to imply selling energy to the grid (on average), since generated energy is never enough to cover annual requirements. However, given the previous discussion on the duration of irrigation cycles (12 hours) and the fact that potentially, hydro generation occurs continuously 24 hours a day, unless storage is considered some fraction of energy could never be directly used by the pumps. Although the two scenarios discussed A and B, involve very different approaches, since produced energy is used to complement energy needs, in effect, the cost avoided by doing so can be considered a gross benefit.

In scenario A, since some measure of storage exists, and discarding for now the interval of several days between cycles to simplify things, one considers that the off-period flow, which lasts for 12 hours, can be stored (especially during the dry season), which means that the turbine can be disconnected for that period, and no energy generation occurs. This way, energy generation is synchronized with irrigation cycles and whatever energy is generated can be immediately used by the pumps.

For scenario B, two hypothesis could be considered. In the first, is it assumed that the optional reservoir can store the basic river flow between irrigation cycles, and that just like in scenario A, the energy demand is synchronized with energy generation, which means that all produced energy is consumed.

In the second, no reservoir is assumed to exist, which means that only a fraction of generated energy in this scenario $E(IV) = 156,72$ MWh would be used by the pumps. Taking the original scenario for simplification, it is possible to determine the annual pump utilization, 41.9% (2 pumps) and 20.3% (3 pumps), and so, these are the fractions of E_a that, on average, could be used by the pumps if no type of storage exists. Thus, in this option two types of benefits would exist, one associated with avoided costs by consuming a fraction of annual generated energy, and the other associated with selling the remainder to the grid. Given that this option would always be economically worst than considering a reservoir, and that no realistic way exists of evaluating the difference in investment associated with considering or not the reservoir (since the installed capacity is the same), this option will not be subjected to economic evaluation.

Thus, the annual gross benefit is just the avoided cost of buying the annual generated energy for both scenarios, A and B, with the previously assumed tariff, see Table 3.16, equation 6.23.

$$R_G^{A/B} = R \times (V_t \times E_a^{A/B} \times 10^3 + 12 \times F_t) \tag{6.23}$$

Scenario A

From Table 5.4, the avoided cost of generated energy in scenario A would lead to the gross profits R_G of Table 6.7:

Table 6.7: Gross benefit for recorded flows with two kaplan turbine variants.

	Kaplan double regulated	Kaplan regulated rotor
	R_G^A [€]	R_G^A [€]
$2018/2019$	33 139	26 805
$2019/2020$	16 976	12 406

Scenario B

For scenario B, the gross profit associated with the avoided cost of buying an annual energy of $E(IV) = 156.72$ MWh at the considered tariff is $R_G^B = 13\,059$ €.

6.6 Economic Results

The results for the annual mean cost and LCOE are presented in Table 6.8.

Note: DR and RR stand for Double Regulated and Regulated Rotor, respectively.

Table 6.8: Mean and levelized cost of energy.

		I_t [€]		$d_{om}I_t$ [€]	E_a [MWh]		c [€/MWh]		$LCOE$ [€/MWh]
Scenario	Season			$d_{om} = 0.01$	Kaplan Type		I_t		$k_a = 11.6536$
A	18/19	min	456 000	4 560	DR	398.44	min	11.44	109.65
							mean	23.64	226.52
		mean	942 000	9 420			max	46.43	444.86
					RR	322.20	min	14.15	135.59
		max	1 850 000	18 500			mean	29.24	280.12
							max	57.42	550.12
	19/20	min	342 000	3 420	DR	203.87	min	16.78	160.73
							mean	34.68	332.26
		mean	707 000	7 070			max	68.08	652.30
					RR	148.86	min	22.97	220.12
		max	1 388 000	13 880			mean	47.49	455.04
							max	93.24	893.36
B	–	min	45 600	456	IV	156.72	min	**2.91**	**27.87**
		mean	94 200	942			mean	**6.01**	**57.59**
		max	185 000	1 850			max	11.80	113.09

It seems then, that scenario A is far from being economically viable. As for scenario B, the best results for the LCOE are obtained considering the minimum and mean values of the investment interval. In G20 countries, the LCOE of small-scale projects ($<$ 10 MW), was in 2018 situated between 36 €/MWh and 100 €/MWh, with 75% of the values being under 76 €/MWh [29]. However, it is likely that for micro-hydro projects, these values are slightly higher since installations with reduced size do not allow, in general, for economies of scale. Also, these values pertain to developed countries, and no information for micro-scale projects is known for Mozambique.

As for the indicators discussed, Table 6.9 summarizes the results, and as expected from the LCOE results, only two options are economically viable, those with a positive NPV, although resulting in values for the IRR lower than the discount rate assumed, $r = 0.07$.

Table 6.9: Investment Indicators.

		I_t [€]		$d_{om}I_t$ [€]	R_G [€]			R_N [€]		NPV [€]	IRR	T_{gr} [years]	T_r [years]	ROI
Scenario	Season			$d_{om} = 0.01$	Option	Kaplan Type		I_t		$k_a = 11.6536$			$k_a = 11.6536$	
A	18/19	min	456 000	4 560	O1	DR	16 336	min	11 776	-318 767	–	38.70	83.07	0.30
								mean	6 916	-861 404	–	136.21	292.19	0.09
								max	-2 164	-1 875 218	–	–	–	–
						RR	13 210	min	8 650	- 355 196	–	52.72	130.09	0.22
		mean	942 000	9 420				mean	3 790	-897 833	–	248.55	533.20	0.05
								max	-5 290	-1 911 648	–	–	–	–
					O2	DR	33 139	min	28 579	-122 952	–	15.96	34.23	0.73
								mean	23 719	-665 588	–	39.71	85.19	0.29
		max	1 850 000	18 500				max	14 639	-1 679 403	–	126.37	271.11	0.09
						RR	26 805	min	22 245	-196 766	–	20.49	43.98	0.57
								mean	17 385	-739 402	–	54.85	116.24	0.22
								max	8 305	-1 753 217	–	222.76	477.87	0.05
	19/20	min	342 000	3 420	O1	DR	8 359	min	4 939	-284 443	–	69.24	148.55	0.17
								mean	1 289	-691 979	–	548.49	1176.65	0.02
								max	-5 521	-1 452 339	–	–	–	–
						RR	6 103	min	2 683	-310 733	–	127.47	273.45	0.09
		mean	707 000	7 070				mean	-967	-718 269	–	–	–	–
								max	-7 777	-1 478 630	–	–	–	–
					O2	DR	16 976	min	13 556	-184 024	–	25.23	54.12	0.46
								mean	9 906	-591 559	–	71.37	153.11	0.16
		max	1 388 000	13 880				max	3 096	-1 351 920	–	448.32	961.76	0.03
						RR	12 406	min	8 986	-237 281	–	38.14	81.65	0.31
								mean	5 336	-644 816	–	132.49	284.24	0.09
								max	-1 474	-1 405 177	–	–	–	–
B	–	min	45 600	456	O1	2 952		min	2 496	- 16 513	–	18.27	39.19	0.64
								mean	2 010	- 70 776	–	46.87	100.54	0.25
		mean	94 200	942				max	1 102	-172 158	–	167.88	360.14	0.07
					O2	13 059		min	12 603	**101 270**	**0.3597**	**3.62**	**7.76**	**3.22**
		max	185 000	1 850				mean	12 117	**47 007**	**0.2099**	**7.77**	**16.68**	**1.49**
								max	11 209	-54 375	–	16.50	35.41	0.71

Chapter 7

Results

In essence, this chapter is comprised of a summary and discussion of the results obtained in this work. A problem description is given, the steps required in achieving a solution are examined, the assumptions made by necessity or convenience are stated and their impact on the results discussed.

7.1 Problem Description

The problem to be analyzed and solved can be best described by the following statements:

- the case study is a sugar cane plantation with 187.9 ha in the district of Magude, Mozambique;
- the plantation is run by a small farmer's association with almost to 200 people;
- the irrigation system has 3 pump/motor units connected to the national electric grid;
- irrigation is made by aspersion and sprinkler units are manually rotated by workers every 12 hours;
- irrigation needs and frequency are dependent on climate annual variability and crop stage development;
- the costs incurring from irrigation are considerable to the farmer's association;
- a new, renewable self-supply system is needed to alleviate energy costs;
- the proximity of the Incomati river suggests an alternative based in a micro-hydro system;
- the flow of the Incomati river near the case study needs to be characterized;
- in conjunction with the river data, the local terrain will determine the type of hydro power plant, the turbine to be installed and additional structures required;
- in addition to a technical study, an economic analysis is necessary to ensure project viability.

7.2 Work Overview

Figure 7.1 shows a flowchart that portraits in a more immediate way, the steps taken in this work, as well as some of the assumptions and decisions made.

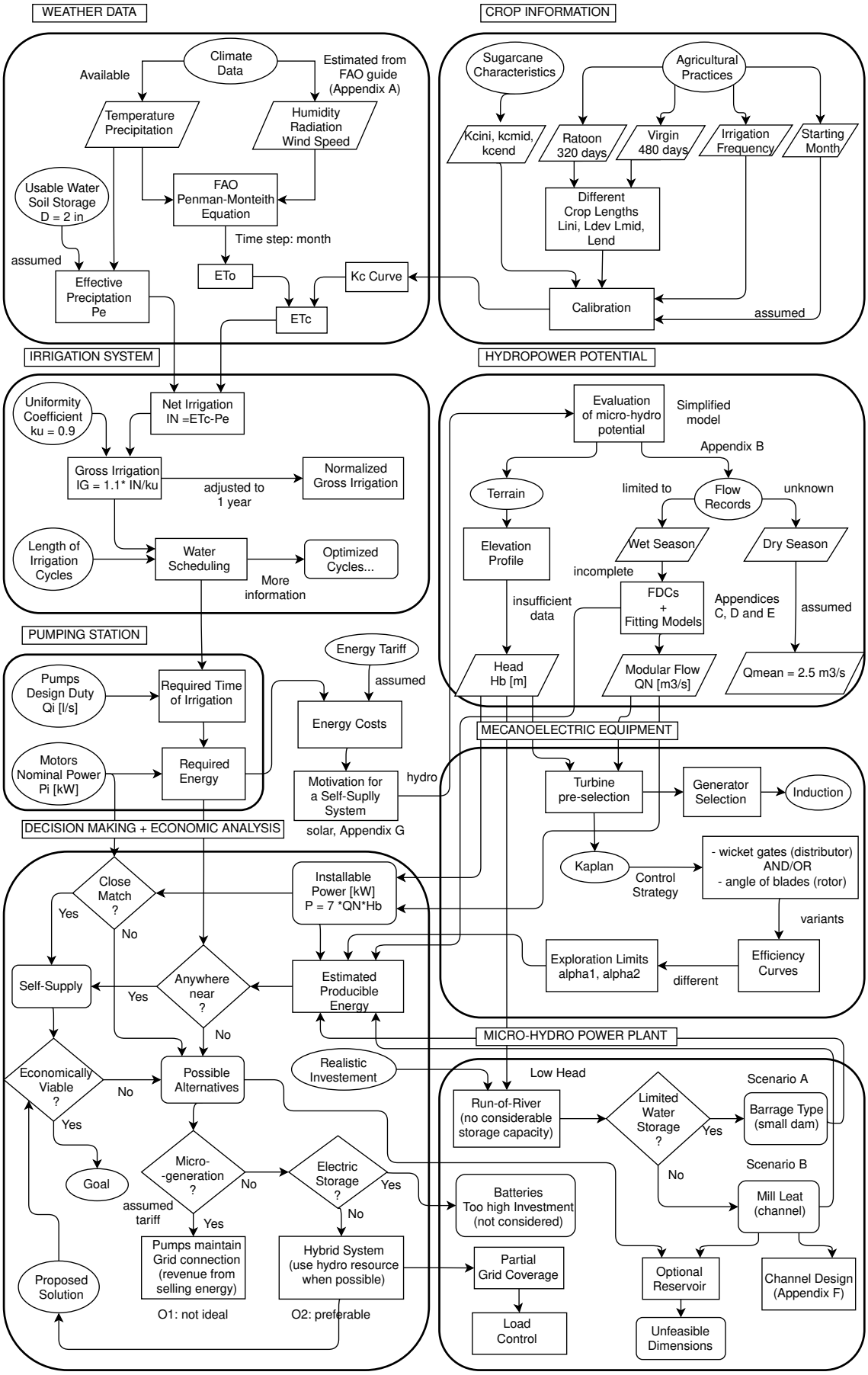

Figure 7.1: Methodology adopted in the progression of this work.

7.3 Relevant Results

7.3.1 Evapotranspiration vs Required Irrigation

Table 7.1 summarizes the total irrigation requirements obtained from the FAO Penman-Monteith method, estimated from effective precipitation, which in turn is based on precipitation and evapotranspiration data.

Table 7.1: Evapotranspiration vs irrigation for the scenarios considered.

Ref. Evapotranspiration		Original Scenario (º)	
ET_o^v [mm/cycle]	ET_o^r [mm/cycle]	I_N^0 [mm/year]	I_G^0 [mm/year]
1768.2	1269.9	1366	??
Crop. Evapotranspiration		**Constructed Scenario (º)**	
ET_c^v [mm/cycle]	ET_c^r [mm/cycle]	$\bar{I}_G^v$ [mm/year]	$\bar{I}_G^r$ [mm/year]
1960.4	1449.3	1293.5	1338.4

For the constructed scenario (virgin and ratoon agricultural practices), a normalization of the total gross irrigation $I_G^{v/r}$ to a period of one year was performed to establish a comparison, equation 7.1, where n is the duration of the crop in question, with 480 days for a virgin crop and 320 days for a ratoon one.

$$\bar{I}_G^{v/r} = \frac{365}{n} I_G^{v/r} \tag{7.1}$$

The virgin/ratoon plantation/replantation cycle is unknown, and the duration of the crop in each of the agriculture practices is different, so the total water requirements of Table 7.1 were normalized for the period of one year and the results averaged: 1360 mm/year.

The infield specifications available, Table 3.10 provide a value of 1366 mm/year for the net irrigation requirements. While this value is almost identical to the average normalized water requirements mentioned above, this is misleading, as one refers to a net irrigation and the other to a gross irrigation. One possible explanation is that the net irrigation requirements of Table 7.1 are grossly underestimated due to a number of factors, ranging from wrong assumptions concerning unknown agriculture practices to incomplete or inaccurate climate data, that greatly affect water requirements. Another possibility is that the original irrigation system, from which this value is reported was not designed with a uniformity coefficient k_u in mind, meaning an even distribution of water was assumed, which would be peculiar, given that irrigation is made by sprinkler.

Another possibility that comes to mind is that the water requirements of the crop assumed in the irrigation system designed for the plantation system were based on typical values for sugarcane reported in literature that do not reflect local climate conditions and/or agricultural practices, or the designer simply assumed a safety margin, or both. Considering that one of the pumps is not working, the eventual failure of equipment would be a motivation for designing an over-sized system with such margin.

Either way, in this work, since irrigation needs depend on climate variability, in evaluating the hydroelectric potential, the obtained monthly water requirements are considered, instead of the reported annual net requirements (1366 mm), as they allow the identification of critical months that would otherwise make a self-supply solution impossible to work year long. This being said, a scenario in which the original reported annual water requirements determine energy consumption is also considered.

7.3.2 Energy Requirements vs Energy Generation

The units installed are characterized as far as their design duty and nominal power. The question then is how many hours per month the pumps need to work to deliver the crop water requirements. For the sake of argument, two hypothesis were considered: 3 pumps and 2 pumps (as the larger pump is not working but could be repaired).

The results obtained allow the system to work with 2 pumps most of the time, see Table 3.13, but as it was shown, this is undesirable, as the system working with the 3 pumps sees its energy consumption decrease for the same number of hours of irrigation, that is, the knocked out pump pushes the efficiency of the system up by 16%, see section 3.5 and this alone is reason enough for the system to work with 3 pumps, as it was meant to, and recommend a repair.

The estimated annual consumption E_{req} under the original and constructed scenarios, as well as the estimated annual producible energy E_a under scenarios A and B, and for the stated variations are summarized in Table 7.2.

Table 7.2: Annual required energy vs annual generated energy for the scenarios considered.

E_{req}			E_a		
Original Scenario (º)			Scenario A		
Pumps	E_i^o [MWh]		Season	E_{DR} [MWh]	E_{RR} [MWh]
2	660.17		18/19	398.44	322.20
3	554.36		19/20	203.87	148.86
Constructed Scenario			Scenario B		
Pumps	$\bar{E}_i^v$ [MWh]	$\bar{E}_i^r$ [MWh]	Season	$E(IV)$ [MWh]	
2	625.15	646.83	-	156.72	
3	524.79	542.99	-	-	-

For the constructed scenario (virgin and ratoon agricultural practices), a normalization of the total energy to a period of one year was performed to establish a comparison, equation 7.2, where n is the duration of the crop in question, with 480 days for a virgin crop and 320 days for a ratoon one.

$$\bar{E}_i^{v/r} = \frac{365}{n} E_i^{v/r},\ i = \{2, 3\} \tag{7.2}$$

The nature of the scheme adopted for scenario A naturally results in increased energy production. Even so, as Table 7.2 shows, this is far from ensuring a self-supply system with complete autonomy. Since this would never be feasible under any realistic economically viable scenario, a change in paradigm was required, leading to scenario B, which is aimed at working all year, and therefore make a better use of the installed capacity, albeit at much lower energy production, requiring far lower values of investment. As a possible boost at energy production under scenario B, a reservoir capable of loading the channel leading to the turbine for the duration of the irrigation cycle was considered, but found to be impractical both due to its required dimensions to store the volume of water determined to power just one pump, but also, to the nonexistence of a workable head.

While scenario A would allow, in theory for a self-supply system during the wet season, Table 5.4, provided a barrage type run-of-river hydroplant is built, and this would already represent a considerable investment, the defining uncertainty here concerns to the availability of the hydro resource during the dry season, as the river flow is not characterized for no data is available. It is possible this solution would work, but without a mean annual chronological flow series to properly evaluate the feasibility of this solution, any decision in theses circumstances is meaningless. In either case, this scenario would definitely represent a higher investment and also greater benefits, whether micro-generation is possible or not, given the limited capacity to store water and regulate somewhat the river flow.

As for scenario B, which implies aiming for lower goals and reducing investment, the channel, designed to work with the river basic flow, which again, is unknown for the dry season but assumed, implies a sharp decrease in energy production making a solution rooted in a self-supply system impossible. What it does however, is allow the turbine to produce a lower but nearly constant energy output year long. It was also considered that a reservoir could load the channel, however, with this solution not even one of the pumps would be able to be shut off from the grid in the dry season for the duration of the irrigation cycle, and adding to this, the reservoir would need to be so large, that effectively, this would be a storage power plant, instead of a run-of-river with limited to no storage.

The technically viable solution then is, it would appear, to consider scenario B, in which the channel is sized to work with the river basic flow. The derivation point will depend on local terrain, to maximize the net height achievable after losses in the channel are discounted, and on the status of the adjacent traversed lands (owners, obstacles, construction difficulty, etc.).

7.3.3 Consumption Metrics

7.3.3.1 Energy Demand

It is useful to characterize energy consumption per unit of water applied, i.e., D_i [kWh/m^3] for both scenarios considered, equation 7.3. Similarly, energy consumption per unit of area covered $D_i^{'}$ [kWh/ha], is computed for both scenarios from equation 7.4.

.

$$D_i^0 = 10^3 \times \frac{E_i^0}{I_N^0 \times A} \qquad \bar{D}_i^{v/r} = 10^3 \times \frac{E_i^{v/r}}{I_G^{v/r} \times A}, \qquad i = \{2, 3\} \tag{7.3}$$

$$D_i^{0^{'}} = 10^3 \times \frac{E_i^0}{A} \qquad \bar{D}_i^{v/r^{'}} = 10^3 \times \frac{E_i^{v/r}}{A}, \qquad i = \{2, 3\} \tag{7.4}$$

The results of equations 7.3 and 7.4 are summarized in Table 7.3 for a command area $A = 187.9$ ha.

Table 7.3: Energy consumption metrics.

Original Scenario (º)					Energy-Water Metric		Energy-Area Metric	
Pumps	E_i^o [MWh]		I_N^0 [m^3/ha]		D_i^o [kWh/m^3]		$D_i^{o^{'}}$ [kWh/ha]	
2	660.17		13 660		0.257		3513.4	
3	554.36				0.216		2950.3	
Constructed Scenario					Energy-Water Metric		Energy-Area Metric	
Pumps	$\bar{E}_i^v$ [MWh]	$\bar{E}_i^r$ [MWh]	$\bar{I}_G^v$ [m^3/ha]	$\bar{I}_G^r$ [m^3/ha]	$\bar{D}_i^v$ [kWh/m^3]	$\bar{D}_i^r$ [kWh/m^3]	$\bar{D}_i^{v^{'}}$ [kWh/ha]	$\bar{D}_i^{r^{'}}$ [kWh/ha]
2	625.15	646.83	12 935	13 384	0.257	0.257	3327.0	3442.4
3	524.79	542.99			0.216	0.216	2792.9	2889.8

It is no surprise that the values of the Energy-Water metric are independent of the scenarios considered, since the energy demand was indirectly estimated from water requirements.

7.3.3.2 Cost of Irrigation

Similarly to the previous discussion, the cost of energy associated with irrigation can be expressed relative to the volume of water used, Ce_i [€/m^3], or relative to the area of plantation under exploration, $Ce_i^{'}$ [€/ha], equations 7.5 and 7.6, respectively.

$$Ce_i^0 = \frac{C_i^0}{I_N^0 \times A} \qquad \bar{C}e_i^{v/r} = \frac{C_i^{v/r}}{I_G^{v/r} \times A}, \qquad i = \{2, 3\} \tag{7.5}$$

$$Ce_i^{0^{'}} = \frac{C_i^0}{A} \qquad \bar{C}e_i^{v/r^{'}} = \frac{C_i^{v/r}}{A}, \qquad i = \{2, 3\} \tag{7.6}$$

The ensuing results are presented in Table 7.4.

Table 7.4: Cost of irrigation metrics.

Original Scenario (º)					Cost-Water Metric		Cost-Area Metric	
Pumps	C_i^o [€]		I_N^0 [m^3/ha]		Ce_i^o [€/m^3]		$Ce_i^{o'}$ [€/ha]	
2	54 881		13 660		0.021		292.1	
3	46 091				0.018		245.3	
Constructed Scenario					**Cost-Water Metric**		**Cost-Area Metric**	
Pumps	$\bar{C}_i^v$ [€]	$\bar{C}_i^r$ [€]	$\bar{I}_G^v$ [m^3/ha]	$\bar{I}_G^r$ [m^3/ha]	$\bar{C}e_i^v$ [€/m^3]	$\bar{C}e_i^r$ [€/m^3]	$\bar{C}e_i^{v'}$ [€/ha]	$\bar{C}e_i^{r'}$ [€/ha]
2	52 584	54 196	12 935	13 384	0.021	0.021	279.9	288.4
3	44 247	45 569			0.018	0.018	235.5	242.5

As before, the cost of irrigation per unit of water applied is only sensitive to the number of working pumps, as the two arrangements present a difference in efficiency estimated at 16%. Otherwise, this metric remains constant across scenarios.

7.3.4 Economic Analysis

The various scenarios and hypothesis considered were tested for viability under often used indicators in power plant investment projects, such as the LCOE, NPV and IRR.

Scenario A was found to be utterly nonviable, presenting levels of LCOE far above those reported for similar hydro projects elsewhere in the world and resulting in negative NPV values across all its variations.

Scenario B was found to be conservatively viable, if the lower to average values on the investment interval for the installed capacity determined, $P = 20\,\text{kW}$ are considered and assuming that all energy generated can be consumed when needed, implying the assumption of storage in the reservoir. This allows to consider the cost avoided by not buying that portion of energy from the grid as a gross benefit, thus being preferable to inject in part or whole, the generated energy in the grid as the remuneration incurred from this is far inferior to the tariff practiced when selling energy to the consumer.

However, one should not assume this is indicative of project viability, and in fact, several times the fact that the FDCs are incomplete and based in only 3 individual seasons was mentioned, definitely affecting the validity of the assumptions made as well as their consequences. Furthermore, no data on similar projects in Mozambique is known, and the cost of investment could be grossly under or overestimated.

Chapter 8

Conclusions

8.1 Achievements

Although a workable value of irrigation needs was known from the infield specifications, this was supposedly an annual value. When researching the specifics of the sugarcane crop in exploring possible solutions, one is lead to the FAO water irrigation guide, where a distinction in agriculture practices and wetting frequency, to name a few, implies a variable water duty for the crop according to the time step in question. Given that the climate data available for both temperature and precipitation, was on a monthly basis, this suggested a value for irrigation needs specific for each month.

Similarly, when asking what value of energy would need to be produced to partially or totally suppress the dependence on the grid, it was natural to consider several scenarios. For the sake of argument, the wort case in respect to energy consumption would coincide with the month for which irrigation needs would peak. And, while the system would not necessarily have to be designed to handle the most energy demanding months, this led to a desire to work with monthly water requirements. Although this approach could be avoided, if access to energy bills was provided, as this would allow an estimation of monthly water requirements, it would still have been preferred as it can allow for the design of a flexible irrigation system. Reportedly, irrigation is suspended for two weeks when precipitation reaches 70 mm in the region. This is obviously an inefficient method for scheduling irrigation and, at this stage, it was unknown what solution would be adopted, specifically if the present system would have to be modified.

As for the installation of a micro-hydro power plant, scenario A naturally results in a greater energy production than scenario B as the volume of water passing through the turbine is considerably larger. Still, this is not cost-effective, and would imply greater construction works with high level of investment and ecological impact. Therefore, scenario B, while in the limit of viability, presents itself as the preferred candidate, at least within the scope of this work, that employed simplified models to estimate energy production.

As to the validation of results, in regard to either the estimated water requirements or energy consumption, since no energy bills are available and no direct line of communication exists with the association, it is not possible to validate the results obtained, and at each step, these influence the next layer of the model. As an example, from Figure 7.1, one sees that any wrong assumption or uncertainty concerning infield practices propagates to the water requirements estimation which in turn influence the estimation of energy consumption, both in terms of demand, that determines the technical viability of the power plant in achieving a self-supply system, but also, in terms of projected energy costs that impact economical viability.

8.2 Future Work

Starting with the water requirements determined according to the FAO Penman-Monteith equation, a better knowledge of missing weather parameters would increase accuracy of the estimated reference evapotranspiration ET_o. Similarly, a better understanding of the agriculture practices, namely the cycle of rotation between ratoon and virgin crops, the usual starting month and the duration of the crop, as well as irrigation scheduling would allow for a better calibration of the single crop coefficient k_c, resulting in a better estimate of the crop evapotranspiration, ET_c. In this regard, it is proposed that local measurements of estimated missing parameters be carried out to better model the climate's influence on the crop water requirements, ultimately impacting irrigation needs. Similarly, a better scheduling of irrigation shifts, assumed as of now to be equally apart and of equal duration, in conjunction with the variation of the climate, would allow for a more efficient use of water, and as a consequence lead to a decrease in energy consumption.

It is known that while irrigation is made by sprinkler, the rotation of sprinklers is performed by hand. However, a dynamic irrigation schedule, based on locally acquired weather data could be designed, implemented and controlled via locally installed sensors connected to an Arduino board, for example, to ensure crop needs at the lowest possible costs. While, the work shifts of workers would be a constraint in scheduling these variable cycles, a move to automatic irrigation would be more efficient in achieving this. As an alternative, the cycles could always start at the same time but an alert be putted out to suspend irrigation (for example) or the system could directly shut off the pumps and or certain lines.

The missing H-Q curves as well as a precise understanding of infield agricultural practices would be useful to better understand the current system and improve upon it. Also, the H-Q curves could indicate the need for maintenance, as typically, these systems move away from the design duty point with age leading to a decreased efficiency.

Concerning the evaluation of hydropower potential, access to longer river flow records, for this location, that include the dry season, would allow to work with a mean chronological daily flow series instead of considering each season separately. This presents itself as a prerequisite in any future work related

to this endeavor. In the same manner, a detailed study of the terrain to properly evaluate the head of the river and the status of the surrounding terrain, namely, if it is sound for construction, what are the ecological impacts, etc, would allow for a better selection of options in the pre-planing phase.

As far as storage is concerned, the possibility of storing water in distributed reservoirs across the plantation could be studied.

Lastly, one could also study the viability of implementing variations of either scenario discussed, A or B, in leading water from a higher elevation, to the existing pumps that in conjunction with the hydraulic circuit could be modified to work as turbines (PAT) in off-periods, to generate energy and/or pump water to a reservoir in a pumped-storage hydroelectricity scheme.

Bibliography

[1] The world bank in mozambique: Overview. https://www.worldbank.org/en/country/mozambique/overview, 2020. Accessed: 2020-10-31.

[2] T. Bucx, M. Marchand, B. Makaske, and C. van de Guchte. Comparative assessment of the vulnerability and resilience of 10 deltas – synthesis report. delta alliance report number 1., 2010.

[3] B. Nhamire and J. Mosca. Electricidade de moçambique: mau serviço, não transparente e politizada. https://cipmoz.org/wp-content/uploads/2018/08/339_Relato%CC%81rio_Electricidade_de_Moc%CC%A7ambique.pdf, 2014.

[4] Crop information, sugar cane. http://www.fao.org/land-water/databases-and-software/crop-information/sugarcane/en/.

[5] R. A. Molijn, L. Iannini, J. Vieira Rocha, and R. F. Hanssen. Sugarcane productivity mapping through c-band and l-band sar and optical satellite imagery. *Remote Sensing*, 11(9), 2019. ISSN 2072-4292. doi: 10.3390/rs11091109. URL https://www.mdpi.com/2072-4292/11/9/1109.

[6] I. Jelsma, A. Bolding, and M. Slingerland. Smallholder sugarcane production systems in xinavane, mozambique: Report from the field. 12 2010.

[7] P. Dias. Anaysis of incentives and disincentives for sugar cane in mozambique. technical notes series, mafap, 2013.

[8] ALER. Energias renováveis em moçambique: Relatório nacional do ponto de situação, 2º edição. Technical report, Associação Lusófona de Energias Renováveis, 2017.

[9] C. D. Konstapel, A. Vermeer, R. L. Voortman, and F. Haupt. Sumário do potencial agrícola das províncias de maputo e gaza. Série Terra e Água Nota Técnica, Nº26, Instituto Nacional de Investigação Agronómica, 1987.

[10] Monthly weather forecast and climate maputo, mozambique. https://www.weather-atlas.com/en/mozambique/maputo-climate#rainfall. Accessed: March, 2020.

[11] Maputo climate (mozambique). https://en.climate-data.org/africa/mozambique/maputo/maputo-535/. Accessed: March, 2020.

[12] G. et Al. Atlas das energias renováveis de moçambique, 2014.

[13] R. G. Allen, L. S. Pereira, D. Raes, and M. Smith. Fao irrigation and drainage paper no. 56. (guidelines for computing crop water requirements).

[14] H. Radwan. *Irrigation Water requirment*, pages 1–302. 09 1993.

[15] S. Silva, J. Dantas Neto, I. Teodoro, J. De Souza, G. Lyra, and M. Santos. Demanda hídrica da cana-de-açúcar irrigada por gotejamento nos tabuleiros costeiros de alagoas. *Revista Brasileira de Engenharia Agrícola e Ambiental*, 19:849–856, 09 2015. doi: 10.1590/1807-1929/agriambi.v19n9p849-856.

[16] A. Z. Mohamed, R. Peters, X. Zhu, and A. Sarwar. Adjusting irrigation uniformity coefficients for unimportant variability on a small scale. *Agricultural Water Management*, 213:1078–1083, 03 2019. doi: 10.1016/j.agwat.2018.07.017.

[17] J. Viholainen, J. Tamminen, T. Ahonen, J. Ahola, E. Vakkilainen, and R. Soukka. Energy-efficient control strategy for variable speed-driven parallel pumping systems. *Energy Efficiency*, 6:2, 08 2013. doi: 10.1007/s12053-012-9188-0.

[18] A. Quintela. *Hidráulica*. Serviço de Educação e Bolsas. Fundação Calouste Gulbenkian, 12º edition, 2011.

[19] Green power partnership, self supply. `https://www.epa.gov/greenpower/self-supply`. Accessed: June, 2021.

[20] M. M. Uamusse, K. Tussupova, and K. M. Persson. Climate change effects on hydropower in mozambique. *Applied Sciences*, 6:2, 19 2020. doi: 10.3390/app10144842.

[21] Tripartite interim agreement between the republic of mozambique and the republic of south africa and the kingdom of swaziland for co-operation on the protection and sustainable utilisation of the water resources of the incomati and maputo watercourses. `http://www.fao.org/faolex/results/details/en/c/LEX-FAOC034943/`, 2002.

[22] A guide to uk mini-hydro developments. `https://www.british-hydro.org/wp-content/uploads/2018/03/A-Guide-to-UK-mini-hydro-development-v3.pdf`, 2012.

[23] R. Castro. *Uma Introdução às Energias Renováveis: Eólica, Fotovoltaica e Mini-Hídrica*, chapter ENERGIA MINI-HÍDRICA, pages 71–86. Number 35 in Colecção Ensino da Ciência e da Tecnologia. IST Press, 2º edition, Outubro 2012.

[24] C. Mataix. *Mecanica de Fluidos Y Maquinas Hidraulicas*. Ediciones del Castilio, S. A., Madrid, 1986.

[25] J. Paiva. *Redes de Energia Eléctrica, Uma Análise Sistémica*. Number 16 in Colecção Ensino da Ciência e da Tecnologia. IST Press, 3º edition, Agosto 2011.

[26] E. Corà. Hydropower techologies, the state-of-the-art. https://consultation.hydropower-europe.eu/assets/consultations/2019.08.13%20HydropowerTechnology_State%20of%20the%20Art%20FINAL.pdf, August 2019.

[27] Hydropower, costs. https://iea-etsap.org/E-TechDS/PDF/E06-hydropower-GS-gct_ADfina_gs.pdf, 6 2010. Accessed: June, 2021.

[28] North west hydro resource model, engineering options, turbine costs. http://www.engineering.lancs.ac.uk/lureg/nwhrm/engineering/turbine_costs.php. Accessed: June, 2021.

[29] Final report cost of energy (lcoe), energy costs, taxes and the impact of government interventions on investments. http://trinomics.eu/wp-content/uploads/2020/11/Final-Report-Cost-of-Energy-LCOE.pdf, October 2020. Accessed: June, 2021.

Appendix A

Evapotranspiration

A.1 Reference Evapotranspiration (ET_o)

Evapotranspiration is a combination of two processes occurring simultaneously: evaporation and transpiration. In the former, water is lost from the soil surface through solar radiation, air temperature, air humidity and wind speed, whereas in the latter, water is predominantly lost through plant stomata [13]. These two processes occur simultaneously, however, since evaporation strongly depends on the fraction of radiation that reaches the soil, this process becomes less predominant in relation to transpiration, as the growing of the crop and the development of a larger canopy casts a broader shadow on the soil and the more canopy in a crop the more important transpiration will be.

The evapotranspiration rate is computed in relation to a reference surface, and is then called the reference evapotranspiration, ET_o, where the reference surface is a hypothetical grass reference crop with specific characteristics [13]. As mentioned before, E_o is only influenced by climatic parameters, thus it can be computed solely from weather data. Where this data is unavailable the guide provides procedures for estimating it.

A.1.1 Penman-Monteith combination Equation

The combination method, introduced by Penman in 1948, combined the energy balance with mass transfer to compute the evaporation from an open water surface from climatic records of sunshine, temperature, humidity and wind speed. Later this method was further extended by others by use of resistance factors that incorporate aerodynamic resistance, r_a manifested as friction from upward flowing air through vegetation, and surface resistance, r_s that accounts for the resistance to the flow of vapour through vegetation stomata openings, total leaf area and soil surface [13].

The Penman-Monteith combination equation is then:

$$\lambda ET = \frac{\Delta(R_n - G) + \rho_a c_p \frac{(e_s - e_a)}{r_a}}{\Delta + \gamma\left(1 + \frac{r_s}{r_a}\right)} \tag{A.1}$$

where

R_n : net radiation $[MJ/(m^2.day)]$

G : soil heat flux $[MJ/(m^2.day)]$

$e_s - e_a$: vapour pressure deficit of the air [kPa]

ρ_a : mean air density at constant pressure $[Kg/m^3]$

c_p : specific heat of the air [KJ/Kg]

Δ : slope of the saturation vapour pressure temperature relationship $[kPa/^\circ C]$

γ : psychrometric constant $[kPa/^\circ C]$

r_s : bulk (surface) resistance [s/m]

r_a : aerodynamic resistance [s/m]

For a grass reference surface, the aerodynamic and surface resistances are just

$$r_a = \frac{208}{u_2} \tag{A.2}$$

$$r_s = 70 \tag{A.3}$$

Substituting (A.2) and (A.3) in (A.1), it follows the FAO Penman-Monteith method to estimate ET_o:

$$ET_o = \frac{0.408\Delta(R_n - G) + \gamma \frac{900}{T+273} u_2 (e_s - e_a)}{\Delta + \gamma(1 + 0.34u_2)} \tag{A.4}$$

where

ET_o : reference evapotranspiration [mm/day]

R_n : net radiation at the crop surface $[MJ/(m^2.day)]$

G : soil heat flux density $[MJ/(m^2.day)]$

T : mean daily air temperature at 2 m height $[^\circ C]$

u_2 : wind speed at 2 m height [m/s]

e_s : saturation vapour pressure [kPa]

e_a : actual vapour pressure [kPa]

$e_s - e_a$: vapour pressure deficit [kPa]

Δ : slope of the saturation vapour pressure temperature relationship $[kPa/^\circ C]$

γ : psychrometric constant $[kPa/^\circ C]$

The FAO Penman-Monteith Equation then requires data concerning air temperature, humidity, radiation and wind speed for the desired time-step calculations. Usually these are daily, weekly, ten-day or monthly calculations, but since the only directly available data is temperature - hourly monthly averages, as discussed before, the missing data will be estimated in accordance with the guide's instructions.

Location:

Table A.1: Location of the case study.

Latitude	Longitude	Altitude
25º01'S	32º41'E	26 m

Note: Data taken from google earth/google maps.

Temperature: The (average) daily maximum and minimum air temperatures are required:

Table A.2: Average daily maximum and minimum air temperatures by month.

	Jan	Feb	Mar	Apr	May	Jun	Jul	Aug	Sept	Oct	Nov	Dec
T_{min} [° C]	23.02	23.20	22.14	19.91	17.31	15.43	14.70	15.96	18.47	19.93	21.19	22.46
T_{max} [° C]	30.46	31.69	30.44	28.29	27.54	25.89	25.14	26.86	29.14	29.55	30.01	30.79

Humidity: As for humidity, the (average) daily actual vapour pressure, e_a, in kilopascals (kPa) is required, but since this is not available, the guide says it can be derived from the dewpoint temperature (ºC). However, the dewpoint is also not available but, when missing, it can be assumed to be equal to the (average) daily minimum air temperature.

Radiation: In regard to the radiation factor, the (average) daily net radiation (MJ.m^{-2}.day^{-1} is required, but when missing it can be derived from the daily (average) hours of sunshine.

Wind speed: The (average) daily wind speed (m.s^{-1}) measured at a height of 2 m is required, but when missing it can be assumed to be 2 meters per second.

Atmospheric Pressure (P)

The atmospheric pressure, P, is given by:

$$P = 101.3\left(\frac{293 - 0.0065\,z}{293}\right)^{5.26} \tag{A.5}$$

where z is the elevation above sea level [m].

For the location in question, z = 26 m results in P = 100.993 kPa.

Latent Heat of Vaporization (λ)

Over normal temperature ranges, λ remains fairly constant, and a value of 2.45 MJ/kg corresponding to an air temperature of approximately 20°C is assumed.

$$\lambda = 2.45 \tag{A.6}$$

Pychrometric Constant (γ)

The psychrometric constant, γ, is given by:

$$\gamma = \frac{c_{p\,P}}{\epsilon\,\lambda} \tag{A.7}$$

where

- γ : pychrometric constant [kPa/° C]
- P : atmospheric pressure [kPa]
- λ : latent heat of vaporization [MJ/Kg]
- c_p : specific heat at constant pressure, $1.013\,10^{-3}$ [MJ/(Kg.° C)]
- ϵ : ratio molecular weight of water vapour/dry air $= 0.622$

For the previously determined value of P = 100.993 kPa, the psychrometric constant is $\gamma = 0.0671$ kPa/° C

Mean Air Temperature (T_{mean})

The FAO Penman-Monteith equation requires the mean daily air temperature (T_{mean}) to calculate the slope of the saturation vapour pressure curves (Δ) and to quote the guide, "for standardization, T_{mean} for 24-hour periods is defined as the mean of the daily maximum (T_{max}) and minimum temperatures (T_{min}) rather than as the average of hourly temperature measurements".

$$T_{mean} = \frac{T_{max} + T_{min}}{2} \tag{A.8}$$

From Table A.2, the monthly average mean temperature is immediately obtained:

Table A.3: Daily average mean temperature by month.

	Jan	Feb	Mar	Apr	May	Jun	Jul	Aug	Sept	Oct	Nov	Dec
T_{mean} [° C]	26.7400	27.4450	26.2900	24.1000	22.4250	20.6600	19.9200	21.4100	23.8050	24.7400	25.6000	26.6250

Mean Saturation Vapour Pressure (e_s)

Saturation vapour pressure can be calculated from air temperature with the relationship expressed by:

$$e^o(\mathsf{T}) = 0.6108\, e^{\left[\frac{17.27\,\mathsf{T}}{\mathsf{T}+237.3}\right]} \tag{A.9}$$

where

$e^o(\mathsf{T})$: saturation vapour pressure at air temperature T [kPa]
T : air temperature [° C]

The guide advises that "due to the non-linearity of the above equation, the mean saturation vapour pressure for (...) a month should be computed as the mean between the saturation vapour pressure at the mean daily maximum and minimum air temperatures for that period":

$$\mathsf{e_s} = \frac{e^o(\mathsf{T_{max}}) + e^o(\mathsf{T_{min}})}{2} \tag{A.10}$$

Again, considering Table A.2, this yields

Table A.4: Daily average mean saturation vapour pressure.

	Jan	Feb	Mar	Apr	May	Jun	Jul	Aug	Sept	Oct	Nov	Dec
e_s [kPa]	3.5846	3.7579	3.5090	3.0848	2.8280	2.5464	2.4335	2.6749	3.0820	3.2315	3.3808	3.5791

Slope of Saturation Vapour Pressure Curve (Δ)

At a given temperature, the slope of the curve is

$$\Delta = \frac{4098\left[0.6108\, e^{\left(\frac{17.27\,\mathsf{T}}{\mathsf{T}+237.3}\right)}\right]}{(\mathsf{T}+237.3)^2} \tag{A.11}$$

where

Δ : slope of the saturation curve at air temperature T [kPa/° C]
T : air temperature [° C]

In the FAO Penman-Monteith equation, the slope of the vapour pressure curve is computed using mean air temperature. Thus, from Table A.2 it follows that

Table A.5: Daily average slope of the saturation vapour pressure curve.

	Jan	Feb	Mar	Apr	May	Jun	Jul	Aug	Sept	Oct	Nov	Dec
Δ [kPa/° C]	0.2064	0.2140	0.2017	0.1800	0.1648	0.1500	0.1441	0.1562	0.1773	0.1861	0.1946	0.2052

Actual Vapour Pressure (e_a) derived from dewpoint temperature

The actual vapour pressure (e_a) is the saturation vapour pressure at the dewpoint temperature (T_{dew}):

$$e_a = 0.6108\, e^{\left[\frac{17.27\, T_{dew}}{T_{dew}+237.3}\right]} \tag{A.12}$$

The dewpoint temperature is unknown, but it can be assumed to be equal to the (average) daily minimum temperature (T_{min}),

$$T_{dew} = T_{min} \tag{A.13}$$

Then, from Table A.2, it follows that

Table A.6: Monthly actual vapour pressure.

	Jan	Feb	Mar	Apr	May	Jun	Jul	Aug	Sept	Oct	Nov	Dec
e_a [kPa]	2.8128	2.8436	2.6666	2.3253	1.9761	1.7531	1.6727	1.8136	2.1258	2.3282	2.5162	2.7190

Vapour Pressure Deficit ($e_s - e_a$)

The difference between the saturation vapour pressure (e_s) and the actual vapour pressure (e_a) for a given time period is called the vapour pressure deficit. For periods such as a month e_s is computed from Equation A.10 using the T_{max} and T_{min} averaged over that time period. Similarly the e_a is computed with equation A.12, using average dewpoint temperatures over that period. Thus, from Tables A.4 and A.6, it follows that:

Table A.7: Daily average actual vapour pressure.

	Jan	Feb	Mar	Apr	May	Jun	Jul	Aug	Sept	Oct	Nov	Dec
$(e_s - e_a)$ [kPa]	0.7717	0.9143	0.8424	0.7595	0.8519	0.7933	0.7608	0.8613	0.9562	0.9033	0.8647	0.8601

Extraterrestrial Radiation for daily periods (R_a)

According to the guide, 'the extraterrestrial radiation, R_a, for each day of the year and for different latitudes can be estimated from the solar constant, the solar declination and the time of the year" by:

$$R_a = \frac{24\,(60)}{\pi}\, G_{sc}\, d_r\, [\omega_s \sin(\varphi)\sin(\delta) + \cos(\varphi)\cos(\delta)\sin(\omega_s)] \tag{A.14}$$

where

R_a : extraterrestrial radiation $[MJ/(m^2.day)]$

G_{sc} : solar constant $= 0.0820\, MJ/(m^2.min)$

d_r : inverse relative distance Earth-Sun

ω_s : sunset hour angle [rad]

φ : latitude [rad]

δ : solar declination [rad]

and with the inverse relative distance Earth-Sun, d_r, and the solar declination, δ, given by:

$$d_r = 1 + 0.033 \cos\left(\frac{2\pi}{365} J\right) \tag{A.15}$$

$$\delta = 0.409 \sin\left(\frac{2\pi}{365} J - 1.39\right) \tag{A.16}$$

where J denotes the number of the day of the year and assumes values between 1 (1 January) and 365 or 366 (31 December).

The sunset hour angle, ω_s, is given by:

$$\omega_s = \arccos[-\tan(\varphi)\tan(\delta)] \tag{A.17}$$

Since the computation of ω_s, d_r and δ is performed on a daily basis, the extraterrestrial radiation R_a is also given on a daily basis, i.e., R_a is an array with 365 values.

Now, the previous discussed parameters that are required for the estimation of ET_o were computed on a monthly basis (because that is the imposed time step with the available data), and so, monthly averages for R_a were performed:

Table A.8: Monthly average extraterrestrial radiation.

	Jan	Feb	Mar	Apr	May	Jun	Jul	Aug	Sept	Oct	Nov	Dec
R_a [MJ/(m^2.day)]	41.5469	38.1371	32.4134	26.4658	22.1987	21.4039	24.2853	29.8252	35.6907	40.3072	42.6700	43.1112

Daylight Hours (N)

The number of hours of daylight, N, is given by:

$$N = \frac{24}{\pi}\omega_s \tag{A.18}$$

where ω_s is given by equation A.17.

As before, this results in a array with 365 elements, so once more, monthly averages were performed:

Table A.9: Daily average daylight hours.

	Jan	Feb	Mar	Apr	May	Jun	Jul	Aug	Sept	Oct	Nov	Dec
N [h]	13.1415	12.5373	11.7685	11.0659	10.5579	10.4662	10.8314	11.4987	12.2439	12.9654	13.4473	13.5262

Solar Radiation (R_s) derived from air temperature differences

In the absence of solar radiation data, the Hargreaves' radiation formula, adjusted and validated at several weather stations in a variety of climate conditions, becomes:

$$R_s = k_{R_s} \sqrt{T_{max} - T_{min}}\, R_a \tag{A.19}$$

where

R_s : solar radiation $[MJ/(m^2.day)]$
T_{max} : maximum air temperature $[^\circ C]$
T_{min} : minimum air temperature $[^\circ C]$
k_{R_s} : adjustment coefficient $(0.16 \,..\, 0.19)$ $[^\circ C^{-0.5}]$

The guide says that 'for interior locations, where land mass dominates and air masses are not strongly influenced by a large water body, $k_{R_s} \simeq 0.16$ and for coastal locations, situated on or adjacent to the coast of a large land mass and where air masses are influenced by a nearby water body, $k_{R_s} \simeq 0.19$.' Given the location of Magude, it is reasonable to assume an intermediate value of $k_{R_s} = 0.175\,^\circ C^{-0.5}$.

It should also be noted that instead of using the determined daily extraterrestrial radiation values in the above formula, the average monthly values were used, yielding:

Table A.10: Daily average solar radiation.

	Jan	Feb	Mar	Apr	May	Jun	Jul	Aug	Sept	Oct	Nov	Dec
R_s $[MJ/(m^2.day)]$	19.8318	19.4464	16.3419	13.4074	12.4252	12.1143	13.7319	17.2319	20.4021	21.8780	22.1766	21.7746

Clear-Sky Solar Radiation (R_{so})

"When calibrated values for a_s and b_s are not available", the equation to be used is:

$$R_{so} = (0.75 + 2\,10^{-5}\, z) R_a \tag{A.20}$$

where z is the elevation above sea level [m].

For monthly averages of the extraterrestrial solar radiation, R_a, it follows that

Table A.11: Daily average clear-sky solar radiation.

	Jan	Feb	Mar	Apr	May	Jun	Jul	Aug	Sept	Oct	Nov	Dec
R_{so} [MJ/(m^2.day)]	31.1818	28.6227	24.3269	19.8631	16.6606	16.0641	18.2266	22.3844	26.7866	30.2514	32.0247	32.3559

Net Solar or Net Shortwave Radiation (R_{ns})

"The net shortwave radiation resulting from the balance between incoming and reflected solar radiation is given by:"

$$R_{ns} = (1 - \alpha R)_s \tag{A.21}$$

where α is the albedo or canopy reflexion coeeficient, which is 0.23 for the grass crop reference.

Table A.12: Daily average net solar radiation.

	Jan	Feb	Mar	Apr	May	Jun	Jul	Aug	Sept	Oct	Nov	Dec
R_{ns} [MJ/(m^2.day)]	15.2705	14.9737	12.5833	10.3237	9.5674	9.3280	10.5736	13.2686	15.7096	16.8461	17.0760	16.7665

Net Longwave Radiation (R_{nl})

The net longwave radiation is given by:

$$R_{nl} = \sigma \left[\frac{T_{max,K}{}^4 + T_{min,K}{}^4}{2} \right] (0.34 - 0.14\sqrt{e_a}) \left(1.35 \frac{R_s}{R_{so}} - 0.35 \right) \tag{A.22}$$

where

- σ : Stefan-Boltzmann constant $[4.903\,10^{-9}$ MJ/(K^4.m^2.day)]
- $T_{max,K}$: maximum absolute temperature during the 24-hour period [K]
- $T_{min,K}$: minimum absolute temperature during the 24-hour period [K]
- e_a : actual vapour pressure [kPa]
- R_s : calculated solar radiation [MJ/(m^2.day)]
- R_{so} : calculated clear-sky radiation [MJ/(m^2.day)]

From Tables A.2, A.6, A.10 and A.11, it follows that

Table A.13: Daily average net longwave radiation.

	Jan	Feb	Mar	Apr	May	Jun	Jul	Aug	Sept	Oct	Nov	Dec
R_{nl} [MJ/(m^2.day)]	2.1240	2.3626	2.4482	2.7215	3.5265	3.7821	3.8427	3.8618	3.5209	3.0614	2.6976	2.4169

Net Radiation (R_n)

The difference between the incoming net shortwave radiation (R_{ns}) and the outgoing net longwave radiation R_{nl}) is called the net radiation (R_n):

$$R_n = R_{ns} - R_{nl} \tag{A.23}$$

Table A.14: Daily average net radiation.

	Jan	Feb	Mar	Apr	May	Jun	Jul	Aug	Sept	Oct	Nov	Dec
R_n [MJ/(m^2.day)]	13.1465	12.6111	10.1351	7.6022	6.0409	5.5459	6.7309	9.4068	12.1887	13.7847	14.3784	14.3496

Soil Heat Flux (G)

For monthly periods, the soil heat flux for a given month i is given by:

$$G_{month,i} = 0.07(T_{month,i+1} - T_{month,i-1}) \tag{A.24}$$

where it is assumed that the monthly average temperature for the month i = 0 is that of i = 12 (December) and in the same manner, the monthly average temperature for month i = 13 is that of month i = 1 (January), from which:

Table A.15: Daily average soil heat flux.

	Jan	Feb	Mar	Apr	May	Jun	Jul	Aug	Sep	Oct	Nov	Dec
G [MJ/(m^2.day)]	0.0574	-0.0315	-0.2341	-0.2706	-0.2408	-0.1753	0.0525	0.2719	0.2331	0.1257	0.1319	0.0798

Wind Speed (u_2)

"Where no wind data is available within the region, a value of 2 m/s can be used as a temporary estimate."

$$u_2 = 2\,\mathrm{m/s} \tag{A.25}$$

Estimated Reference Evapotranspiration (ET_o)

Plugging all previous information in equation A.4, it follows that

Table A.16: Estimated daily reference evapotranspiration from the Penman-Monteith equation.

	Jan	Feb	Mar	Apr	May	Jun	Jul	Aug	Sept	Oct	Nov	Dec
ET_o [mm/day]	4.4281	4.5031	3.7949	3.0298	2.7769	2.5746	2.7503	3.4785	4.3234	4.6967	4.8183	4.8479

A.1.2 An Alternative Equation for ET_o when weather data is missing

In the absence of data on solar radiation, relative humidity and/or wind speed, the estimation of these parameters is performed using the procedures presented in the previous section in order to compute the ET_o from the Penman-Monteith equation.

Now, the ET_o is estimated using the Hargreaves ET_o equation:

$$ET_o = 0.0023(T_{mean} + 17.8)(T_{max-T_{min}})^{0.5} R_a \tag{A.26}$$

where all parameters have been previously defined.

So, taking the monthly average values of extraterrestrial solar radiation from Table A.8, it follows that

Table A.17: Estimated daily reference evapotranspiration from the alternative equation.

	Jan	Feb	Mar	Apr	May	Jun	Jul	Aug	Sept	Oct	Nov	Dec
ET_o [mm/day]	4.7366	4.7180	3.8636	3.0124	2.6801	2.4984	2.7775	3.6231	4.5517	4.9906	5.1610	5.1871

A.2 Crop Evapotranspiration (ET_c)

The guide indicates a general procedure for calculating ET_c:

$1)$ Compute ET_o
$2)$ Select stage lengths (verified and supplemented locally)
$3)$ Single crop coefficient, K_c
$4)$ Select values for $K_{c\ ini}$, $K_{c\ mid}$ and $K_{c\ end}$
$5)$ Adjust $K_{c\ ini}$ to reflect wetting frequency of soil surface
$6)$ Adjust $K_{c\ mid}$ and $K_{c\ end}$ to local climatic conditions
$7)$ Construct K_c curve
$8)$ Determine $ET_c = K_c ET_o$

1) Computed ET_o

The reference evapotranspiration, ET_o was estimated by the Penman-Monteith equation and by the alternative Hargreaves equation:

Table A.18: Estimated daily reference evapotranspiration by two different methods.

ET_o [mm/day]	Jan	Feb	Mar	Apr	May	Jun	Jul	Aug	Sep	Oct	Nov	Dec
Penman-Monteith	4.4281	4.5031	3.7949	3.0298	2.7769	2.5746	2.7503	3.4785	4.3234	4.6967	4.8183	4.8479
Hargreaves	4.7366	4.7180	3.8636	3.0124	2.6801	2.4984	2.7775	3.6231	4.5517	4.9906	5.1610	5.1871

It should be noted that the results from the Penman-Monteith equation, where the missing data was estimated, are more accurate than the alternative equation when missing data is not accounted for and instead only the extraterrestrial solar radiation is weighted in. In light of this, from now on, only the values obtained from the Penman-Monteith equation will be considered.

Although there are alternatives to the Penman-Monteith Equation, the later is reported as the most accurate and therefore widely used. So, while the FAO guide gives an alternative equation, for when weather data is missing - only uses temperature data -, the Penman-Monteith FAO method allowing for the use of approximate parameters is still more accurate in predicting the real water requirements of crops.

2) Stage Lengths

The guide provides a table with the lengths (in days) of crop development stages for various planting periods and climatic regions. As seen before, Magude is located at a latitude of 25°S which puts it in the immediate vicinity of the south hemisphere tropic, and so, the following lengths were considered:

Table A.19: Assumed lengths (days) of crop development stages of sugar cane for Magude.

Practice	L_{inic}	L_{dev}	L_{mid}	L_{late}	L_{tot}
Virgin	50	70	220	140	480
Ratoon	30	50	180	60	320

3) Single Crop Coefficient (K_c)

The guide provides a table as a means of choosing the type of the coefficient approach. Since the time step assumed thus far is on a monthly basis and the purpose is to determine the average water requirements for irrigation, the choice must then fall for the single crop coefficient.

4) Selection of values for $K_{c\ ini}$, $K_{c\ mid}$ and $K_{c\ end}$

Similarly, the guide provides a table with the single (time-averaged) crop coefficients, Kc for use with the FAO Penman-Monteith ETo.

Table A.20: Sugar cane crop coefficients $K_{c\ ini}$, $K_{c\ mid}$ and $K_{c\ end}$.

Crop	$K_{c\ ini}$	$K_{c\ mid}$	$K_{c\ end}$
Sugar Cane	0.40	1.25	0.75

5) Adjustment of $K_{c\ ini}$ to wetting frequency

With an initial estimate for $K_{c\ ini}$ taken from the previous table, now the interval between wetting events must be estimated to properly adjust the value of $K_{c\ ini}$.

Wetting events can either refer to rainfall or irrigation. With regard to rainfall, which was discussed in previous sections, the only data available is the monthly averages. The frequency of rainy days or the interval between rains is unknown.

As for the irrigation events, from the infield specification data, we know the irrigation is made by sprinkler with the relevant data on the irrigation management taken from Table 3.10. Assuming the smallholders association follows the irrigation scheme as laid out by the project, then there are 35 cycles of irrigation per year, where each cycle lasts for 6 days with 12 hours a day as stated in the infield specifications.

Assuming the type of sugar cane planted has a lifecyle of exactly one year, then, for each crop planted, there are $35 \times 6 = 210$ days of irrigation and $365 - 210 = 155$ days with no irrigation occurs. And supposing that the cycles are equally apart, then, the interval between irrigation cycles is just

$$\frac{155}{34} \simeq 4.56 \,\text{days}$$

Note: The species of sugar cane planted or even the agriculture practice (virgin/ratoon) is unknown, and so, one can only guess how long the duration of the crop actually is. However, from Table A.19, the total length of the culture is either 480 days $\simeq 1.3$ years for virgin cane or 320 days $\simeq 0.9$ years for ratoon cane). Direct conversation with the association could eliminate this uncertainty by allowing to better calibrate the lengths of crop development stages. Nevertheless, the values will be assumed as they are in the computations ahead.

Another important issue is the date of plantation of the crop, specifically the month, which varies greatly according to the type of cane or the mode of plantation (whole year cane, year and a half cane, winter cane, etc). The reason why this is so important is due to the frequency of raining and the type of the wetting event in question. The guide differentiates between 'Light wetting events (infiltration depths of 10 mm or less): rainfall and high frequency irrigation systems' and 'Heavy wetting events (infiltration depths of 40 mm or more): surface and sprinkler irrigation'. An inadequate choice between these may be detrimental to the correct calibration of $K_{c\ inic}$.

In this analysis it will be assumed that the plantation occurs before August. The latest satellite images from google earth, indicate that a new crop was planted and already irrigated (dark circles) before the beginning of August 2020 and no discernible culture was yet evident at this time. Again, for a better understanding of the crop management practices there should be a local correction of these parameters,

namely through communication with the association, as the guide suggests, but one is limited to the available information.

From this discussion, and correlating with the monthly average precipitation for the months preceeding August, specifically May, June and July, which have the lowest (average) daily values of precipitation ($<$1 mm), one would have to assume light wetting events. On the other hand there is obviously irrigation by sprinkler, and with such low values of daily precipitation and naturally expected long periods between rains (for these months), it stands to reason the wetting is almost entirely assured by sprinkler irrigation, which would classify as a heavy wetting event. Again, without further information from the field, this is impossible to determine. For the time being, we will assume light wetting events during the initial stage of the sugar cane development.

Thus, for light wetting events, those between 3 and 10 mm per event, the adjustment of $K_{c\ inic}$ is performed graphically, in accordance with Figure A.1 adapted from the guide.

For the months in question, the ones where it is assumed that the plantation of a new crop might have occurred, May, June or July, the determined ET_o is within the interval $[2.57 - 2.78]$ mm/day. The interval between wetting events was determined to be around 4.56 days (if the infield specifications from the original design are followed).

Graphically, it will look something like this (roughly)

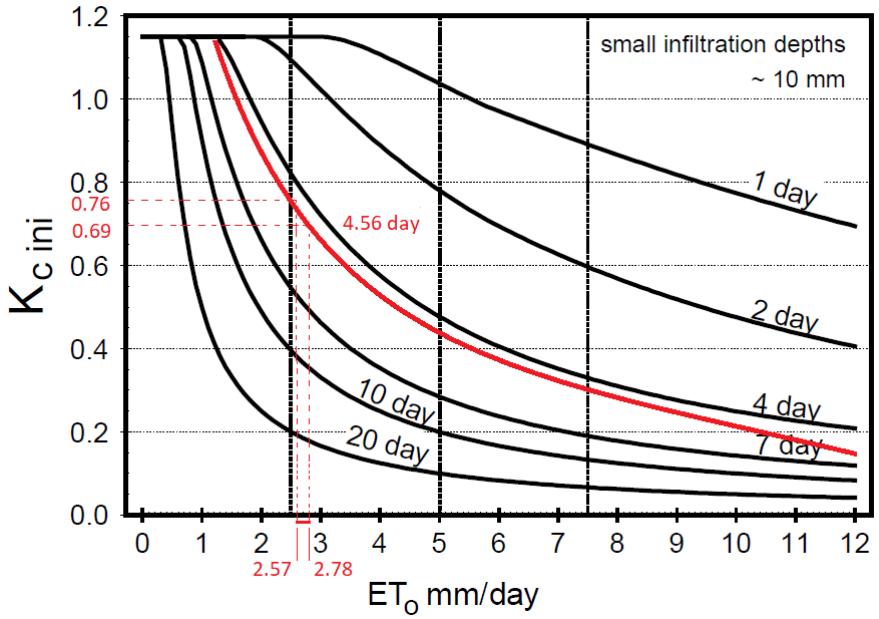

Figure A.1: Correction for $K_{c\ ini}$ under light wetting events and assumed irrigation time intervals.

Then, $K_{c\ ini}$ is between 0.69 and 0.76. The mean of these values is assumed: $K_{c\ ini} = 0.725$

In addition, wetting by sprinkler, as is the case at the Magude plantation, has a fraction f_w of soil surface wetted equal to 1, so no additional correction is necessary for $K_{c\ ini}$.

6) Adjustment of $K_{c\ mid}$ and $K_{c\ end}$ to local climatic conditions With no wind and humidity data available and without local information, is impossible to correct $K_{c\ mid}$ and $K_{c\ end}$.

7) Crop Coefficient Curve

In order to construct the crop coefficient curve, an annual crop will be assumed. The construction on the curve needs only three points, $K_{c\ ini}$, $K_{c\ mid}$ and $K_{c\ end}$ and follows the steps described in the guide:

1) Divide the growing period into four growth stages that describe crop development (initial, crop development, mid-season, and late season), determine the lengths of the growth stages, and identify the three Kc values that correspond to $K_{c\ ini}$, $K_{c\ mid}$ and $K_{c\ end}$.

2) Adjust the Kc values to the frequency of wetting and/or climatic conditions of the growth stages.

3) Construct a curve by connecting straight line segments through each of the four growth stages. Horizontal lines are drawn through $K_{c\ ini}$ in the initial stage and through $K_{c\ mid}$ in the mid-season stage. Diagonal lines are drawn from $K_{c\ inic}$ to $K_{c\ mid}$ within the course of the crop development stage and from $K_{c\ mid}$ to $K_{c\ end}$ within the course of the late season stage.

For virgin sugar cane, the curve obtained is

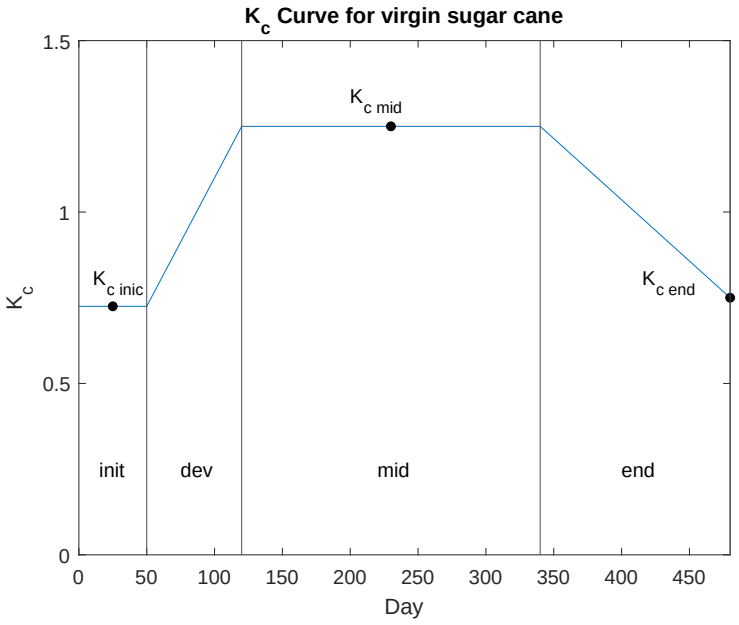

Figure A.2: K_c curve for virgin cane, assuming 480 days of crop cycle.

Whereas for ratoon sugar cane, the curve obtained is

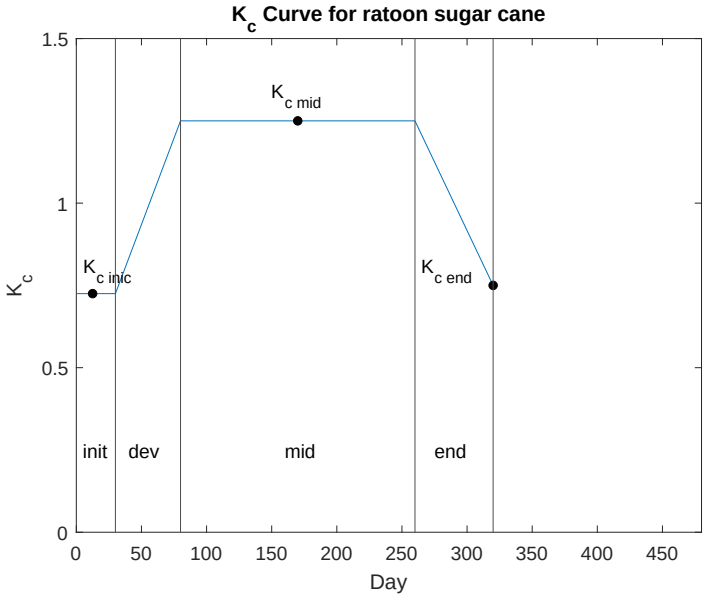

Figure A.3: K_c curve for ratoon cane, assuming 320 days of crop cycle.

8) Determination of ET_c

Given that the reference ETo was computed in a monthy time step, monthly values for Kc are necessary to compute ET_c. A general procedure is to construct the K_c curve, overlay the curve with the lengths of the months in question, and to derive graphically from the curve the K_c value for the period under consideration.

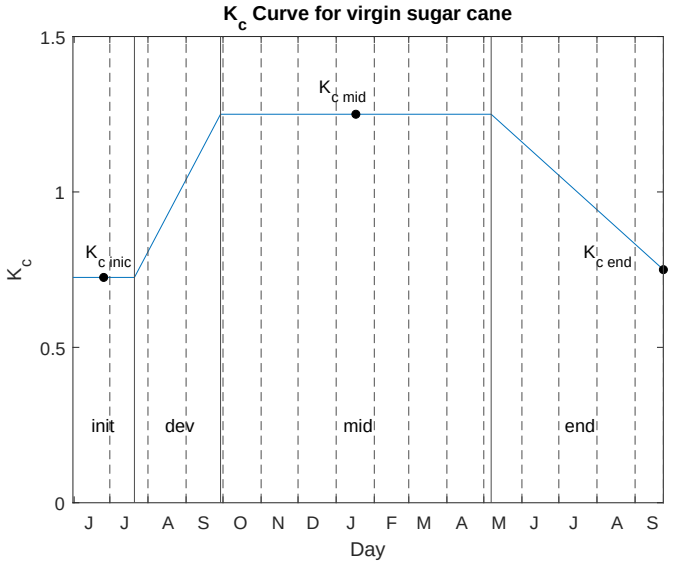

Figure A.4: K_c curve for virgin cane, assuming June as the commencement of crop cycle.

Previously it was assumed the plantation of the crop began somewhere between May and July. For the purpose of these computations let us assume the crop is usually planted in the beginning of June. This being the case, then the graph becomes that of Figure A.4.

Taking the values determined for the reference evapotranspiration, ET_o, and extracting the correspondent K_c for each month, results in

Table A.21: Estimated daily ETc by the crop coefficient method - virgin cane, plantation in June.

	Jun	Jul	Aug	Sept	Oct	Nov	Dec	Jan	Feb	Mar	Apr	May	Jun	Jul	Aug	Sept
ET_o [mm/day]	2.5746	2.7503	3.4785	4.3234	4.6967	4.8183	4.8479	4.4281	4.5031	3.7949	3.0298	2.7769	2.5746	2.7503	3.4785	4.3234
K_c	0.7250	0.7500	0.9375	1.1500	1.2500	1.2500	1.2500	1.2500	1.2500	1.2500	1.2500	1.2033	1.0917	1.0000	0.9000	0.8000
ET_c [mm/day]	1.8666	2.0627	3.2611	4.9719	5.8709	6.0229	6.0598	5.5351	5.6289	4.7436	3.7873	3.3414	2.8107	2.7503	3.1306	3.4587

Computing the monthly averages yields:

Table A.22: Estimated monthly ETc by the crop coefficient method - virgin cane, plantation in June.

	Jun	Jul	Aug	Sept	Oct	Nov	Dec	Jan	Feb	Mar	Apr	May	Jun	Jul	Aug	Sept
ET_c [mm/month]	55.9977	63.9436	101.0929	149.1562	181.9970	180.6875	187.8553	171.5871	157.6087	147.0514	113.6178	103.5837	84.3210	85.2581	97.0492	79.5500

This results in a total of 1960.4 mm/cycle.

The procedure for the ratoon cane is the same and the result is 1449.3 mm/cycle.

Appendix B

Flow Data

Here, a compilation of the data used in Chapter 4 to model the river flow is presented. Unfortunately, measurements are only available for the wet season and for a limited number of years.

All data points were taken from hydrologic bulletins produced by ARA-Sul and hosted at https://www.ara-sul.gov.mz/bolentins-hidrologicos/.

At the time of last access, May 2021, only the bulletins for the wet season of 2020/2021 were available. Up until recently, records for the wet seasons of 2018/2019 and 2019/2020 were also hosted at the online repository.

It is worth mentioning that there are minor gaps in the data, either from unavailable measurements or due to missing bulletins in the repository. These gaps occur in very small numbers compared to the length of the season for which measurements were recorded and are marked with the symbol (*).

The flow comes in SI units.

B.1 2018/2019

Table B.1: Flows for the 2018/2019 wet season.

# Bulletin	Date	Flow
3	01-11	1.83
	02-11	1.95
	03-11	2.20
	04-11	2.20
	05-11	2.46
4	06-11	1.83
5	07-11	1.95
6	08-11	2.20
7	09-11	2.20
8	10-11	*
	11-11	2.07
	12-11	1.95
9	13-11	1.72
10	14-11	1.61
11	15-11	1.83
12	16-11	1.83
14	17-11	1.95
	18-11	2.07
	19-11	1.83
	20-11	1.40
15	21-11	1.30
16	22-11	1.61
17	23-11	1.61
18	24-11	1.50
	25-11	1.40
	26-11	1.50
19	27-11	1.11
21	28-11	0.94
	29-11	1.11
22	30-11	1.20
23	01-12	1.02
	02-12	2.20
	03-12	1.11
24	04-12	1.50
25	05-12	1.40
26	06-12	1.11
27	07-12	1.30
28	08-12	1.50
	09-12	1.72
	10-12	2.46
29	11-12	3.03
30	12-12	2.88
31	13-12	1.95
32	14-12	1.95
33	15-12	1.72
	16-12	4.34
	17-12	6.55
34	18-12	5.29
35	19-12	5.29
	20-12	5.09
37	21-12	6.33
	22-12	*
41	23-12	4.90
	24-12	4.17
	25-12	2.88
	26-12	2.73
	27-12	1.02
42	28-12	4.17
43	29-12	4.90
	30-12	5.49
	31-12	5.29
44	01-01	3.99
45	02-01	4.53
46	03-01	4.17
47	04-01	4.34
48	05-01	3.99
	06-01	4.53
	07-01	5.49
49	08-01	5.49
50	09-01	8.19
51	10-01	19.22
52	11-01	21.17
53	12-01	21.17
	13-01	39.92
	14-01	46.08
54	15-01	34.95
55	16-01	13.60
56	17-01	17.72
57	18-01	13.60
58	19-01	10.87
59	20-01	8.19
60	21-01	7.47
61	22-01	6.12
62	23-01	4.53
63	24-01	3.33
64	25-01	2.46
65	26-01	1.83
66	27-01	1.61
67	28-01	1.61
68	29-01	1.83
69	30-01	1.83
70	31-01	1.72
71	01-02	1.61
72	02-02	1.80
	03-02	2.07
	04-02	4.17
	05-02	5.90
73	06-02	7.00
74	07-02	7.71
75	08-02	7.47
76	09-02	6.77
	10-02	7.71
	11-02	7.95
77	12-02	7.71
79	13-02	4.90
	14-02	4.53
80	15-02	4.17
81	16-02	3.18
82	17-02	3.18
83	18-02	3.18
84	19-02	2.46
85	20-02	2.59
86	21-02	4.17
87	22-02	92.18
88	23-02	122.25
89	24-02	113.62
	25-02	92.18
90	26-02	76.05
91	27-02	64.28
92	28-02	55.45
93	01-03	13.28
94	02-03	73.77
	03-03	60.80
	04-03	58.77
95	05-03	49.11
96	06-03	43.15
97	07-03	70.78
98	08-03	69.31
99	09-03	52.86
100	10-03	43.15
101	11-03	38.13
103	12-03	37.06
	13-03	29.02
104	14-03	26.27
105	15-03	22.40
106	16-03	18.84
107	17-03	19.99
	18-03	21.58
108	19-03	16.99
109	20-03	14.91
110	21-03	13.60
111	22-03	14.24
112	23-03	18.09
	24-03	20.38
	25-03	22.40
114	26-03	27.63
	27-03	33.93
115	28-03	33.42
116	29-03	29.97
117	30-03	23.23
	31-03	22.81
	01-04	20.38
	02-04	15.59
118	03-04	12.96
119	04-04	16.64
120	05-04	15.25
121	06-04	14.24
	07-04	13.92
	08-04	12.96
	09-04	14.57
122	10-04	19.99
	11-04	27.17
124	12-04	38.67
	13-04	44.31
	14-04	41.44
	15-04	37.59
	16-04	33.93
125	17-04	29.02
126	18-04	26.27
127	19-04	24.08
	20-04	21.99
	21-04	19.22
	22-04	16.64
128	23-04	15.25
129	24-04	13.92

B.2 2019/2020

Table B.2: Flows for the 2019/2020 wet season.

# Bulletin	Date	Flow
	29-11	2.46
	30-11	2.73
2	01-12	2.59
	02-12	2.46
	03-12	2.88
3	04-12	1.50
4	05-12	1.11
5	06-12	0.71
6	07-12	0.64
8	08-12	1.02
	09-12	1.02
9	10-12	1.50
10	11-12	3.49
11	12-12	4.71
12	13-12	3.49
13	14-12	3.18
14	15-12	10.30
15	16-12	16.64
16	17-12	17.72
17	18-12	17.35
18	19-12	15.93
19	20-12	16.64
20	21-12	17.72
21	22-12	16.99
22	23-12	8.44
23	24-12	6.55
24	25-12	4.90
25	26-12	4.17
26	27-12	3.33
27	28-12	2.73
28	29-12	2.07
30	30-12	2.20
	31-12	2.46
31	01-01	3.33
32	02-01	3.03
33	03-01	2.59
34	04-01	2.32
35	05-01	2.32
36	06-01	2.20
37	07-01	2.46
38	08-01	2.46
39	09-01	2.46
40	10-01	3.18
41	11-01	5.09
43	12-01	5.49
	13-01	5.29
44	14-01	4.71
45	15-01	3.99
46	16-01	3.49
47	17-01	3.03
48	18-01	2.46
49	19-01	3.33
50	20-01	3.66
51	21-01	3.66
52	22-01	104.41
54	23-01	29.50
	24-01	23.65
57	25-01	19.60
	26-01	12.34
	27-01	12.34
	28-01	10.87
	29-01	8.70
*	30-01	*
	31-01	*
	01-02	*
67	02-02	5.49
	03-02	5.49
	04-02	4.71
	05-02	3.82
	06-02	3.03
68	07-02	2.32
69	08-02	1.83
70	09-02	1.50
71	10-02	4.34
72	11-02	8.70
73	12-02	32.92
74	13-02	166.73
75	14-02	166.73
76	15-02	131.19
77	16-02	95.60
78	17-02	89.66
79	18-02	71.52
80	19-02	52.86
81	20-02	39.22
82	21-02	30.94
83	22-02	24.51
84	23-02	19.22
85	24-02	14.91
87	25-02	12.65
	26-02	8.96
88	27-02	12.65
89	28-02	12.34
90	29-02	10.58
91	01-03	12.65
	02-03	12.65
92	03-03	11.74
93	04-03	10.30
96	05-03	9.75
	06-03	8.96
	07-03	7.95
97	08-03	7.00
98	09-03	6.77
99	10-03	5.70
101	11-03	5.29
	12-03	4.71
102	13-03	4.34
103	14-03	3.82
104	15-03	3.49
105	16-03	5.49
106	17-03	4.17
107	18-03	4.34
108	19-03	4.34
109	20-03	4.71
110	21-03	4.71
111	22-03	4.71
112	23-03	6.12

B.3 2020/2021

Table B.3: Flows for the 2020/2021 wet season.

# Bulletin	Date	Flow
2	16-11	1.83
	17-11	1.83
	18-11	1.95
	19-11	1.95
	20-11	2.20
3	21-11	2.20
	22-11	2.07
	23-11	2.20
4	24-11	2.32
	25-11	2.20
	26-11	2.59
	27-11	2.32
5	28-11	2.59
	29-11	2.59
	30-11	3.18
6	01-12	3.33
7	02-12	3.66
8	03-12	3.66
9	04-12	3.49
10	05-12	3.18
11	06-12	3.03
12	07-12	3.18
13	08-12	1.11
14	09-12	0.86
15	10-12	0.57
16	11-12	0.39
17	12-12	0.17
	13-12	0.21
	14-12	1.20
18	15-12	1.50
19	16-12	1.61
20	17-12	2.07
21	18-12	2.73
22	19-12	3.49
23	20-12	4.17
24	21-12	3.99
25	22-12	3.03
26	23-12	2.07
27	24-12	2.20
28	25-12	2.32
29	26-12	2.73
30	27-12	2.59
31	28-12	2.73
32	29-12	3.82
33	30-12	5.70
34	31-12	6.33
*	01-01	*
	02-01	*
37	03-01	5.09
38	04-01	5.70
39	05-01	4.34
40	06-01	3.33
41	07-01	2.88
42	08-01	3.03
43	09-01	2.88
44	10-01	2.59
45	11-01	1.95
46	12-01	1.50
47	13-01	1.02
48	14-01	0.71
49	15-01	0.71
50	16-01	4.90
51	17-01	1.72
52	18-01	4.34
53	19-01	5.09
54	20-01	5.09
55	21-01	4.90
56	22-01	4.71
57	23-01	4.17
58	24-01	4.34
59	25-01	6.77
	26-01	13.92
60	27-01	14.57
61	28-01	442.54
62	29-01	398.73
63	30-01	315.56
64	31-01	241.04
65	01-02	206.59
66	02-02	196.53
67	03-02	418.52
68	04-02	526.83
69	05-02	427.68
70	06-02	362.29
71	07-02	555.88
72	08-02	574.97
73	09-02	518.67
74	10-02	518.52
75	11-02	518.67
76	12-02	365.69
77	13-02	375.97
78	14-02	469.16
79	15-02	514.62
80	16-02	492.21
81	17-02	603.12
82	18-02	518.67
83	19-02	422.17
84	20-02	357.23
85	21-02	322.82
86	22-02	276.72
87	23-02	246.58
88	24-02	220.84
89	25-02	222.16
90	26-02	216.90
91	27-02	282.65
92	28-02	239.67
93	01-03	267.93
94	02-03	243.81
95	03-03	224.81
99	04-03	191.59
	05-03	177.17
	06-03	163.32
	07-03	153.31
100	08-03	140.46
101	09-03	132.20
102	10-03	131.19
103	11-03	123.22
104	12-03	111.75
105	13-03	101.73
106	14-03	98.20
107	15-03	130.18
108	16-03	105.32
109	17-03	91.34
110	18-03	82.32
111	19-03	76.05
112	20-03	68.58
113	21-03	67.13
114	22-03	82.32
115	23-03	94.74
116	24-03	93.03
117	25-03	91.34
118	26-03	91.34
119	27-03	24.08
120	28-03	21.99
121	29-03	68.58

Appendix C

Chronological Daily Flow Series

Here, the data from the previous Appendix is plotted to give meaningful context.

Note: The yy-axis scale of the plots of figures C.1 and C.2 is the same to establish a comparison. As for figure C.3, the abnormally high levels of flow meant the adoption of a different scale.

C.1 2018/2019

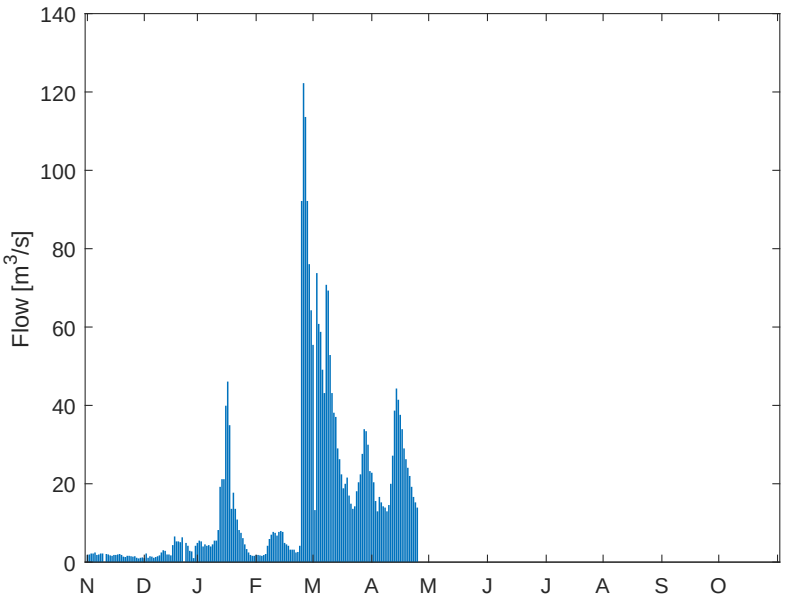

Figure C.1: Recorded Flows - 2018/2019 Wet Season, Magude - E43

C.2 2019/2020

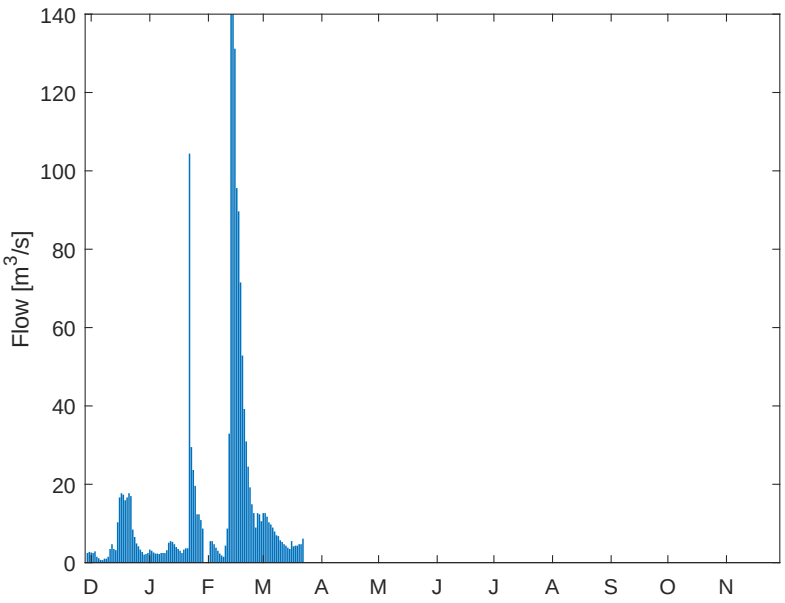

Figure C.2: Recorded Flows - 2019/2020 Wet Season, Magude - E43

C.3 2020/2021

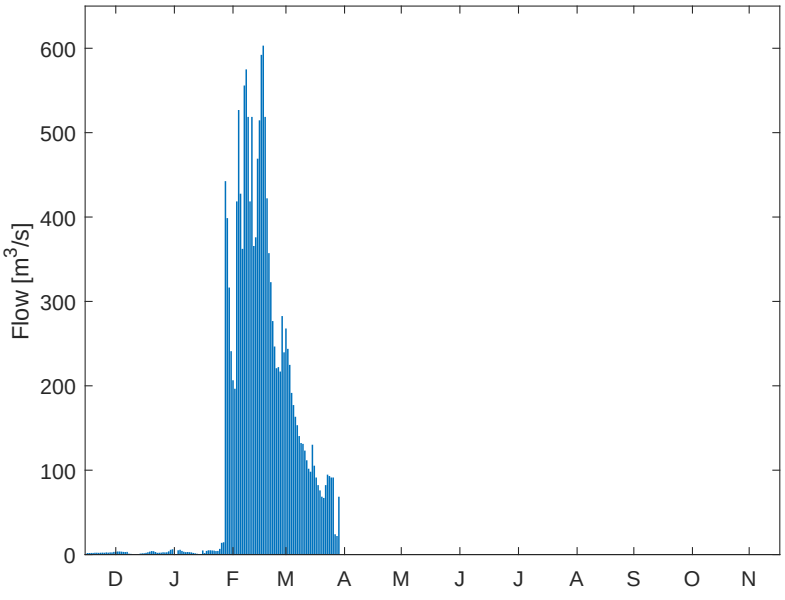

Figure C.3: Recorded Flows - 2020/2021 Wet Season, Magude - E43

Appendix D

Flow Duration Curves

Here, the flow duration curves are presented.

D.1 2018/2019

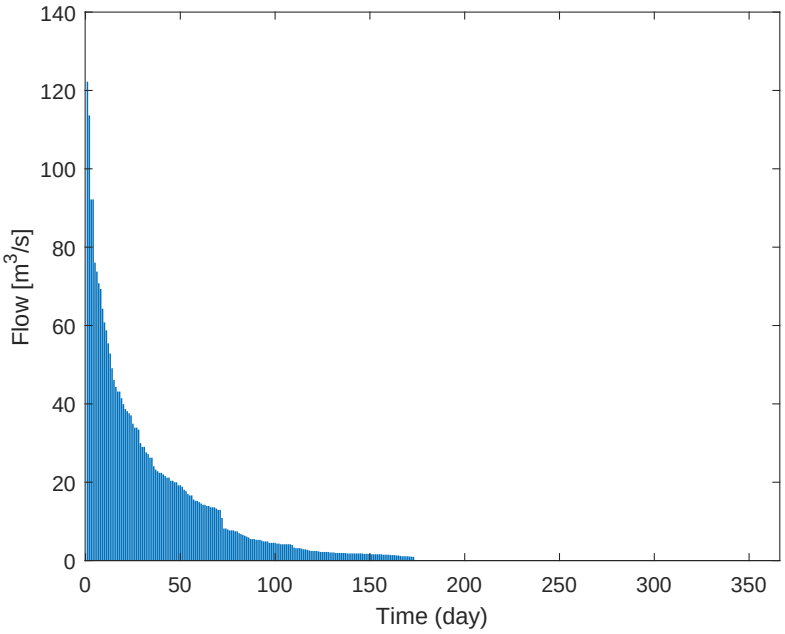

Figure D.1: Flow Duration Curve - 2018/2019 Wet Season, Magude - E43

D.2 2019/2020

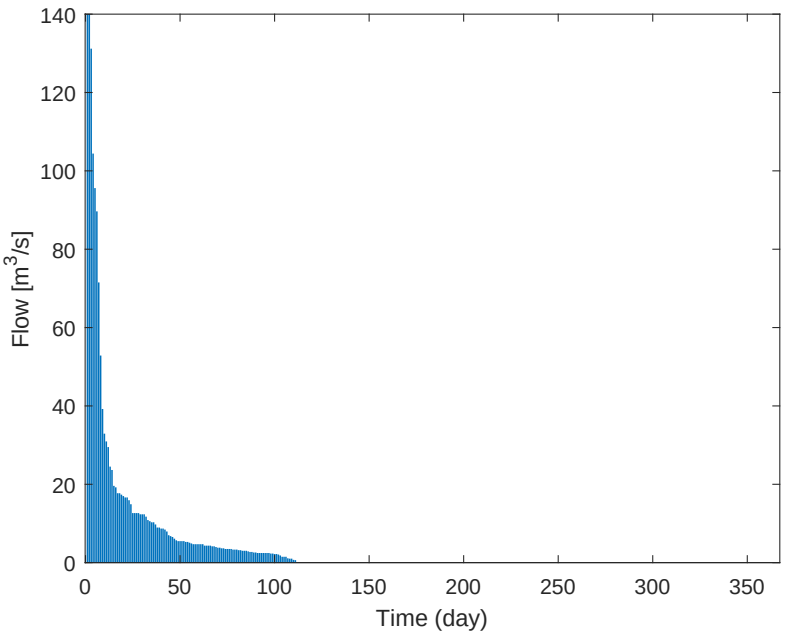

Figure D.2: Flow Duration Curve - 2019/2020 Wet Season, Magude - E43

D.3 2020/2021

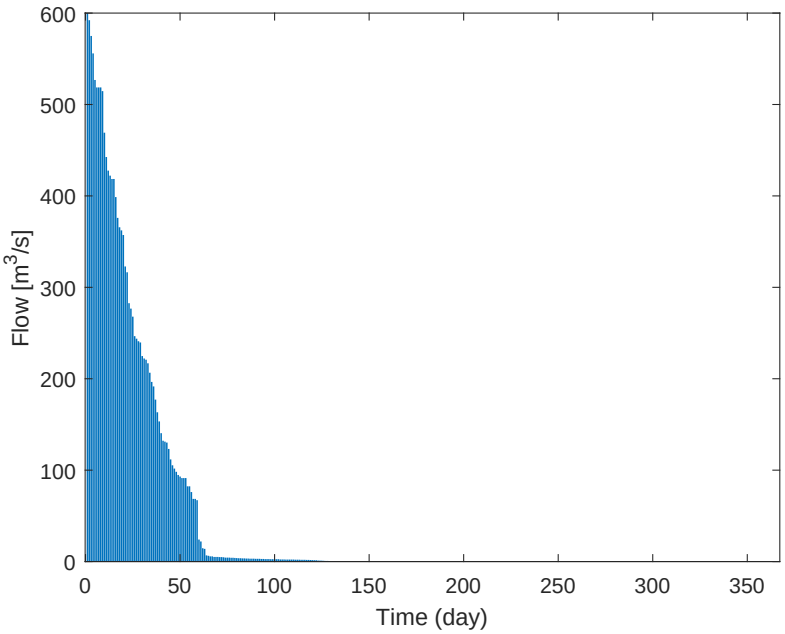

Figure D.3: Flow Duration Curve - 2020/2021 Wet Season, Magude - E43

Appendix E

Modeled Flows

Here, the datapoints of the flow duration curves are plotted against the fitted curves. As such, the 2018/2019 and 2020/2021 wet seasons are reasonably modeled by a two-parameter exponential, equation (E.1).

$$Q(t) = ae^{-b/t} \tag{E.1}$$

By contrast, the flow duration curve of the 2019/2020 wet season is better modeled by a reciprocal function as that of equation (E.2).

$$Q(t) = a\frac{1}{t} \tag{E.2}$$

E.1 2018/2019

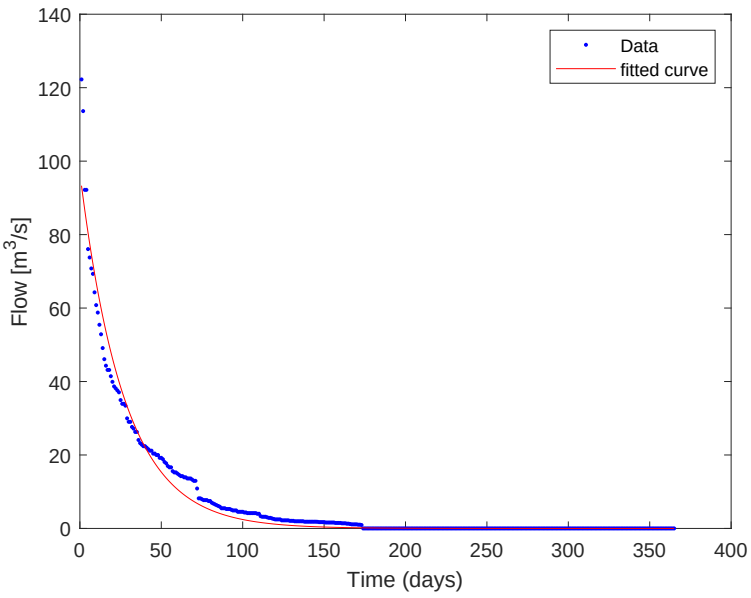

Figure E.1: Fitting of the 2018/2019 FDC.

E.2 2019/2020

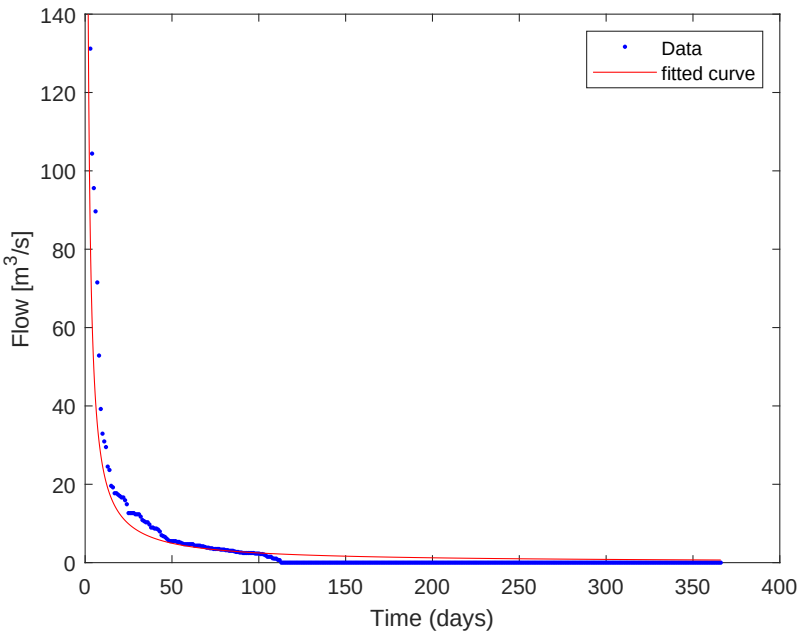

Figure E.2: Fitting of the 2019/2020 FDC.

E.3 2020/2021

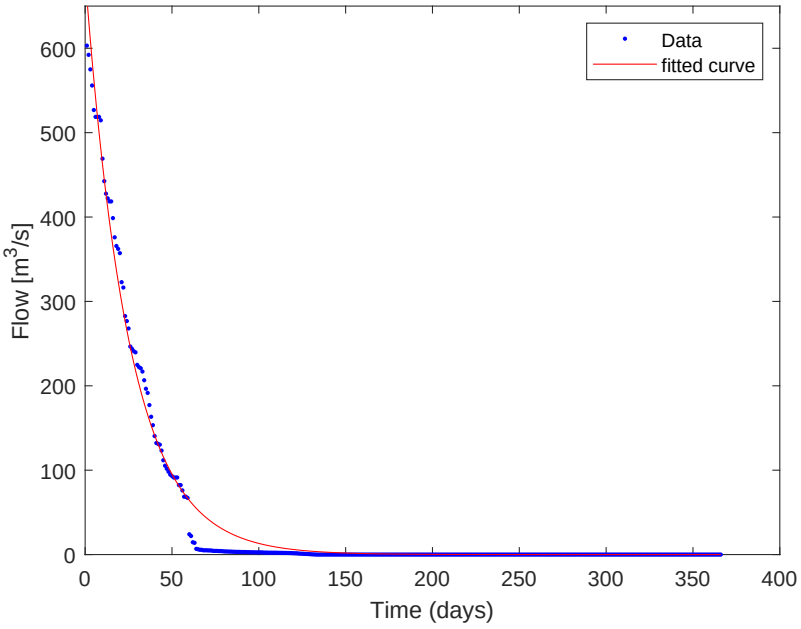

Figure E.3: Fitting of the 2020/2021 FDC.

Appendix F

Channel Design

An optimization of the dimensions of the cross section for a rectangular channel, Figure F.1 has to start with the search for the optimum aspect ratio, i.e., the ratio of channel depth y to channel width b.

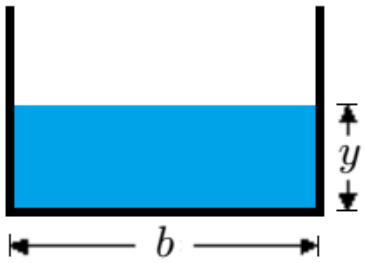

Figure F.1: Channel cross section.

The cross section $A\,[\mathrm{m}^2]$ is defined by

$$A = by \tag{F.1}$$

while the so called wetted perimeter $P\,[\mathrm{m}]$ is given by

$$P = 2y + b \tag{F.2}$$

The optimum cross section of the channel is one that results in the maximum volume-carreying capacity, and therefore one with a maximum hydraulic radius $R_h\,[\mathrm{m}]$, which is defined as the ratio of the cross section to the wetted perimeter, equation F.3.

$$R_h = \frac{A}{P} \tag{F.3}$$

which is the same as saying that the lesser the P, the greater the R_h. Taking equations F.1 and F.2 and expressing the wetted perimeter as a function of the area, we obtain:

$$P = 2y + b = 2y + \frac{A}{y} \tag{F.4}$$

If the constraint is the minimum use of resources required to excavate and coat the channel, then

$$\frac{dP}{dy} = 0 \iff 2 - \frac{A}{y^2} = 0 \iff A = 2y^2 \tag{F.5}$$

Plugging equation (F.5) in equation (F.1), it follows that

$$y = \frac{b}{2} \tag{F.6}$$

Defining the aspect ratio AR of the cross section as the ratio of the channel height to its width,

$$\text{AR} = \frac{y}{b} = \frac{1}{2} \tag{F.7}$$

it follows that the optimum dimensions of the cross section are such that the width is twice the height and the hydraulic radius becomes

$$R_h = \frac{A}{P} = \frac{by}{2y + b} = \frac{2y^2}{4y} = \frac{y}{2} \tag{F.8}$$

Now, supposing such a channel has a given slope S, and a Gauckler–Manning coefficient n, the mean velocity of the fluid $v\,[\text{m/s}]$ is dictated by the Gauckler-Manning formula, equation F.9

$$v = \frac{k}{n} R_h^{2/3} \sqrt{S}, \qquad k = 1 \text{ (SI units)} \tag{F.9}$$

Moreover, from the continuity equation, F.10, the flow $Q\,[\text{m}^3/\text{s}]$that passes through a cross section of the channel is the product of its cross section by the mean velocity of the fluid crossing it,

$$Q = vA \tag{F.10}$$

Combining equations F.9 and F.10, it follows that the flow Q is just

$$Q = \frac{R_h^{2/3} \sqrt{S} A}{n} \tag{F.11}$$

Direct substitution of equations F.1 and F.8 in F.11 results in

$$Q = \frac{1}{n} \left(\frac{y}{2} \right)^{\frac{2}{3}} \sqrt{S} (2y^2) \tag{F.12}$$

After some manipulation it follows that the channel height $y\,[\text{m}]$ can be written as a function of n, Q and S:

$$y = 2^{\frac{7}{8}} \left(\frac{nQ}{\sqrt{S}} \right)^{\frac{3}{8}} \tag{F.13}$$

Then, the Froud number is defined by equation F.14

$$F_r = \frac{v}{\sqrt{gy}} \tag{F.14}$$

Appendix G

Photovoltaic Potential

As mentioned in Chapter 4, the only two viable (at first glance) renewable energy sources capable of powering the irrigation system are solar and hydro. Here, a brief overview of the solar potential is presented, as a means to justify Figure 4.1.

G.1 Irradiance

The same online PVG tool used to derived the temperature series used in Appendix A, also allows for the consultation of several solar databases for the African continent. For the region of Magude, Mozambique, the average daily records, on a hourly basis, of global irradiance for the period of 2005 - 2016 were obtained, Figure G.1. The consulted database was PVGIS-SARAH, for a grid-connected fixed mounting, with an optimized slope angle of 28 $^{\circ}$.

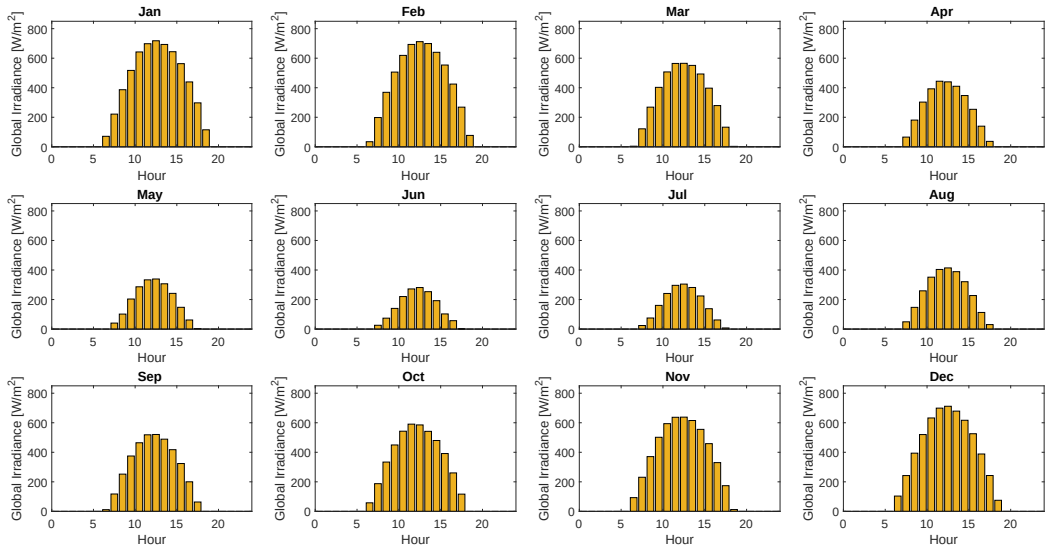

Figure G.1: Daily average global irradiance by month.

Given the required power demand, a preliminary study discarded low power PV modules, and so, for computation purposes, the panel chosen was the Canadian Solar KuPower CS3K-305P 305W Solar Panel, whose characteristics (electric, temperature and mechanical) are presented in Figure G.2.

ELECTRICAL DATA | STC*

CS3K	295P	300P	305P	310P
Nominal Max. Power (Pmax)	295 W	300 W	305 W	310 W
Opt. Operating Voltage (Vmp)	32.5 V	32.7 V	32.9 V	33.1 V
Opt. Operating Current (Imp)	9.08 A	9.18 A	9.28 A	9.37 A
Open Circuit Voltage (Voc)	39.1 V	39.3 V	39.5 V	39.7 V
Short Circuit Current (Isc)	9.57 A	9.65 A	9.73 A	9.81 A
Module Efficiency	17.75%	18.05%	18.36%	18.66%
Operating Temperature	-40°C ~ +85°C			
Max. System Voltage	1500V (IEC/UL) or 1000V (IEC/UL)			
Module Fire Performance	TYPE 1 (UL 1703) or Class C (IEC 61730)			
Max. Series Fuse Rating	30 A			
Application Classification	Class A			
Power Tolerance	0 ~ + 5 W			

* Under Standard Test Conditions (STC) of irradiance of 1000 W/m², spectrum AM 1.5 and cell temperature of 25°C.

MECHANICAL DATA

Specification	Data
Cell Type	Poly-crystalline
Cell Arrangement	120 [2 X (10 X 6)]
Dimensions	1675 X 992 X 35 mm (65.9 X 39.1 X 1.38 in)
Weight	18.5 kg (40.8 lbs)
Front Cover	3.2 mm tempered glass
Frame	Anodized aluminium alloy
J-Box	IP68, 3 bypass diodes
Cable	4.0 mm² (IEC), 12 AWG (UL)
Cable Length (Including Connector)	Portrait: 400 mm (15.7 in) (+) / 280 mm (11.0 in) (-); landscape: 1160 mm (45.7 in)*
Connector	T4 series or H4 UTX or MC4-EVO2
Per Pallet	30 pieces
Per Container (40' HQ)	840 pieces

* For detailed information, please contact your local Canadian Solar sales and technical representatives.

ELECTRICAL DATA | NMOT*

CS3K	295P	300P	305P	310P
Nominal Max. Power (Pmax)	219 W	223 W	227 W	230 W
Opt. Operating Voltage (Vmp)	30.2 V	30.4 V	30.6 V	30.8 V
Opt. Operating Current (Imp)	7.26 A	7.34 A	7.42 A	7.49 A
Open Circuit Voltage (Voc)	36.7 V	36.8 V	37.0 V	37.2 V
Short Circuit Current (Isc)	7.72 A	7.78 A	7.85 A	7.91 A

* Under Nominal Module Operating Temperature (NMOT), irradiance of 800 W/m², spectrum AM 1.5, ambient temperature 20°C, wind speed 1 m/s.

TEMPERATURE CHARACTERISTICS

Specification	Data
Temperature Coefficient (Pmax)	-0.37 % / °C
Temperature Coefficient (Voc)	-0.29 % / °C
Temperature Coefficient (Isc)	0.05 % / °C
Nominal Module Operating Temperature	42 ± 3°C

Figure G.2: Canadian Solar KuPower CS3K-305P - Partial Datasheet.

G.2 Estimated Energy Produced by one Panel

The average temperature of the panel $T_{panel}\,[^\circ C]$ is given by equation G.1

$$T_{panel} = \mathsf{T}_{amb} + \frac{Irrad}{800} \times (NOCT - 20) \tag{G.1}$$

in which $T_{amb}\,[^\circ C]$ is the ambient temperature, $I\,[\mathrm{W/m^2}]$ is the global irradiance, and $NOCT\,[^\circ C]$ is the Nominal Operating Cell Temperature.

The PV panel output power is obtained from equation G.2

$$P_{out} = P_{max} \times \frac{Irrad}{800} \times [1 - NPC(T_{panel} - 45)] \tag{G.2}$$

in which the $NPC[\%/^\circ C]$ is the maximum power temperature coefficient.

Both the hourly irradiance and temperature data were restricted to the period between 07:00 hours to 19:00 hours. For the considered time interval, the estimated energy produced by this PV panel is just the sum of the hourly output power, Table G.1.

Table G.1: Estimated monthly average energy generated by one PV panel.

Month	Jan	Feb	Mar	Apr	May	Jun	Jul	Aug	Sep	Oct	Nov	Dec
Energy [kWh]	51.91	45.35	38.02	26.38	18.96	14.56	16.86	24.73	32.51	39.84	43.66	50.07

So, on average, one of these panels would be able to produce 400.3 kWh/year.

Plotting the data of Table G.1, with June as the starting month, it follows the graph of Figure G.3, used in determining the monthly variability of pv production discussed in section 4.1.

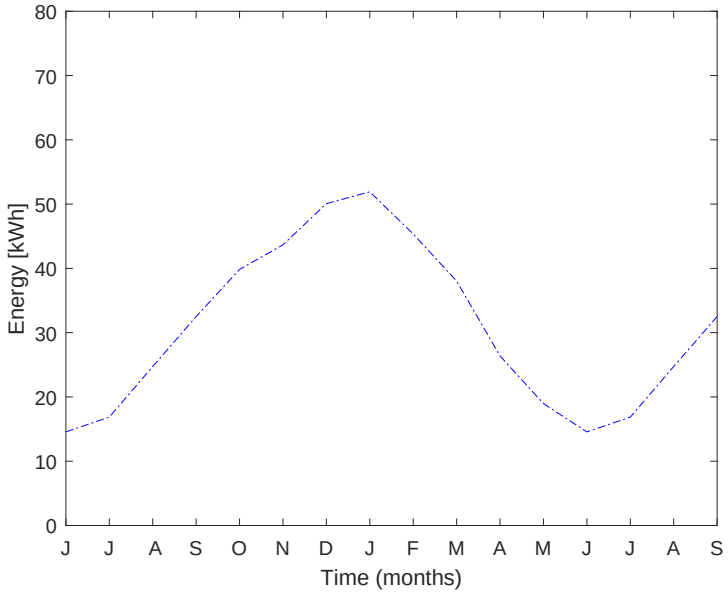

Figure G.3: Estimated monthly average energy produced by one panel from 07:00 to 19:00 hours.

It should be noted that in Figure 4.1, the irradiance was plotted fixing time at t = 13:00 hours, that roughly corresponds to its daily maximum value.